Biologie

The role of the Four and a half LIM only protein 2 (FHL2) in bleomycin induced lung fibrosis

Inaugural-Dissertation
zur Erlangung des Doktorgrades
der Naturwissenschaften im Fachbereich Biologie
der Mathematisch-Naturwissenschaftlichen Fakultät
der Westfälischen Wilhelms-Universität Münster

vorgelegt von
Abdulaleem Ali Alnajar

2013

Dekanin/Dekan: Prof. Dr. Dirk Prüfer

Erster Gutachter: PD Dr. Viktor Wixler

Zweiter Gutachter: Prof. Dr. Martin Bähler

Tag der mündlichen Prüfung(en): 21.06.2013

Tag der Promotion: 12.07.2013

Incription:

I woud like to incript my work to the spirit of my father and my mother (the reason of my success). Also, I incript my work to my darlings, lovely wife and children.

Table of contents

Abstract

Pulmonary fibrosis is a progressive fibrotic disease which takes place when regenerative processes have failed or long-term inflammation occurs. It is characterized by activation of tissue fibroblasts and deregulated synthesis of extracellular matrix proteins. It causes scarring of alveolar compartments of the lung where gas exchange occurs and results in tissue damage.

While fibrotic alterations may be induced by variety of causes, available data increasingly indicate that chronic inflammation and aberrant wound healing play an important role in the development of the disease. Bleomycin (BLM) is a chemotherapeutical drug with a serious side effect. Namely, it induces lung fibrosis. BLM causes alveolar cell damage by intercalating into DNA and by inducing lipid peroxidation. Today it is one of the best established animal models of lung fibrosis.

FHL2 (four-and-a-half LIM domain protein 2) is a scaffolding protein which is able to interact with numerous cellular proteins regulating signaling cascades and gene transcription. It is involved in tissue remodeling and tumor progression and existing data suggest that FHL2 might supports fibrogenesis by maintaining the transcriptional expression of αSMA and excessed synthesis and assembly of matrix proteins in activated fibroblasts. Therefore we hypothesized that FHL2 is a protein that supports fibrogenesis.

To study the role of FHL2 in development of fibrosis, we chose the bleomycin-mediated lung fibrosis model and studied the development of the disease in WT mice in comparison with FHL2 knockout animals. Contrary to our expectation, FHL2-deficient mice developed more severe lung pathology after application of BLM than WT mice. Our histological, tissue cell culture and molecular cell biology studies showed that FHL2 does not aggravate the bleomycin-induced lung fibrosis but rather restrained it by attenuating lung inflammation. We showed that FHL2 inhibits the transcription of the pro-inflammatory matrix protein tenascin C and simultaneously stimulates the expression of the macrophage activating C-type lectin receptor DC-SIGN. Consequently, upon bleomycin application FHL2 knockout mice developed a severe and long-lasting lung inflammation due to enhanced expression of tenascin C and impaired accumulation of activated and inflammation ceasing macrophages. Finally, the particular importance of macrophages in restricting fibrotic alterations was proofed by in vivo depletion of lung macrophages during development of BLM-induced lung fibrosis.

Zusammenfassung

Die Lungenfibrose geht mit einer Transformation von Lungenfibroblasten zu Myofibroblasten und einer Überexpression und Ablagerung von extrazellulären Matrixproteinen einher. Die verstärkte Bildung von Bindegewebe führt letztendlich zu zunehmenden Gewebsschäden und einer stark eingeschränkten Lungenfunktion. Die Lungenfibrose ist eine sich progressiv entwickelnde Erkrankung, wenn Gewebsregenerationen fehlgeschlagen oder langanhaltende Entzündungen überhandgenommen haben.

Bleomyzin (BLM) ist ein Antibiotikum, das in der Tumortherapie eingesetzt wird. Es hat jedoch einen starken Nebeneffekt, die Entwicklung der Lungenfibrose. BLM interkaliert in die DNA und induziert zusätzlich Oxidation von Lipiden, was zu verstärkten Gewebsschäden führt. Auch in Nagern kann eine Lungenfibrose durch Applikation von BLM hervorgerufen werden und ist heutzutage das bestuntersuchte Tiermodel zur Lungenfibrose.

FHL2 (Viereinhalb-LIM-Domänen Protein 2) ist ein Adapterprotein, das mit mehreren zellulären Proteinen wechselwirkt und als solches mehrere Signalübertragungskaskaden und Gentranskriptionen reguliert. Es ist in Gewebeumbauprozesse und Tumorprogression involviert. Des Weiteren wurde gezeigt, dass FHL2 als Kofaktor der Transkription die Expression von aSMA und als integrinbindendes Protein die Assemblierung von extrazellulären Matrixproteinen fördert. Daher sollte in dieser Arbeit geprüft werden ob und inwieweit das FHL2 Protein die Entwicklung der Lungenfibrose begünstigt.

Um dieser Fragestellung nachzugehen, wurde die Entwicklung der Bleomyzin-induzierten Lungenfibrose in FHL2 Wiltyp und Knockout Mäusen verglichen. Erstaunlicherweise zeigten FHL2-defiziente Tiere einen schwereren Krankheitsverlauf als Wildtyp Mäuse. Histologische, zellkulturische sowie molekularbiologische Studien zeigten jedoch, dass die Abwesenheit von FHL2 *per se* nicht zu einer Steigerung der Fibrosierung des Lungengewebes führt, sondern eine verstärkte inflammatorische Reaktion in der Lunge hervorruft. Die Entzündung des Lungengewebes in FHL2 Knockout Mäusen nach BLM Induktion ist im Vergleich zu Wildtyp Tieren nicht erhöht, sondern entwickelt sich wesentlich früher und flammt langsamer ab als in Wildtyp Mäusen. Es konnte gezeigt werden, dass dies auf zwei wichtigen Funktionen des FHL2 Proteins beruht, die in der Knockout Maus fehlen. Zum einen hemmt FHL2 als Kofaktor der Transkription die Expression des entzündlichen Proteins Tenascin C. Zum anderen, ist FHL2 essentiell für die Expression von DC-SIGN, des C-Typ Lektinrezeptors der Makrophagen, nach deren Stimulation mit kohlehydratreichen

Gewebslysaten. Dementsprechend wurde in FHL2 Knockout Lungen nach BLM Applikation das Tenascin C verstärkt exprimiert und die residenten Makrophagen unzulängluich aktiviert, was zu einer erhöhten und langanhaltenden Entzündung führt.

1. Introduction

1.1. Lung fibrosis

The primary function of the lung is to provide a sufficient size and highly efficient area for gas exchange (Robert et al. 2010; Nkyimbeng Takwi 2008). The lung has two well defined interstitial connective tissue compartments arranged in series: the parenchymal interstitium and the loose connective tissue (peribronchovascular sheaths, interlobular septa and visceral pleura). The parenchymal interstitium of the alveolar wall makes up about 33% of the total interstitial volume (Figure 1) (Nkyimbeng Takwi 2008; Robert et al. 2010).

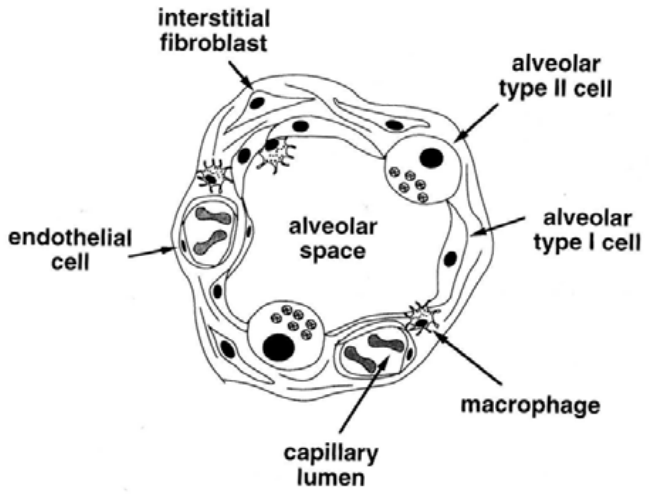

Figure 1: Schematic view of the lung parenchyma that surrounds an alveolar space showing the major cells that line and lie within the putative interstitial space (Nkyimbeng Takwi 2008; Robert et al. 2010).

Fibrosis usually takes place when regenerative processes have failed and /or long- term inflammation occurs after tissue damage. It is characterized by activation of fibroblasts which leads to excess deposition of extracellular matrix (ECM) components (Krieg et al. 2007; Wynn 2011; Wynn 2007; Pottier et al. 2007). Tissue damage may result from various stimuli, including infections, autoimmune reactions, toxins, radiation and drugs or chemical insults (such as bleomycin, gentamicin and cisplatin) (Wynn 2008; Nuno 1998; Pinart et al. 2008; Mouratis &Aidinis 2011; Pottier et al. 2007).

The lung fibrosis is an acute&chronic inflammatory disease, which results in scarring of the alveolar compartment of the lung where gas exchange occurs (William et al. 2007; Herbert 2005; Robert et al. 2011; Wynn 2011). Fibrosis can also involve other areas of the lung, such as bronchi and pleura, but in general the unqualified term pulmonary fibrosis usually indicates alveolar pathology of the lung (Jantz & Antony 2006; William et al. 2007; Wick et al. 2009).

The lung fibrosis corresponds to the end stage of lung injury. The progression of this disease results in the widening of interstitial matrix, eventual compression and destruction of normal lung parenchyma, with damage of capillaries. These factors are related to the extent of tissue scarring (Razzaque & Taguchi 2003; Wynn 2011). The scar formation ultimately leads to organ malfunction, disruption of gas exchange, and death from respiratory failure (Wynn 2011; Raghu et al. 2006).

Idiopathic pulmonary fibrosis (IPF) is one of the most common forms of lung fibrosis. It is diagnosed in 34,000 new patients per year in the United States (Raghu et al. 2006) and is often a severely debilitating and fatal condition; the median survival of patients with IPF is approximately 3 years from the time of diagnosis (Irina et al. 2008; Daniil et al. 1999).

1.1.1. Stages of wound healing and development of lung fibrosis:

Fibrogenesis is often defined as an out of control wound healing response (Mutsaers et al. 1997). The development of wound repair and lung fibrosis has three distinct stages: i) the acute inflammatory stage (includes migration of inflammatory cells into the wounded area and secretion of inflammatory mediators), ii) the stage of active fibroblast migration and proliferation and a iii) the tissue remodeling stage (Figure 2) (Razzaque & Taguchi 2003; Wynn 2011; Wick et al. 2009; Robert et al. 2011; Mutsaers et al. 1997; Rajendra 1994).

After lung tissue injury, epithelial cells release large amounts of bioactive lipids and inflammatory mediators that initiate an antifibrinolytic coagulation cascade, which triggers platelet activation and blood clot formation (Annie & Moises 2002; Wynn 2011; Wynn 2008). This is followed by migration of leukocytes (e.g., neutrophils, macrophages, and T- cells) into the site of injury. Neutrophils are the most abundant inflammatory cell at the earliest stages of

wound healing, but are quickly replaced by macrophages after neutrophil degranulation (Shaw et al. 2009; Wynn 2011; Wynn 2008; Martin 2009). The activated macrophages and neutrophils remove dead cells and eliminate invading microrganisms (Shaw et al. 2009; Wynn 2011). The recruited leukocytes secrete profibrotic cytokines such as tumor necrosis factor (TNF), interleukin-1 (IL-1), interleukin-13 (IL-13), transforming growth factor (TGF-β) and different ELR+ motif (Glu-Leu-Arg domain) containing CXC chemokines (Wick et al. 2009; Robert et al. 2011; Wynn 2011; Jack et al. 1993). Also, the macrophages secrete matrix metalloproteinases (MMPs), e.g. MMP-12, which largely regulate the inflammatory cytokine and chemokine secretion and migration of cells into the site of inflammation (Dean et al. 2008).

In the subsequent phase, fibrocytes from the bone marrow and resident fibroblasts proliferate and differentiate into myofibroblasts, which release ECM components (Wynn 2011; Wick et al. 2009; Robert et al. 2011). Fibroblasts and myofibroblasts may also be derived from epithelial cells undergoing epithelial/endothelial-mesenchymal transition (EMT) (Hinz et al. 2007; Wynn 2011). In the final remodeling and resolution phase, activated myofibroblasts can promote wound repair by regulating wound contraction and restoration of blood vessels (Wynn 2011; Mutsaers et al. 1997). However, fibrosis often develops if any stage in the tissue repair program is dysregulated or when the lung-damaging stimulus persists (Wynn 2011; Annie & Moises 2002; Rajendra 1994). The stages of wound healing and development of lung fibrosis are described in more detailes in sections below.

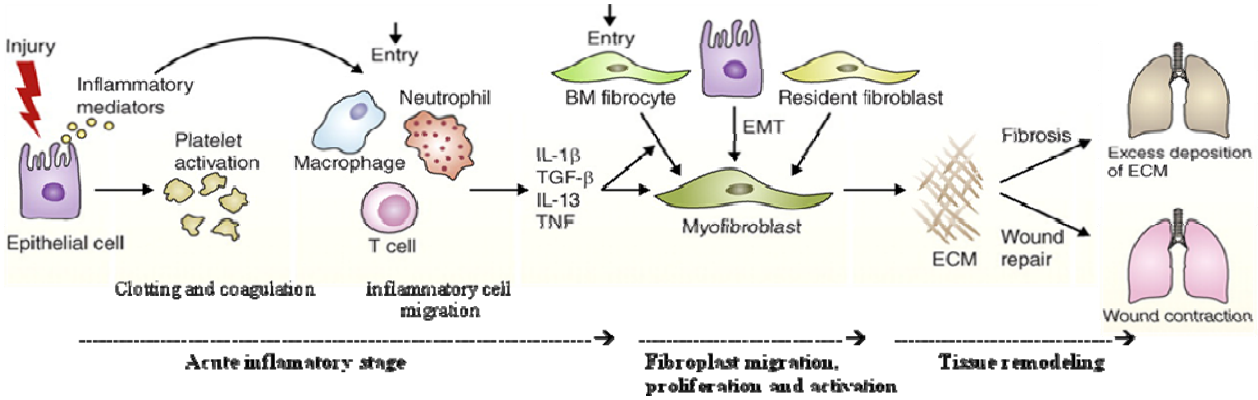

Figure 2: Disruptions in normal wound healing contribute to the development of lung fibrosis (Wynn 2011).

1.1.1.1. Acute inflammatory stage:

The alveolar surface of the lung is lined by type 1 and type 2 epithelial cells. Type 1 cells, which cover more than 90% of the alveolar surface area of the peripheral lung, are highly attenuated cells that interface with pulmonary capillaries (see Figure 1) (Moises and Annie 2006; Wynn 2011). The geometry of these cells is ideally suited for gas exchange (Annie & Moises 2002).

The damage of epithelial cells and/ or endothelial cells as result of tissue injury plays an important role in fibrogenesis (Kisseleva & Brenner 2008; Wynn 2011). These cells secrete numerous inflammatory mediators, including, transforming growth factor (TGF-β1), platelet-derived growth factor (PDGF), tumor necrosis factor-alpha (TNF-α), interleukins, members of ELR+ motif (Glu-Leu-Arg domain) containing CXC chemokines and members of the fibroblast growth factor family (FGF) (Strieter et al. 2007; Kisseleva & Brenner 2008). These inflammatory mediators induce platelet aggregation and degranulation, blood clot formation and are responsible for active recruitment of inflammatory cells and for accumulation of provisional ECM (Strieter et al. 2007; Kisseleva & Brenner 2008; Wynn 2011).

Platelet aggregation and their subsequent degranulation in turn promotes blood vessel dilation and increased permeability, allowing efficient recruitment of inflammatory cells (e.g., granulocyte neutrophils, macrophages, and lymphocytes) to the site of injury (Wynn 2011; Wick et al. 2009; Robert et al. 2011; Rajendra 1994; Kisseleva & Brenner 2008).

1.1.1.1.1. Inflammatory cell migration stage

Migration of inflammatory cells to the site of the acute injury is a part of wound healing (Kisseleva & Brenner 2008; Pinart et al. 2008; Wick et al. 2009). The cellular components of the immune system appear at the site of injury in a specific sequence and time frame as shown in Figures 2 and 3 (Wynn 2011; Martin 2009).

Neutrophils are the first immune cells that arrive at the site of injury within minutes (the time frame for the highest activity lies between the first 3 to 24 h) (Shaw et al. 2009; Kisseleva &

Brenner 2008). Following neutrophils, the macrophages migrate to the site of tissue injury within 24-48 h and become the predominant immune cell type (Martin 2009; Timothy et al. 2006; Wick et al. 2009). T- and B- lymphocytes are also recruited to the site of injury, although to some what later time points, and further facilitate secretion of fibrogenic cytokines (Kisseleva & Brenner 2008). The pro-inflammatory-fibrotic factors which have been secreted by the inflammatory cells regulate the migration and proliferation of fibroblasts (Wynn 2011; Kisseleva & Brenner 2008).

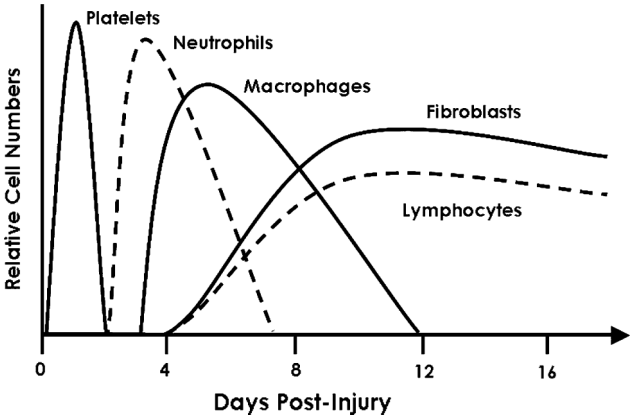

Figure 3: Immune cell content of the healing wound. The cellular components of the immune system in the wound in a specific sequence and time frame (Martin 2009).

- Neutrophils

Neutrophils are polymorphonuclear leukocytes, which play a central role in innate immunity by phagocytosing and destructing invading microorganisms through production of reactive oxygen intermediates and releasing proteolytic enzymes (Timothy et al. 2006; Driss & Janos 2010). During wound healing and development of lung fibrosis, neutrophils are one of the first-responders of inflammatory cells that migrate towards the site of inflammation. They migrate through the blood vessels, then through interstitial tissue (Shaw et al. 2009; Wynn 2011; Kisseleva & Brenner 2008). They also produce a variety of cytokines and chemokines that amplify the inflammatory response and trigger fibroblast proliferation and recruitment (Timothy et al. 2006; Wynn 2011; Razzaque & Taguchi 2003).

-Macrophages

Macrophages (MΦ) are phagocytic cells derived from monocytes (Nishida & Hamaoka 2008). They express a number of specific surface proteins, including F4/80 in case of mice, and can be identified by flow cytometry or immunohistochemical staining (Khazen et al. 2005). It has been shown that macrophages can be activated by lipopolysaccharide (LPS), a component of the gram negative bacterial cell wall (Fanying and Clifford 1997).

Activated macrophages release chemokines (such as CCL2 and CCL3), cytokines (such as tumor necrosis factor (TNF), interleukin-1 (IL-1), interleukin-6 (IL-6), interleukin-13 (IL-13), macrophage inflammatory protein-1 (MIP-1) and reactive oxygen species (ROS) (Smith et al. 1994; Robert et al. 2011; Wynn 2011).

Lung macrophages are integrated into all stages of wound healing and fibrosis and they role in regulation of these processes is multifunctional but very essential (Wynn and Barron, 2010; Herbert 2005). The macrophages phagocytose cell debris, induce apoptosis, recruit inflammatory cells and myofibroblasts and regulate vascularization, but they are also involved in induction of scar formation (Nishida & Hamaoka 2008; Timothy et al. 2006). Lung macrophages terminate and resolve the lung inflammation and fibrosis by secreting mediators that induce myofibroblast apoptosis, by removing cellular debris that can drive inflammation, by clearance of alveolar edema fluid, by regulation of angiogensis and proliferation/differentiation of epithelial cells to repair the damage, by digesting and engulfing ECM components, and by stimulating the production of matrix metalloproteinases (MMPs) (Wynn and Barron 2010; Nishida & Hamaoka 2008; Wynn 2011; Herold et al. 2011). From MMPs secreted by macrophages the MMP-12 plays an essential important role. It does not only degrade extracellular matrix proteins but also regulate the recruitment of inflammatory cells to sites of tissue injury as well as cytokine and chemokine secretion (Zuo et al. 2002; Nishida & Hamaoka 2008; Dean et al. 2008; Iredale et al. 1998). The macrophage-specific metalloelastase (MMP-12) inactivates different ELR+ CXC- and CC chemokines, which underscores the absolute essential role of macrophage in terminating polymorphonuclear leukocyte influx during inflammation (Dean et al. 2008). Macrophages can be selectively

depleted from tissues in vivo by using clodronate containing liposomes, allowing investigating the role of these cells in fibrotic processes (Rooijen and Sanders 1994). Macrophage depletion during the recovery phase of renal fibrosis led to a failure of matrix degradation and persistent scarring (Nishida & Hamaoka 2008). In myocardial wound healing, macrophage depletion impaired wound healing (Van Amerongen et al. 2007). Other studies show that injection of macrophages into healing cutaneous wounds augments the repair process (David et al. 1989).

-Lymphocytes:

Lymphocytes are a type of leukocytes in vertebrate immune system (Charles et al. 2001). Under the microscope, lymphocytes can be divided into large and small lymphocytes. Large granular lymphocytes include natural killer cells (NK cells). Small lymphocytes consist of T-cells (thymus cells) and B cells (bursa-derived cells) (Charles et al. 2001). The basis for lymphocyte immune function is the highly selective clonal expansion of individual lymphocytes following exposure to specific antigens (Charles et al. 2001). Lymphocytes, together with monocyte-derived macrophages, are common participants in inflammatory responses associated with various forms of tissue injury (Russel 1994).

T- cells have an immportent role during wound healing and development of fibrosis. In the wound, the active hypertrophic scar tissue was infiltrated with T- cells, and also they are characteristic for the remission phase of hypertrophic scar formation (Boyce et al. 2000; Bernabei et al. 1999).

Infiltration of T- lymphocytes into the lung is common in patients with lung fibrosis and in animal models for this disease as well. These cells have a role in regulating the accumulation of extracellular matrix and modulation of the inflammatory and healing responses in the lung and they may work in a profibrotic or an antifibrotic (Naohito et al. 1996; Wynn 2011; Irina et al. 2008). Activated T- lymphocytes may produce proinflammatory mediators such as IFNγ, TNFα, Il-4 or Il-13 as part of the overall inflammatory pattern (Atamas et al. 2003). Also, T cells regulate fibroblast proliferation and apoptosis and differentiation of other cells such as

macrophages during wound healing or lung fibrosis development (Atamas et al. 2003, Naohito et al. 1996).

B-cells can play important roles in the pathogenesis of various autoimmune diseases, e.g. rheumatic arthritis, either by secretion of auto-antibodies or production of proinflammatory cytokines or auto-antigen presentation (Hogan et al. 2010). B-cells can produce a wide spectrum of cytokines under inflammatory conditions, including IL-4, IL-6, TGF-β and IFN-γ (Hogan et al. 2010). B-cells may also play a regulatory role by modulating the production of IL-10; an anti-inflammatory cytokine which can suppres harmful immune responses resulting in the prevention of innate cell mediated inflammatory responses (Mauri et al. 2003; Hogan et al. 2010). The depletion of B- cells in the tight-skin mouse model for systemic sclerosis results in reducing of skin fibrosis and autoimmunity (Hasegawa et al. 2006).

1.1.1.1.2. Mediators of fibrotic alterations

- Cytokines and chemokines:

During development of wound healing and lung fibrosis, inflammatory reactions in the lung are orchestrated by inflammatory and stationary cells as well as inflammatory cytokines and chemokines secreted by them (Commins et al. 2010; Wick et al. 2009; Robert et al. 2011). Cytokines are small secreted cell-signalling proteins with paracrine, autocrine and even endocrine functions (Commins et al. 2010). Chemokines are an important subgroup of cytokines (Commins et al. 2010). Cytokines and chemokines are essential mediators of inflammation and immunity during development of lung fibrosis (Chung 2001; Wynn 2011; Wick et al. 2009; Robert et al. 2011; Jack et al. 1993).

Tumor necrosis factor (TNF), interleukin-1 (IL-1), interleukin-6 (IL-6) and interleukin-13 (IL-13) are proinflammatory cytokines, that promote inflammation by activating a variety of inflammatory mediators that are crucial in the cascade of events leading to tissue inflammation (Borish and Steinke 2003; Chung 2001). These cytokines promote the matrix

metalloproteinase (MMP) secretion and the proliferation of fibroblasts. They are mostly secreted by macrophages (Wynn 2011; Borish and Steinke 2003; Chung 2001).

TNF-α is an important mediator of innate immunity. It has direct cytotoxic effects and induces further immune responses (Chung 2001). TNF-α stimulates the expression of other proinflammatory mediators, leukocyte adhesion factors, and CCL (CC chemokine ligand) (Wynn 2011; Chung 2001). Furthermore, TNF-α enhances resolution of inflammation by promoting of apoptosis of neutrophils (Emmet et al. 2011; Kettritz et al. 2000). TNF-α inhibitors are mainly used in the treatment of rheumatoid arthritis and other auto-immune diseases (Feldmann & Maini 2003; Meyer 2008). Further, TNFα increases MMPs synthesis in myofibroblasts regulating thus matrix proteins degradation, such as collagen, during fibrosis (Debra et al. 1996).

IL-1 is an important cytokine involved in acute and chronic inflammation, and it is involved in various disorders of the lung (Kolb et al. 2001). IL-1 induces the activation of ROS-expressing neutrophils, which can further damage epithelial cells (Wynn 2011; Kolb et al. 2001). IL-1 also promotes production of TGF-β, a major profibrotic cytokine and activator of myofibroblasts (Krieg et al. 2007; Wynn 2011). TGF-β induces the expression of αSMA (alpha smooth muscle actin), which is incorporated into β-actin microfilaments and confers high contractile properties to myofibroblasts (Hinz et al. 2007). IL-6 is an important pleiotropic cytokine with both pro- and anti-inflammatory properties including a wide range of biological activities in immune regulation, hematopoiesis and inflammation (Chi-Hang et al. 2012; Papanicolaou et al. 1998). Many studies have shown that induction of IL-6 requires activation of the NF-kB which is often involved in immune and inflammatory responses (Beg et al. 1996; Papanicolaou et al. 1998; Chi-Hang et al. 2012). In rheumatoid arthritis (RA), IL-6 inhibits the proliferation of fibroblastic synovial cells (Norihiro et al. 2000). Furthermore, IL-6 plays an important role in the development of bleomycin-induced lung inflammation and fibrosis, possibly through up-regulation of CCL3 and TGFβ (Fumitake et al. 2008).

Chemokines have been classified into 4 subfamilies, based on the presence of cysteins at the amino terminal part: CXC (α-chemokines) and CC (β-chemokines), CX3C and C (Commins et al. 2010; Wynn 2008). Among chemokine subfamilies, CXC chemokines can be further subclassified into Glu-Leu-Arg (ELR) + and ELR− CXC chemokines, based on the presence or absence of a tripeptide motif ELR at the NH2 terminus. Characteristic of ELR+ chemokines is their ability to specifically recruit neutrophil polymorphonuclear leucocytes (PMN) into inflamed tissues (Cinzia et al 2006).

Several CC chemokines are produced by activated macrophages and other inflammatory cells which regulate fibrogenesis by controlling myofibroblast recruitment (Wynn 2008; Strieter et al. 2007). CCL3 (macrophage inflammatory protein 1α) and CCL2 (monocyte chemoattractant protein-1), are chemotactic for mononuclear phagocytes, they were identified as profibrotic mediators (Wynn 2008). Macrophages and epithelial cells are believed to be the key sources of CCL3 (Smith et al. 1994). Studies in the bleomycin model of pulmonary fibrosis showed that anti-CCL3 antibodies could significantly reduce the development of fibrosis (Smith et al. 1994; Smith et al. 1995).

-S100A8/A9

S100 proteins compose a family of low molecular weight Ca-binding proteins found in vertebrates (Zimmer et al. 1995; Foell et al. 2004). The name S100 is derived from the fact that these proteins are 100% soluble in ammonium sulfate at normal pH (Zimmer et al. 1995; Foell et al. 2004). The S100 proteins were firstly identified by Moore in 1965 (Foell et al. 2004). They regulate the cytoskeletal metabolism and the oxidant & antioxidant balance (Bargagli et al. 2011). S100 proteins belong to the alarmin family, which are endogenous molecules found at high levels during inflammatory conditions and at sites of inflammation (Chan et al. 2012). S100 proteins are biomarkers for inflammatory disorders, but also act as pro-inflammatory proteins by activating immune and endothelial cells (Bargagli et al. 2011; Foell et al. 2004).

S100A8 and S100A9 are highly expressed by neutrophils, monocytes and activated endothelial and epithelial cells (Ryckman et al. 2003; Bargagli et al. 2011). The “alarmins“ S100A8/A9 have different roles during inflammation. They modulate the pro-inflammatory response by regulating neutrophil adhesion and migration (Chan et al. 2012) but also may as ligands for TLR4 receptor stimulate activation of immune cells (Vogl et al 2007; Nature Medicine). S100A9, also known as calgranulin B, is overexpressed in breast, lung and colorectal cancer cells and in target tisues of many autoimmune inflammatory diseases such as rheumatoid arthritis, juvenile idiopathic arthritis, chronic inflammatory bowel disorder and myositis (Bargagli et al. 2011; Gebhardt et al. 2006). S100A9 has also been associated with the pathogenesis of chronic and acute lung diseases such as cystic fibrosis, chronic obstructive pulmonary disease (COPD), and Acute Respiratory Distress Syndrome (ARDS) (Foell et al. 2004; Bargagli et al. 2011; Lorenz et al. 2008).

-DC-SIGN (CD209)

DC-SIGN (**D**endritic **C**ell-**S**pecific **I**ntercellular adhesion molecule-3-**G**rabbing **N**on-integrin) also known as CD209 (**C**luster of **D**ifferentiation 209) is a protein which is encoded by the CD209 gene in humans (Curtis et al. 1992). CD209 (DC-SIGN) is a C-type lectin receptor present on both macrophages and dendritic cells (Soilleux et al. 2002). DC-SIGN on macrophages binds to mannose type carbohydrates, a class of pathogen associated molecular patterns (PAMPs) commonly found on viruses, bacteria and fungi. This binding activates phagocytosis (McGreal et al. 2006; Cambi and Figdor 2003; McGreal et al. 2005; Kerrigan & Brown 2009). DC-SIGN has also an important role in adhesion and migration of macrophages and dendritic cells during inflammation (McGreal et al. 2005; Cambi and Figdor 2003). Forthermore, DC-SIGN plays an important role in inflammatory response, proliferation and initiating of the immune response (Zhou et al. 2006; van den Berg et al. 2012). The intracellular signaling pathway induced by this C-type lectin modulates the response of other pattern recognition receptors (PRRs), such as TLRs. DC-SIGN activates the serine/threonine

protein kinase RAF1 and there by induces phosphorylation of the NF-*k*B subunit p65 at serine residue 276 (Figure 4) (van den Berg et al. 2012). This signaling pathway leads to the expression of specific cytokines, such as IL-6, which have a role in regulation of immune responses (van den Berg et al. 2012; Zhou et al. 2006).

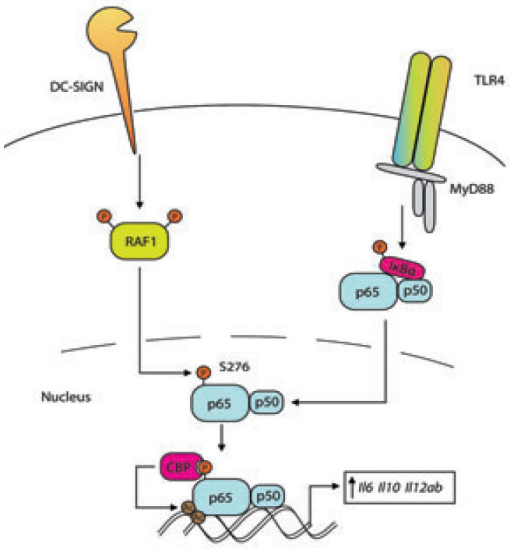

Figure 4: DC-SIGN signaling modulates TLR signaling. DC-SIGN binds ligands such as mycobacteria and HIV-1. DC-SIGN induces RAF1 phosphorylation, which modulates TLR induced NF-κB activation. Upon TLR stimulation the canonical NF-*k*B subunit p65 is released from its inhibitor and translocates to the nucleus. Phosphorylated RAF1 induces p65 phosphorylation at Ser276 that functions as a binding site for the histone acetylase CBP. Acetylation of p65 induces enhanced and prolonged Il6, Il10 and Il12ab transcription (van den Berg et al. 2012).

1.1.1.2. Fibroblast activation stage:

Fibroblast migration, proliferation and activation is stimulated by different inflammatory cytokines, chemokines and growth factors which are secreted by inflammatory cells during development of wound healing and lung fibrosis (Kisseleva & Brenner 2008; Wynn 2011). In the "second" stage of wound healing fibroblasts become activated and converted into myofibroblasts that synthesize and secrete ECM components (Wynn 2011; Kisseleva & Brenner 2008). Myofibroblasts possess ultrastructural features that are intermediate between fibroblasts and smooth muscle cells; they are characterized by high expression of alpha-smooth muscle actin (aSMA) (Hinz et al. 2007; Hinz 2007; Kisseleva & Brenner 2008).

Myofibroblasts are generated during a processes termed epithelial/endothelial-mesenchymal (EMT/EndMT) transition from a variety of sources including resident mesenchymal cells, epithelial and endothelial cells as well as from circulating fibroblast-like cells called fibrocytes that in turn are derived from bone-marrow (stem cells) (Hinz et al. 2007; Krieg et al. 2007). Fibroblasts and myofibroblasts are the cells responsible for the synthesis and secretion of extracellular matrix proteins that are at the core of the fibrotic transformation of the lung (Hinz 2007; Wynn 2011). Myofibroblast interacts with ECM via integrin receptors. This interaction is an important factor for understanding complex events in fibrosis (Eckes et al. 2000).

Myofibroblasts are activated by several growth factors and cytokines. Being activated myofibroblasts synthesize and secrete high amounts of ECM components, including fibronectin, tenascins, collagens as well as matrix metalloproteinases (MMPs) and their inhibitors (Krieg et al. 2007; Wynn 2011). During fibrosis the proliferation of myofibroblasts as well as synthesis of collagens and tissue inhibitors of MMPs (TIMPs) are increased, while myofibroblast apoptosis and MMPs-collagenase expression are decreased (Schuppan et al. 2001). Moreover, myofibroblasts have additional function in ECM contraction, through formation of stress fibers containing smooth muscle actin; myofibroblasts can exert substantial remodeling forces on the granulation tissue (Wynn 2007; Hinz 2007).

1.1.1.3. Matrix remodeling stage:

Tissue remodeling is the final stage of wound healing and lung fibrosis development, in this stage, myofibroblasts promote wound contraction, a process where the edges of the wound migrate toward the center and epithelial/endothelial cells divide and migrate over the temporary matrix to regenerate the damaged tissue (Wynn 2011; Rajendra 1994; William et al. 2007). Fibrosis develops when the wound is severe, the tissue-damaging irritant persists, or when the repair process becomes dysregulated. Thus, many stages in the wound repair process can run abnormal and contribute to scar formation (Razzaque & Taguchi 2003; Wynn 2011). The balance between matrix formation and degradation is disrupted in fibrotic diseases, usually due to the increased production and decreased degradation of extracellular matrix proteins (Razzaque & Taguchi 2003).

The extracellular matrix (ECM) is a complex structural entity surrounding and supporting cells that are found within mammalian tissues (Steven et al. 1997). There are two main forms of ECM; interstitial matrix and basement membrane or basal lamina. Both of them are composed of aggregates of matrix proteins (Murray 2010; Korpos et al. 2010; Steven et al. 1997). The interstitial matrix forms the majority of the connective tissue between cells and acts as scaffold for migrating cells. Basement membranes form sheet-like matrix barriers that separate epithelial cells from underlying mesenchymal cells (Korpos et al. 2010; Murray 2010).

Generally, ECM regulates different cellular functions, such as cell proliferation and differentiation, migration, adhesion, cell metabolism and gene expression. It regulates these functions through signaling via cellular adhesion receptors. Besides this, ECM is also a reservoir for extracellular signaling molecules such as cytokines and growth factors (Rajendra 1994; Steven et al. 1997). Figure 5 shows cell-ECM interactions and that binding of matrix molecules to cell receptors initiates' different cell signaling mechanisms (Steven et al. 1997).

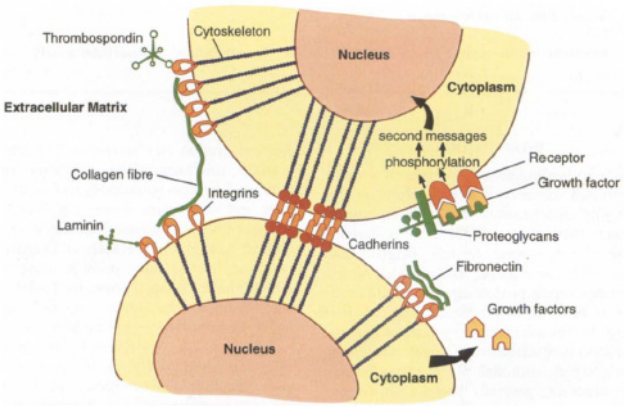

Figure 5: ECM-cell and cell-cell interactions (Steven et al. 1997).

The generation of ECM is predominantly achieved through the production of collagenous and non-collagenous proteins (e.g. fibronectin, laminin and tenacin c), whereas degradation of ECM is predominantly achieved by various proteolytic enzymes, such as matrix metalloproteinases (MMP) (Wynn 2008; Razzaque & Taguchi 2003). In addition, tissue inhibitors of metalloproteinases (TIMPs) also play an active role in matrix remodeling by neutralizing MMP activities (Wynn 2008). These proteins and enzymes are described in more details in following section.

1.1.1.3.1. Extracellular matrix proteins

The matrix proteins play an essential role in tissue injury remodeling and failure in synthesis of these proteins or their deposition might result in fibrosis (Wynn 2011; Rajendra 1994; William et al. 2007). During inflammation, the extracellular matrix (ECM) acts as a scaffold for cell infiltration and as a reservoir for cytokines and growth factors (Steven et al. 1997). ECM compounds such as fibronectin or vitronectin have tri- peptide cell binding sites, Arg-Gly-Asp (RGD), to which integrins bind and represent the majority of integrin adhesive interactions (Shiokawa et al. 1999). Collagens and laminin have their own binding sites for integrins (Calderwood et al. 1997). In addition, some ECM molecules can also directly act as inflammatory stimuli by inducing transcription of proinflammatory genes (Fui et al. 2010). These ECM molecules display a class of endogenous signals or damage-associated molecular

patterns (DAMPs) molecules (Fui et al. 2010). Expression of these molecules is specifically induced upon tissue injury, for example the expression of tenascin-C, biglycan or fibronectin (Midwood et al. 2009; Fui et al. 2010).

-Collagens

Collagens (COLs) are the most abundant proteins found in the animal kingdom. It is the major protein comprising the ECM (Van der Rest & Garrone 1991; Gay & Miller 1979). There are at least 30 different collagen genes dispersed through the human genome (Van der Rest & Garrone 1991). These 30 genes generate proteins that combine in a variety of ways to create over 20 different types of collagen fibrils (Van der Rest & Garrone 1991; Gay & Miller 1979). Types I, II and III COL are the most abundant types in formation of fibrils (Tomoaki et al. 2005; Van der Rest & Garrone 1991). Type IV COL forms a two-dimensional reticulum and is a major component of the basal lamina (Tomoaki et al. 2005; Van der Rest & Garrone 1991). The fundamental higher order structure of COLs is a long and thin diameter rod-like protein (Schuppan et al. 2001).

Collagen type I is the most abundant component of the ECM and is composed of glycine- and prolinerich two-a1(I) and one-a2(I) chains (Ramirez et al. 2006). The pro-COL1A1 and COL1A2 polypeptide chains are synthesized by fibroblasts, osteoblasts or odontoblasts (Ramirez et al. 2006).

Type III collagen is a member of the fibrillar collagen family and is a homotrimer composed of a single α type chain (Tomoaki et al. 2005; Van der Rest & Garrone 1991).Type III COL is a component of the small argyrophilic collagen fibers that characterize reticular connective tissue (Gay & Miller 1979). It can be present in banded collagen fibrils regardless of fibril diameter (Van der Rest & Garrone 1991). Type III COL is co-expressed in most tissues with type I COL and can also form heterotypic fibrils with type I COL (Tomoaki et al. 2005). Studies with monoclonal antibodies suggested that type III COL is along with COL type I a component of straight fibrils (Van der Rest & Garrone 1991; Tomoaki et al. 2005).

-Fibronectin

Fibronectin (FN) is a ubiquitous ECM glycoprotein that is assembled into a fibrillar matrix in all tissues (Purva et al. 2010). FN molecules typically exist as dimers composed of two subunits linked by a disulphide bond: Due to alternative splicing; at least 20 different variants of fibronectin are present in humans (Pankov and Yamada, 2002; Murray 2010). According to its solubility, FN can be subdivided in two broader categories; soluble plasma FN and less-soluble cellular FN (Purva et al. 2010; Murray 2010; Pankov and Yamada, 2002). The basic domain structure of both plasma and cellular FN is homologous and contains RGD (Arg-Gly-Asp) binding sites. These binding sites are responsible for interaction with integrin α5β1 and integrin αvβ3 and are therefore critical for fibronectin-cell interaction (Shiokawa et al. 1999; Murray 2010). FN contributes to the ECM by providing a degree of elasticity following the formation of fibrils (Purva et al. 2010; Murray 2010). FN fibrillogenesis occurs following binding to integrin α5β1 that elicits the formation of a dense network of fibrils on the cell surface (Murray 2010; Wierzbicka-Patynowski and Schwarzbauer 2003).

-Tenascin-C

Tenascins are proinflammatory ECM glycoproteins. Four isoforms have been recognized in vertebrates: tenascin-C, tenascin-X, tenascin-R and tenascin-W (Jones and Jones 2000; Peter & Frederick 2000).

Tenascin-C (TNC) polypeptides form a hexabrachion and were discovered as first of the tenascin family (Peter & Frederick 2000). TNC is secreted by mesenchymal cells and is highly expressed in adult lung parenchyma following acute lung injury (Jones and Jones 2000; Kaarteenaho-Wiik et al. 2001). High TNC levels are also associated with chronic inflammation in auto-immune diseases, such as rheumatoid arthritis and in tumor stroma (Midwood & Orend 2009; Midwood et al. 2009; Fui et al. 2010). Its expression can be modulated by many factors, including growth factors, mechanical stress, inflammatory cytokines and MMPs (Fui et al. 2010).

Several studies have shown that TNC mediates a number of cellular activities. For example, it stimulates the migration and proliferation of cells (Fui et al. 2010). It also interacts with fibronectin (FN), and supports adhesion of a variety of cell types including fibroblasts and endothelial cells (Chang et al. 1995; Maseruka et al. 1997; End et al. 1992; Fui et al. 2010). TNC induces cytokine synthesis in primary human macrophages and synovial fibroblasts via activation of toll-like receptors 4 (TLR4) pattern recognition receptor (Midwood et al. 2009). Also, it can stimulate cytokine and matrix metalloproteinase (MMPs) synthesis in murine synovial fibroblasts via activation of α9 integrins (Kanayama et al. 2009; Fui et al. 2010). Furthermore, TNC induces inflammatory mediators and promote matrix degradation in osteoarthritic cartilage (OA) (Lisha et al. 2011).

1.1.1.3.2. Matrix metalloproteinases and their inhibitors

Matrix metalloproteinases (MMPs) are enzymes that belong to the family of zinc-containing endopeptidases collectively assigned to the metzincin superfamily (Woessner 1994). The metzincin superfamily comprises enzymes with similar metalloproteinase domains; this superfamily is further subdivided into discovered multigene families: astacins, seralysins, adamalysins and MMPs (Overall & Lopez-Otin 2002; Woessner 1994).

MMPs have many roles during development of wound healing or lung fibrosis. MMPs are expressed at very low levels in normal healthy tissues (Nagase et al. 1999). In contrast, MMP expression can be detected in all repair or remodeling processes, in all diseased or inflamed tissues and in all cell types grown in culture (Parks et al. 2004). The production of MMPs and other proteases is described in various cells such as granulocytes, macrophage, epidermal cells and fibroblasts/ myofibroblasts (Parks et al. 2004; Ruiz et al. 2003). MMPs play a major role on cell behaviors such as cell proliferation, migration (adhesion/dispersion), differentiation, and apoptosis (Parks et al. 2004; Overall & Lopez-Otin 2002).

In early stages of fibrosis development, the MMPs regulate the efficiency of leucocytes infiltration and cytokine and chemokine secretion (Dean et al. 2008; Roderick et al. 2006;

Philippe and Claude 2007; Parks et al. 2004). In later stages, MMPs and their inhibitors (including the tissue inhibitors of MMPs (TIMPs)) regulate the collagen turnover and the ECM remodeling (Nagase et al. 1999; Ji Kim et al. 2009; Ruiz et al. 2003). Also, MMPs cleave many other types of peptides and proteins; but they have also many other important functions that may be independent of proteolytic activity (Parks et al. 2004; Nagase et al. 1999).

Human MMPs are classified into six different subgroups: collagenases, gelatinases, stromelysins, matrilysins, membrane type MMPs, and other MMPs (Woesser 1994; Ruiz et al. 2003). Collagenases (MMP-1, MMP-8 and MMP-13) degrade mainly fibrillar collagens, whereas gelatinases (MMP-2 and MMP-9) have, among others, substrate affinity for basement membrane type IV collagen, thus the collagenases and gelatinases play an important role in fibrosis (Ruiz et al. 2003; Ji Kim et al. 2009). Matrilysin (MMP-7) was identified by transcriptional profiling analysis as significantly upregulated in bleomycin-induced lung fibrosis (Zuo et al. 2002).

MMP-12 is mainly produced by macrophages and has been shown to be associated with inflammatory skin diseases, inflammatory respiratory disease, atherosclerosis and cancers (Soazig et al. 2005; Vincent et al. 2009). Furthermore, MMP-12 is an important inflammatory mediator in acute and chronic pulmonary inflammatory diseases, such as pulmonary fibrosis and chronic obstructive pulmonary disease (COPD) (Belvisi et al. 2003; Soazig et al. 2005). The major substrates for MMP-12 are the elastic ECM components such as elastin but MMP-12 can also digest collagen type I, fibronectin and proteoglycans (Vincent et al. 2009). In addition to that, MMP-12 regulates the cytokines and chemokines function. For example, it specifically cleaves human ELR+CXC chemokines (CXCL1, -2, -3, -5, and -8) at Glu-Leu-Arg (ELR) motif, which results in lose of chemotactic activity (Dean et al. 2008). Furthermore, MMP-12 processes and inactivates monocyte chemotactic proteins CCL2, -7, -8, and -13 during acute inflammation (Dean et al. 2008) and is, thus, an important component in ceasing the acute inflammation phase during wound healing.

Generally, MMPs are secreted into the extracellular space or anchored to the plasma membrane as inactive proenzymes (Bode et al. 1999; Nagase et al. 1999), thus, they require

activation. In vivo, MMPs are generally activated by other proteinases and in vitro, MMPs are activated by chemical and physical agents such as aminophenylmercuric acetate (APMA), low pH and heat treatment (Parks et al. 2004; Visse & Nagase 2003). The catalytic activity of MMPs is tightly regulated at multiple levels including gene expression (transcription and translation), compartmentalization and inhibition by their endogenous inhibitors and the tissue inhibitors of metalloproteinases (TIMPs) (Nkyimbeng Takwi 2008; Visse & Nagase 2003; Nagase et al. 1999).

Tissue inhibitors of metalloproteinases (TIMPs) are specific regulators of MMP activity that bind and inhibit their specific active MMPs (Visse & Nagase 2003; Nkyimbeng Takwi 2008). In vertebrates the TIMP family consists of four members, TIMP-1, TIMP-2, TIMP-3, and TIMP-4 (Nkyimbeng Takwi 2008; Brew et al. 2000). Their expression is regulated during development and tissue remodeling. TIMPs have been shown to bind with high degree of specificity to the proenzyme forms of MMP-2 and MMP-9, an interaction that provides an extra level of MMP activity regulation (Nkyimbeng Takwi 2008; Olson et al. 1997). Moreover, TIMP-1 and TIMP-2 are capable to inhibit the activities of all known MMPs and playa key role in maintaining the balance between extracellular matrix deposition and degradation in different physiological processes (Brew et al. 2000; Nkyimbeng Takwi 2008; Visse & Nagase 2003).

1.1.6. Animal models for lung fibrosis

To study the role of FHL2 in development of lung fibrosis, we chose the bleomycin-mediated lung fibrosis model, because bleomycin-induced fibrosis is easily reproducible in different species of mammals (e.g., mouse, rat, dog and pig) and is clinically relevant. It can be delivered intratracheally, intravenously, intraperitoneally or intranasally, which results in development of fibrosis within a time frame between 14-28 days (Walters et al. 2008; Bethany 2008; Moore & Hogaboam 2008).

Bleomycin (BLM) is a glycopeptide antibiotic produced by the bacterium *Streptomyces verticillus* and was discovered in 1966, by Homao Umezawa (Umezawa et al. 1966). The commercially available form of BLM consists of predominantly BLM- A2 (55-70%) and BLM- B2 (25-32%) and the Figure 6 show the chemical structure of bleomycin (Hay et al. 1991). BLM is a cytostatic drug commonly employed in the treatment of cancer and Hodgkin`s lymphoma (Benntt and Reich 1979). As a side effect of its therapeutic use, bleomycin induces in some patients a chronic pulmonary inflammation that may progress into fibrosis (Mouratis & Aidinis 2011; Hay et al. 1991). The BLM molecule has two main structural components; a bithiazole component which partially intercalates into the DNA helix, and pyrimidine and imidazole components which bind iron and oxygen forming an activated complex capable of releasing damaging oxidants in close proximity to the polynucleotide chains of DNA (Figure 6) (Hay et al. 1991). BLM is also able to cause cell damage independent from its effect on DNA by inducing lipid peroxidation (Breuer et al. 1995; Bethany 2008; Hay et al. 1991). Also, BLM induces lung epithelial and endothelial cells apoptosis which is a key event in progression of lung fibrosis (Mungunsukh et al. 2010; Fridlender et al. 2007). The side effect of BLM is mostly basen on augmented concentration of reactive oxygen species, decrease in nicotinamide adenine dinucleotide (NAD) and adenosine triphosphate (ATP), and overproduction of mature collagen fibrils (Breuer et al. 1995; Bethany 2008).

By intratracheal injection, the BLM causes a lung injury, which becomes manifested in alveolar cells damage, interstitial edema and influx of inflammatory cells. This may lead to

development of lung fibrosis, characterized by activation of fibroblast and enhanced deposition of matrix proteins (Hay et al. 1991; Nuno et al. 1998; Marios & Vassilis 2011).

The mouse lung fibrosis resembles the features of the human idiopathic lung fibrosis, but in contrast to the human lung fibrosis, the bleomycin-induced lung fibrosis in mice is transient (Degryse et al. 2011).

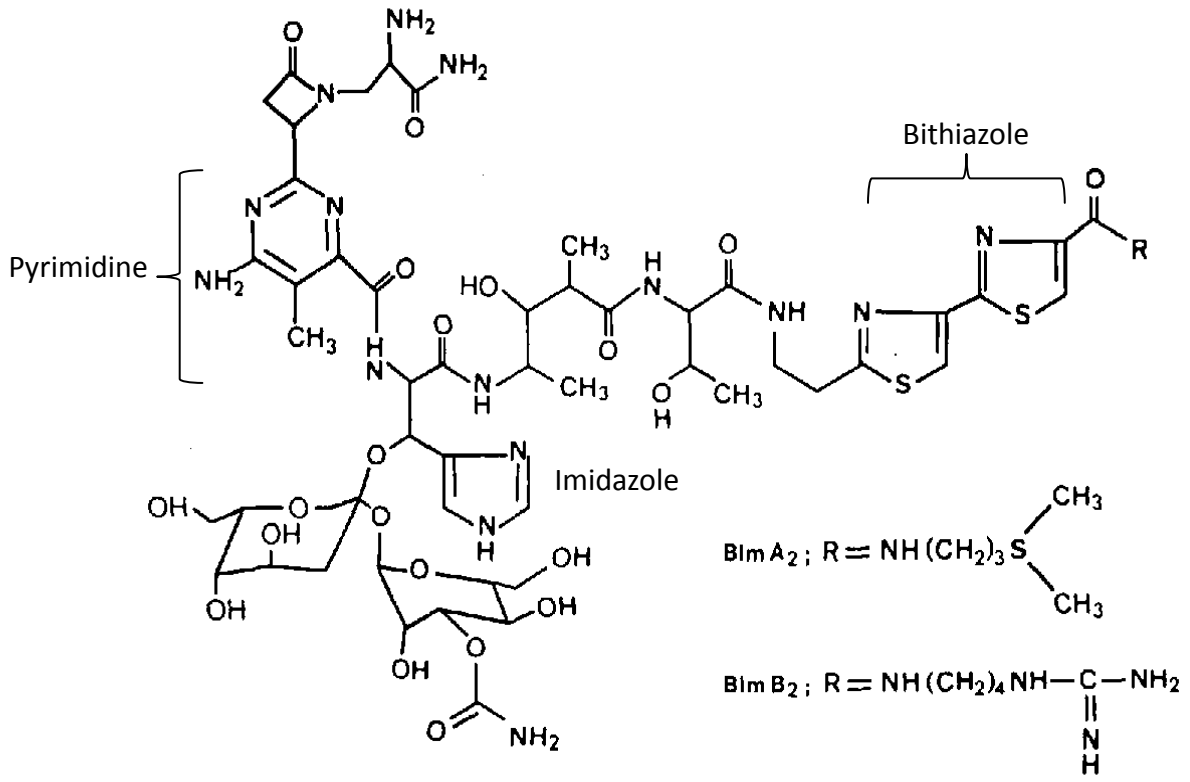

Figure 6: The chemical structure of bleomycin and its active sites (bithiazole ring and pyrimidine and imidazole structures) (Hay et al. 1991).

1.2. The LIM-only protein “FHL2”

1.2.1. LIM proteins

FHL2 is an adaptor protein and belongs to the group of LIM proteins that regulates diverse processes in the cell. These include; the control of cell differentiation and growth. These proteins can either associate with the actin cytoskeleton or could be responsible for the transcription. LIM proteins make are able to interact with numerous cellular proteins, allowing formation of protein clusters with different complexity and specific activity (Bach 2000; Henke 2007; Kadrmas and Beckerle 2004; Gabriel et al. 2009).

The nomenclature of LIM derives from **L**IN-11 (C. elegance-linage protein), **I**SL-1 (rat insulin enhancer binding protein) and **M**EC-3 (C. elegance-linage transcription factor) (Nordhoff et al. 2012). A LIM domain is composed of two finger motifs, which bind two zinc ions and mediate interactions with other proteins (Figure 7A) (Bach 2000; Dawid et al. 1998; Kadrmas and Beckerle 2004; Meyer 2008). Depending on the presence of additional motifs, LIM proteins are grouped into four main families: nuclear-only, LIM-only, LIM-actin associated and LIM-catalytic proteins (Kadrmas and Beckerle 2004; Gabriel et al. 2009).

FHL proteins belong to the subset of the LIM-only proteins because they contain only LIM domains. FHL proteins have a certain feature in their structural design: they contain aspecific number of LIM domains, namely, four-and-half LIM domains (FHL). Thus, they consist of four double and one single zinc finger and therefore, they can bind 9 zinc ions totally, see Figure 7B (Morgan and Madgwick 1996; Genini et al.1997).

A)

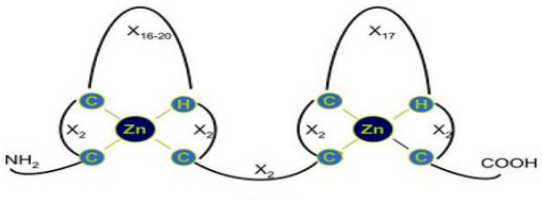

B)

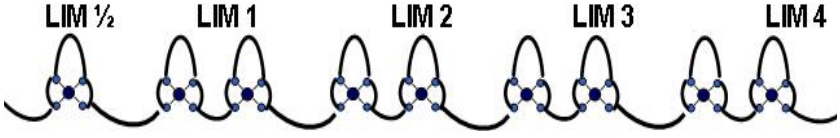

Figure 7: (A) Schematized structure of a LIM domain: the double zinc finger motif **(B)** Structure of FHL2 (Four-and-half LIM domains). (Zn: zinc, C: cysteine, H: histidine, X: any amino acid) (Meyer 2008).

1.2.2. FHL subtypes

There are several subtypes of FHL proteins, they include FHL1, FHL2, FHL3, FHL4 and ACT (Activator of CREM in testis), which are similar in their structural design (Morgan and Whawall 2000). The tissue-specific occurrence of FHL proteins and ACT is different. FHL1 is the only protein of the FHL family with a relatively ubiquitous distribution in human tissues (Morgan and Magdwick 1999a). FHL2 is found to be particularly strong expressed in the heart and skeletal muscles and to a less extent in the ovary, testis, prostate and other endocrine structures (pituitary gland, adrenal medulla) (Chan et al. 1998; Fimia et al. 2000; Genini et al. 1997; Muller et al. 2000; Henke 2007; Scholl et al. 2000; Johannessen et al. 2006). FHL3 is strongly expressed in heart and skeletal muscles, but only weak in the ovary, spleen and adrenal gland (Morgan and Madgwick 1999a; Henke 2007). FHL4 and ACT are synthesized specifically in testis (Morgan and Madgwick 1999b).

1.2.3. Genetic coding and structure of FHL2

The human FHL2 gene was discovered in 1997 on the chromosomal region 2q12-q13 and consists of 7 exons (Figure 8) (Chan et al. 1998). By comparing this gene sequence with the nucleotide database of the Gene Bank, it was found that FHL2 is identical with two other known proteins. One of them, it is SLIM-3 (skeletal muscle LIM-protein 3), which showed a particularly strong expression in the skeletal muscles (Morgan and Madgwick 1996). The other molecule with a homologous structure to FHL2 was DRAL (down regulated in rhabdomyosarkoma LIM protein) (Genini et al. 1997). Actually, SLIM-3, DRAL and FHL2 is the same protein. Different researches described it and gave the proteins different names (Johannessen et al. 2006; Genini et al. 1997; Henke 2007; Morgan and Madgwick 1996).

The FHL2 gene is transcribed into a 1.5 kb RNA molecule, which is translated into a protein with 279 amino acids (Johannessen et al. 2006). The comparison of the amino acid sequence between FHL2 and the other proteins of the FHL family, including ACT, shows that it is not only similar in the structural design, but also in the sequence of their gene, which suggests a common genetic ancestry (Johannessen et al. 2006). Thus, human FHL2 protein is 47.9%

identical with human FHL1, 51.8% with human FHL3, 47.1% with mouse FHL3 and 58.5% with ACT (Morgan and Whawell 2000; Johannessen et al. 2006).

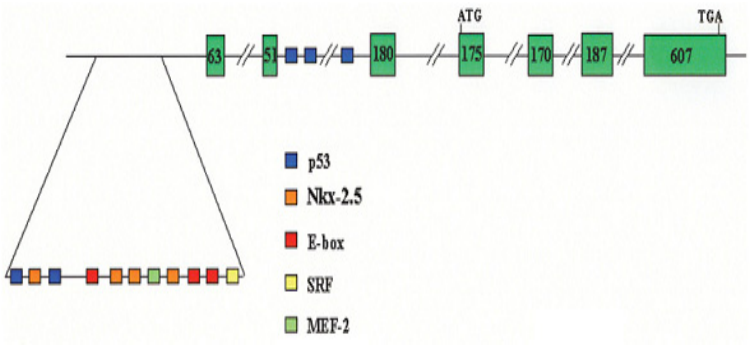

Figure 8: Schematic representation of the fhl2. Exons are depicted with boxes bound to each other by interrupted lines representing the introns. Numbers in the boxes indicate the size of the exons in bp. The smaller boxes in front of exon 1 and intron 2 illustrate the presence of putative transcription factor binding sites (Johannessen et al. 2006).

1.2.4. Expression and cellular localization of FHL2

As already mentioned, FHL2 shows the highest expression in heart cells, but can also be find in in different other cell types, including myoblasts, prostate epithelial cells, rhabdomyosarcoma cells, fibroblasts and several types of tumor cells (Gabriel et al. 2009; Gabriel et al. 2004; Wixler et al. 2000). The LIM-only protein FHL2 is involved in a wide range of cellular processes, which is reflected by its different localization in the cell. First, it was found to be localized at the cell membrane where it participates in cell adhesion, cell identity and cell differentiation (Muller et al. 2000; Wixler et al. 2000). Second, FHL2 regulates signal transduction by interaction with various cytoplasmatic and cytoskeletal proteins (Muller et al. 2000; Wixler et al. 2007; Park et al, 2008). Third, FHL2 was found in the nucleus, where it works as a transcriptional cofactor selectively stimulating expression of specific DNA segments (Du et al. 2002; Labalette et al. 2004; Li et al. 2001; Muller et al. 2002).

The molecular mass of the FHL2 protein is 32 kDa which is well below the cut-off (50-kDa) for the active transport through the nuclear pores, which may explain the lack of an apparent

nuclear localization signal and/or nuclear export signal but could lead to passive shuttling between the cytoplasm and the nucleus (Wixler et al. 2000; Wixler et al. 1999; Samsonet al. 2004).

The localization and expression of FHL2 is controlled by various stimuli. For example; pro-fibrotic cytokines (such as TGFβ) and S1P (*sphingosine-1-phosphate*) induce its expression, while pro-inflammatory cytokines TNFα and IL-1 downregulate it (Joos et al. 2008; Phillipar et al. 2004; Meyer 2008).

1.2.5. Function of FHL2 and its interaction partners

FHL2 is able to interact with many different proteins and depending on the interaction partner, different LIM-domains are involved. FHL2 can interact with more than 50 different proteins (Johannessen et al. 2006).

FHL2 was found to play a role in the regulation of signal transduction, gene expression and cytoskeleton modulation, as well as in cell adhesion, survival and mobility (Bai et al. 2005; Muller et al. 2002; Johannessen et al. 2006).

FHL2 interacts with the cytoplasmic part of different α-integrin chains like, α3A, α3B, α7A and α7B subunits (Samson et al. 2004; Wixler et al. 2000; Wixler et al. 1999), but also with several β subunits (Samson et al. 2004; Wixler et al.2000). Further, FHL2 interacts with various structural proteins of the cytoskeleton, such as actin, myosin, titin, and vinculin, suggesting a role of FHL2 in the organization of the cytoskeleton (Coghill et al. 2003; El Mourabit et al. 2004; McGrath et al. 2006; Johannesson et al. 2006).

Further studies showed that FHL2 is involved as an adapter protein in the assembly of focal contacts and that it fulfills this function through interaction with different integrins and FAK (Park et al. 2008). Furthermore, FHL2 controls cell migration and besides this the development of focal contacts and the assembly of extracellular matrix proteins (Wixler at al, 2007; Park et al, 2008). The interaction between FHL2 and ERK lead to prevention of passage of ERK into the nucleus, which in turn affects ERK-dependent gene expression (Purcell et al. 2004).

The function of FHL2 as a cofactor of transcription may vary according to interaction partners and cell type, because FHL2 can act both as activator and repressor (Johannessen et al. 2006). As activator, FHL2 selectively interacts with the androgen receptor (AR) and acts as a coactivator for the expression of AR-specific genes (Muller et al. 2000). FHL2 also acts as a coactivator of the CREB-mediated gene expression (Fimia et al. 2000; Johannessen et al. 2007). Further, FHL2 directly binds to β-catenin and acts as a regulator of β-catenin-Lef/Tcf-transcription complexes (Martin et al, 2002; Labalette et al. 2004; Wei et al. 2003). In this respect, FHL2, however, shows a dual function, which is cell type-dependent. It inhibits the Lef /Tcf-driven transcription in myoblasts, but increased it in epithelial cells (Martin et al. 2002; Chen et al. 2003).

FHL2 has been shown to interact with the proteins of the AP-1 complex, which is a heterodimer of protonkogenes c-Jun and Fos and one of the key transcription factors in MMP expression (Morlon and Sassone-Corsi 2003; Martin et al. 2007). Furthermore, the FHL2 deficiency results in increased translocation of p65 to the nucleus, as well as in increased transcription of NF-*k*B-dependent genes, assuming that it regulates the activity of the NF-*k*B pathway (Bai et al. 2005).

1.2.6. FHL2 is an important mediator in inflammation, wound healing and fibrosis

Inflammation is always a consequence of tissue injuryand results either in wound healing or fibrotic disease (Wynn 2011; Pottier et al. 2007). The latter is characterized by migration of immune-inflammatory cells, activation of fibroblasts and dysregulated synthesis of extracellular matrix proteins (Wynn 2011; Razzaque & Taguchi 2003). FHL2 is highly expressed in activated fibroblasts and shuttles between the cell membrane and nucleus playing an important role during development of the disease (Muller et al. 2002; Johannessen et al. 2006).

In inflammation, FHL2 is an important regulator of the innate cellular immune response to influenza A virus (IAV) infection (Nordhoff et al. 2012). Also, FHL2 promotes epithelial-mesenchymal transition in colon cancer (Wenjing et al. 2010). Konig and others showed that FHL2 is an important regulator of dendritic cell (DCs) migration towards the chemotactic

factor CCL19 (Konig et al. 2010). The LIM-only protein FHL2 regulates interleukin-6 expression through p38MAPK mediated NF-*k*B pathway in muscle cells, the pleiotropic cytokine that play an important role in inflammatory response (Chi-Hang et al. 2012). Through association with proteins of the TRAF (tumour necrosis factor receptor-associated factor) family FHL2 sequesters TRAF6 from RANK receptor in osteoclasts, inhibiting activation of the NF-*k*B pathway and stimulating bone resorption (Bai et al. 2005). Also, FHL2 has a role in the limitation of cytokine- induced MMP expression and constitutes an important regulator of inflammatory tissue damage in arthritis (Meyer 2008).

Fhl2- deficient mice revealed a delayed skin wound healing, reduced migration of mesenchymal precursor cells, reduced expression of α- smooth muscle actin (α-SMA), and impaired wound contraction (Wixler et al. 2007). Fhl2 is strongly up-regulated in α-SMA positive mesenchymal cells of wounded skin and acts there as a coactivator of serum response factor-mediated α-SMA expression. In addition to the support of the aSMA-mediated myofibroblast contraction, Fhl2 also influences the migration capability of fibroblasts, which has to entry the wound area for replacing the clot and forming the granulation tissue (Wixler et al. 2007).

During cell adhesion and ECM assembly, FHL2 interacts with several α- and β- integrins, as well as with FAK and α-actinin regulating formation of focal adhesions sites and the capability of cells to generate mechanical forces (Wixler et al. 2000). Inactivation of FHL2 shows impaired focal adhesion clustering, a less-organized cytoskeleton, reduced Rac1 activation, lowered cell motility, and impaired ECM assembly (Park et al. 2008; Wixler et al. 2000). Deficiency of FHL2 also results in enhanced FAK phosphorylation (Y86 & Tyr925), enhanced integrin-dependent activation of Ras-Raf-MEK-ERK pathway, less bundled stress fibers and reduced contraction of collagen matrices (Wixler et al. 2007; Park et al. 2008).

In additional to its role in regulation of the MAP kinase ERK signaling pathway, FHL2 is also involved in regulation of NF-*kB* pathway and p38 MAP kinase signaling cascades, which in turn play a role in development of fibrotic disease (Bai et al. 2005; Muller et al. 2002).

Further, FHL2 upregulates as a cofactor of transcription the expression of aSMA and some matrix proteins, but inhibits the expression of matrixmetalloproteinases-1, -3 and -13 (MMP) (Kirfel et al. 2008; Philippar et al. 2004; Meyer, 2008). FHL2 may act as a cofactor of Jun and Fos that are known as transcription factors of several cytokines (such as TNF-α and IL-2) and collagenases MMP-1(Morlon and Sassone-Corsi 2003).

Aims of the thesis:

Lung fibrosis is a progressive fibrosing disease of unknown aetiology. It causes scarring of alveolar compartments of the lung where gas exchange occurs and results in tissue damage. It is characterized by activation of tissue fibroblasts and deregulated synthesis of extracellular matrix proteins. Available data increasingly indicate that chronic inflammation and aberrant wound healing play an important role in the development of the disease.

FHL2 (four-and-a-half LIM domain protein 2) is a scaffolding protein that is able to interact with numerous membranes, cytosolic and nuclear proteins. By formation of a protein complex with integrins and focal adhesion kinase, FHL2 supports clustering of integrins and integrin-driven assembly of matrix proteins. By interaction with cytosolic proteins FHL2 is involved in regulation of NF-*k*B and MAPK signalling cascades. Besides modulating signalling molecules, FHL2 shuttles between cytosol and nucleus, regulating as a cofactor of transcription the expression of aSMA and some matrix proteins, but inhibiting the expression of matrix metalloproteinases. During skin wound healing FHL2 is upregulated in activated fibroblasts, but only transiently. Pro-fibrotic cytokines, such as TGFβ and S1-P (*sphingosine 1-phosphate*) induce its expression, while the pro-inflammatory cytokine IL-1 downregulates the gene.

In this study we aimed to define the role of the FHL2 protein in fibrotic alterations. We chose the BLM-induced lung fibrosis, which is the best studied animal model for pulmonary fibrosis yet and compared the development of lung fibrosis between FHL2-WT and FHL2-KO mice.

2. Materials and methods

2.1. Materials

2.1.1. Chemicals materials

Table 1:

Material	**Company**
Acrylamide / bisacrylamide 30%	Carl Roth, Karlsruhe, Germany
Adenosine triphosphate (ATP)	Carl Roth, Karlsruhe, Germany
Agar	Oxoid, Hampshire, United Kingdom
Ammonium peroxodisulfate (APS)	Carl Roth, Karlsruhe, Germany
Bromophenol blue	Carl Roth, Karlsruhe, Germany
Chloroform	Sigma; Germany
Dithiothreitol (DTT)	Carl Roth, Karlsruhe, Germany
Ethanol	Carl Roth, Karlsruhe, Germany
Ethylenediaminetetra acetic acid (EDTA)	Carl Roth GmbH & Co., Germany
Glycerol	Carl Roth, Karlsruhe, Germany
Glycin	Carl Roth, Karlsruhe, Germany
H_2O_2	Merck, Darmstadt, Germany
KH2PO4	Carl Roth GmbH & Co., Germany
Leupeptin	Sigma-Aldrich, Munich, Germany
Luciferin	Applichem, Darmstadt, Germany
Luminol	Carl Roth, Karlsruhe, Germany
Magnesium acetate	Carl Roth, Karlsruhe, Germany
Methanol	Carl Roth, Karlsruhe, Germany
$MgCl_2$	Carl Roth, Karlsruhe, Germany
Non-fat dried milk powder blotting grade	Applichem, Darmstadt, Germany
NP-40 (IgePal)	Carl Roth, Karlsruhe, Germany
P-coumaric acid	Sigma-Aldrich, Munich, Germany
Pepton	Carl Roth GmbH & Co., Germany
Ponceau S red	Carl Roth GmbH & Co., Germany
2-Propanol	Carl Roth, Karlsruhe, Germany

Sodium Chloride (NaCl)	Carl Roth, Karlsruhe, Germany
Sodium deoxycholate	Carl Roth, Karlsruhe, Germany
Sodium dodecylsulfat (SDS)	Carl Roth, Karlsruhe, Germany
Sodium glycerophosphate	Sigma-Aldrich, Munich, Germany
Sodium pyrophosphate	Sigma-Aldrich, Munich, Germany
Sodium vanadate	Carl Roth GmbH & Co., Germany
Sodium-MES	Carl Roth, Karlsruhe, Germany
TEMED	Carl Roth, Karlsruhe, Germany
TRIS-HCl	Carl Roth GmbH & Co., Germany
Triton-X-100	Sigma-Aldrich, St.Loius, MO, USA
Trizol reagent	Life technologies, USA
β-mercaptoethanol	Carl Roth, Karlsruhe, Germany

2.1.2. Buffer and solutions

Triton lysis buffer:

Tris-HCl pH 7.4	20 mM	NaCl	137 mM
$MgCl_2$	10 mM	Triton X-100	1%
Glycerol	10%	EDTA pH8	2 mM
Sodium glycerophosphate	50 mM	Sodium pyrophosphate	20 mM
Aprotinin	5mg/ml	Leupeptin	5 mg/ml
Pefablock	200 mM	Sodium ortho-vanadate)	2 mM

RIPA lysis buffer:

Tris-HCl pH8	25 mM	NaCl	137 mM
Glycerol	10%	Sodium dodecylsulfat (SDS)	0.1% Sodium
deoxycholate	0.5%	NP-40 (IgePal)	1% EDTA
Aprotinin	5mg/ml	Leupeptin	5 mg/ml
Pefablock	200 mM	Sodium ortho-vanadate)	2 mM

SDS-PAGE sample buffer (4x Laemmli)

1M Tris / HCl pH 6.8	10 ml	β-mercaptoethanol	5 ml
87% Glycerol	23 ml	Sodium dodecoelsulfat (SDS)	5 g
2% bromophenol blue	2.5 ml	1M EDTA	0.2 ml
d. H2O	ad 50 ml		

SDS-PAGE separating gel:

Tris-HCL pH 8.9	370mM	Sodium dodecylsulfat (SDS)	0.1%
APS	0.1%	TEMED	0.02%
Acrylamid/bisacrylamid	7.5-15%		

SDS-PAGE stacking gel:

Tris-HCL pH 6.8	178mM	Sodium dodecylsulfat (SDS)	0.1%
APS	0.1%	TEMED	1%
Acrylamid/bisacrylamid	4.3%		

SDS-PAGE running buffer:

Tris-HCL pH8.4	25 mM	Glycine	250 mM
Sodium dodecoelsulfat (SDS)	0.1%		

Ponceau S reagent

Ponceau S	2%	Trichloroacetic TCA	3%

Transfer buffer for western blots (blotting buffer):

Tris-HCL pH8.4	25 mM	Glycine	192 mM
Methanol	10%		

ECL detection reagent

1M Tris / HCl pH 8.5	2µl	250 mM Luminol	200 µl
90 mM p-coumaric acid	80µl	H2O	ad 20 ml
35% H_2O_2	6.1 µl ad freshly		

Stripping puffer for western blotting membranes:

Tris / HCl pH 6.8	62.5 mM	β-mercaptoethanol	100 mM
Sodium dodecoelsulfat (SDS)	2%		

TBS- Triton X-100 buffer (20x):

Tris-HCl pH 7.6	50 mM	NaCl	155 mM
Triton X-100	0.2%		

Luciferase harvesting buffer:

Sodium-MES pH7.8	50 mM	Tris-HCL pH7.8	50 mM
DTT	1 mM	Triton X-100	0.2%

Luciferase assay buffer:

Sodium-MES pH7.8	125 mM	Tris-HCL pH7.8	125 mM
Magnesium acetate	25 mM	ATP	49 mM

Luciferin solution:

Luciferin	0.95 mM	KH2PO4 pH7.8	5 mM

Freezing medium of eukaryotic cells

D-MEM high glucose	80%	FCS	10%
DMSO	10%		

LB-medium:

Pepton	1% (w/v)	yeast extract	0.5% (w/v)
NaCL	1% (w/v)		

LB-Amp-medium:

LB-Medium		Ampicillin	100 µg/ml

LB-Agar-platten:

LB-Medium		Agar	1.5 % (w/v)

Paraformaldehyde (PFA 4%):

For preparation of a 20% stock solution of paraformaldehyde (PFA), 20g of PFA was added to 80 ml of PBS. Then, 2µl of 5N NaOH per 1ml of PBS was added and heating at 65 °C for approx 15-20 min until the granules fully dissolved and the solution became translucent. Finally, the solution was filtered and stored at -20 °C. For 4% PFA, the stock solution was dilutied by PBS.

2.1.3. Animal injection and histological materials

Table 2:

Material / Substance	**Company**
AZAN trichrome	Roth, Karlsruhe, Germany
Cover slips 24x36mm	VWR, Menzel, Germany
Diethyl ether (99.5%)	Roth, Karlsruhe, Germany
Eosin Y alcoholic solution	Roth, Karlsruhe, Germany
Formaldehyde alcohol free ≥37%	Roth, Karlsruhe, Germany
Histological glass slides Superfrost Plus®	Thermo scientific, Germany
Hydrogen peroxide 30% pro analysi	Merck Darmstadt, Germany
Isopropanol (99.8%)	Roth, Karlsruhe, Germany
Mayer's Hematoxylin solution	Roth, Karlsruhe, Germany
Needles 20G (0.9mm x 25mm)	BD Biosciences, USA
Paraffin	Allegiance Health Care, Corp. IL, U.S.A
Paraffin embedding medium Paraplast Plus®	Microm international GmbH, Germany
Roti-Histol (Xylolersatz)	Roth, Karlsruhe, Germany
Surgical materials (e.g. scissors, scalpel and tongs)	FEATHER, Japan
Syringes 1ml, 5ml, 10ml Inject Luer®	BD Biosciences, USA
Tissue-Tek Glas mounting medium	SAKURA; Germany
Universal-embedding cassettes y	GML alfaplast, Germany

Table 3: ***Injection solutions***

Solution/ Substance	**Company**
Bleomycin sulphate ®	Sigma-Aldrich, St.Loius, MO, USA
Clodronate liposomes	Sigma-Aldrich, USA
Control liposomes (PBS)	Sigma-Aldrich, USA
Ketamin 10%	CEVA- Sante animale, Germany
Phosphate buffered saline (PBS)	Baxter S.A., München, Germany
Starch4%	REWE Market, Germany
Xylazin 2%	CEVA- Sante animale, Germany

2.1.4. Biological materials

2.1.4.1. Cell culture materials

- Eukaryotic cells:

- HeLa cells: human epithelial cell line derived from a cervical cancer
- HEK209 cells: human embryonic kidney cell line
- Primary fibroblasts from wild-type mice
- Primary macrophages from FHL2-deficient and wild-type mice

- Bacterial strains:

- Escherichia coli DH5a: for cloning / propagation of plasmid DNA (Grant et al., 1990). Genotype: F-endA1 hsdR17 (rm-, mk +) supE44 thi-1 α-recA1 gyrA96 relA1 Deor D (lacZYA-argF) U169 α80dlacZαM15

- Plasmid vectors and promoters

- pCS2+MT: eukaryotic expression vector for the expression of myc-tagged proteins 5x/6x (Wixler et al., 2000)
- pCS2+MT/ FHL2: eukaryotic expression vector for expression of myc-tagged FHL2 (Wixler; IMV, Muenster, Germany)

-The human TNC promoter comprised a 2000 bp long sequence including the TATA box and the first 83 bp of the first exon.

- siRNAs

- siFHL2: sequence (5` → 3` CAACGACUGCUUUAACUGU); Eurofins MWG Operon, Germany.

Table 4: ***Cell culture media, reagents and supplements***

Media / Supplements	**Company**
Ampicillin- antibiotic	Sigma-Aldrich, Germany
Bovine serum albumin (BSA) 35%	MP Biomedicals, Heidelberg, Germany
Dimethyl sulfoxide (DMSO)	Sigma-Aldrich, Munich, Germany
D-MEM high glucose	PAA laboratories, Austria
Fetal Calf Serum (FCS)	Biochrom GmbH, Berlin, Germany
Gentamicin- antibiotic	PAA laboratories, Austria
HiPerFect Transfection	Qiagen: Roche, Mannheim
Lipopolysaccharide(LPS)	Sigma-Aldrich, Germany
Opti-MEM	Gibco Invitrogen, Darmstadt, Germany
Penicillin/ streptomycin100x	PAA laboratories, Austria
Polyethylenimine (PEI)	Sigma-Aldrich, Germany
RPMI 1640	PAA laboratories, Austria
Sodium hydrogen carbonate	Gibco Invitrogen, Darmstadt, Germany
Transformal growth factor-beta (TGF-β)	R & D Systems GmbH, Wiesbaden-Engelstedt
Trypan blue solution	Sigma-Aldrich, Germany
Trypsin-EDTA10x	PAA laboratories, Austria
Tumor necrosis factor-alpha (TNFα)	Sigma-Aldrich, Germany

2.1.4.2. Primers for RT-PCR

The primers used were assigned using the Universal Probe Library Assay Design Center at www.roche-applied-science.com/sis.

Table 5:

cDNA	**Primer: 5` → 3`** **(F= Forward primer, R= Reverse primer)**	**probe Nr.**
Mouse-GAPDH	F: gtccaccagcctgttgctgta R: cccactcttccaccttcgatg	80
Human-GAPDH	F: gcatcctgggctacactgag R: tgctgtagccaaattcgttg	

cDNA	**Primer: 5` → 3`** **(F= Forward primer, R= Reverse primer)**	**probe Nr.**
Mouse-FHL2	F: tgcgtgcagtgcaaaaag R: tgtgcacacaaagcattcct	32
Human-FHL2	F: gtgcaccaaccccatcag R: caccagtgagagggagcact	59
Mouse-TNC	F: gggctatagaacaccgatgc R: catttaagtttccaatttcaggttc	76
Mouse-MMP12	F: ttgtggataaacactactggaggt R: aaatcagcttggggtaagca	51
Mouse-CD209a	F: accaagaactgacccagttga R: cttggaagtgcgtccagtc	51
Mouse-IL-6	F: tgagatctactcggcaaacctgtg R: cttcgtagagaacaacataagtcagatacc	SYBR Green
Mouse-TNFα	F: tcttctcattcctgcttgtgg R: ggtctgggccatagaactga	49
Mouse-TGFβ	F: tggagcaacatgtggaactc R: cagcagccggttaccaag	72

2.1.4.3. Antibodies and enzymes

-Enzymes:

Dnase I: Roche, Mannheim, Germany

Colagenase A: Roche, Mannheim, Germany

Rnase A: Invitrogen AG, Darmstadt, Germany

Proteinase K: Roche, Mannheim, Germany

-Antibodies:

Table 6: Primary antibodies for Western blotting and IHC

material	**targetprotein size**	**using**	**company**
Mouse-anti-ß-actin	42kDa	w. blot	Sigma-Aldrich, Munich, Germany
Monoclonal- anti-α-Tubulin	50 kDa	w. blot	Sigma-Aldrich, Munich, Germany
Mouse- Anti-FHL2 (clone F4B2-B11)	32kDa	w. blot	Wixler et al., 2007
Rabbit-anti-lamininγ1	180 kDa	w.blot	Wixler et al., 2007
Rat- anti-TNC	190-240 kDa	w.blot	Abcam, UK
Rabbit- anti-TNC	190-240 kDa	ICH	Epitomics, USA
Rabbit- anti-FN	94-220 kDa	w.blot	Sigma-Aldrich, Munich, Germany
Rabbit- anti-COL1	140-210 kDa	w.blot	Merck Chemicals GmBH, Germany
Rabbit- anti-COL3	300 kDa	w.blot	Abcam, UK
Mouse- anti-aSMA	42 kDa	w.blot	Sigma-Aldrich, Munich, Germany
Rabbit- anti-MMP12	45 kDa	ICH	Biorbyt-Tools for 39cience, Germany
Rat- anti-F4/80	160 kDa	ICH	AbD sero Tec, Germany
Rabbit- anti-CD3	23 kDa	ICH	Abcam, UK
Goat- Pax-5 (C-20)	46 kDa	ICH	Santa Cruz Biotechnology, Germany
Rabbit- anti-S100A9	13 kDa	ICH	Abcam, UK

Table 7: Primary antibodies for flow cytometry

material	company
APC hamster-anti-mouse CD11c	eBiosciences, Germany
APC rat-anti-mouse CD8a	eBiosciences, Germany
APC-streptavidin	BD Biosciences, Germany
Biotin IL-6 anti-mouse	eBiosciences, Germany
Biotin TNFα anti-mouse	eBiosciences, Germany
biotin-labeled rat-anti-mouse GR-1	BD Biosciences, Germany
FITC-rat-anti-mouse CD11b	BD Biosciences, Germany
FITC-rat-anti-mouse CD45.2	BD Biosciences, Germany
PE CD4 rat-anti-mouse	BD Biosciences, Germany
PE MHCII rat-anti-mouse	eBiosciences, Germany
PE rat-anti-mouse F4/80	eBiosciences, Germany

Table 8: Secondary antibodies

material	description	using	company
anti-mouse	IgG-HRP-lab.	w. blot	Amersham, Freiburg, Germany
anti-rabbit	IgG-HRP-lab.	w. blot	Amersham, Freiburg, Germany
anti-goat	IgG-HRP-lab.	w. blot	Santa Cruz, Heidelberg, Germany
anti-rat	IgG-HRP-lab.	w. blot	SIGMA, USA
anti-mouse	IgG biotin-lab.	IHC	Linaris GmbH Wertheim, Germany
anti-rabbit	IgG biotin-lab.	IHC	Linaris GmbH Wertheim, Germany
anti-goat	IgG biotin-lab.	IHC	Linaris GmbH Wertheim, Germany
anti-horse	IgG biotin-lab.	IHC	Linaris GmbH Wertheim, Germany

Prestained protein marker → Sigma Aldrich, Karlsruhe

2.1.4.4. Molecular-biological kits

- AMAXA- mause Machrophage Nucleofactor Kit: AMAXA GmbH, Germany

-BCA Protein Assay kit: Pierce, Bonn, Germany

- Bradford Protein Assay Reagent: Bio-Rad, Muenchen, Germany

- Brilliant II SYBR Green® QPCR Master Mix: Agilent, Waldbronn, Germany

-High-Capacity cDNA Reverse Transcription Kit (ABI 4368814): AB Applied Biosystems

- QIA filter Plasmid-Max-Kit: Qiagen, Hilden

-Qiagen RNeasy® Mini kit: Qiagen, Hilden

- Sircol collagen assay kit: Biocolor Ltd., U K

- TagMan®-PCR Meister Mix: Roche, Mannheim, Germany

- Vector® Red Alkaline Phosphatase Substrate Kit I, Vector Laboratories, via Linaris GmbH, Wertheim-Bettingen

- Vector® Vectastain ABC Kit, Vector Laboratories, via Linaris GmbH, Wertheim-Bettingen

2.1.5. Consumables

Table 9:

Material	**Company**
Cell Culture Dishes	Greiner Labortechnik, Solingen, Germany
Cell Culture flasks	Greiner Labortechnik, Solingen, Germany
Cell strainer (Filter Falcon)- 70µm	BD Biosciences, USA
Disposable pipettes 5ml, 10ml, 20ml	Becton Dickinson Biosciences, Germany
Eppendorf tubes 0.5ml, 1ml, 1.5ml , 2ml	Eppendorf, Germany
Falcon tubes 15ml, 50ml	Becton Dickinson Biosciences, Germany
Glass plates	Bio-Rad, Muenchen, Germany
Lysing matrix D tube	MP Biomedicals, USA
Nitrocellulose membrane protran	Schleicher & Schuell, Dassel
Whatman GB002 paper	Schleicher & Schuell, Dassel

2.1.6. Machines, systems and software

Table 10:

Machines, systems and software	**Company**
Acrylamide gel electrophoresis apparatus	Bio-Rad, Muenchen, Germany
Bacteria incubator	Heraeus, Hanau, Germany
shaking bacteria	Infors, Bottmingen, Switzerland
Bio Photometer	Eppendorf, Hamburg, Germany
Centrifuge (bench-top) 5810R	Eppendorf, Hamburg, Germany
Centrifuge Eppendorf 5417R	Eppendorf, Hamburg, Germany
CO2 Incubator for cell culture (Hera cell 240)	Heraeus, Hanau
Digital camera microscope	Zeiss, Goettingen, Germany
Flow cytometry(FACSCalibur)	Becton Dickinson, Heidelberg, Germany
ELISA Reader	Biotek, USA
AxioVert 25 microscope	Zeiss, Germany
Liquid nitrogen tank (-181°C)	Tec-Lab, Germany
Luminometer LB96V	EG&G Berthold, Bad Wildbach

Microtome HM 355S	ThermoFisher scientific, Germany
NanoDrop spectrophotometer	Thermo Scientific, Germany
Neubauer hemocytometer	Merck KGaA, Darmstadt, Germany
pH-meter	Knick, Germany
Roche- RT-PCR Cycler- 480II	Roche, Mannheim, Germany
Sterile hood (cells)	BDK, Germany
Tank western blot chamber	Bio-Rad, Muenchen, Germany
Digital detection system Stella	raytest Isotopenmeßgerate GmbH, Germany
Thermcycler (N99nBiometra T Gradient)	Eppendorf, Germany
Tissue embedding machine EG 1150H	Leica Microsystems, Nussloch, Germany
Ultra-Turrax Homogeniser type T8	IKA-Werke, staufen, Germany
Water bath	GFL type 1012, Burgwedel, Germany

2.2. Methods

2.2.1. Animal methods

Animal experiments were conducted with the approval of the ethics commission and in compliance with the guideline uses of experimental animals at the University Hospital of Muenster.

In our experiment the following mouse strains were used:

FHL2-/- mice (genetic background C57BL / 6), here referred also as FHL2 KO mice

FHL2 +/+ mice (genetic background C57BL / 6), here referred also as WT mice

These mice were used at age of 2-4 months to study the development of lung fibrosis after bleomycin treatment and the inflammatory status of this disease as well.

2.2.1.1. Bleomycin administration

Here, several WT and FHL2KO mice were used in the study. Pulmonary fibrosis was induced in mice by intranasal administration of a single dose of bleomycin (usualy 2U/kg body weight, in some experiments 3U/kg or 5U/kg we also used) that was reconstituted in PBS. Control animals received only PBS intranasally. After anesthesia of mice with 10 ml/g anesthesia solution (0.5 mlXylazin 2% and 0.5 ml Ketamin 10% in 9 ml PBS), the bleomycin solution was injected into the lungs, drop by drop via nose at a volume of 25-35µl/nose (total= 50-70µl/mouse). The mice are weighted regularly (each 3 day) to define the changes of the body weight during the fibrosis development.

For the analysis, mice were euthanized 7, 10, 14, 21 and 28 days after bleomycin or saline administration and the bronchoalveolar lavage fluid (BALF), the lung cells, lung tissue lysate or the intact lung tissue were isolated and analyzed by different methods.

2.2.1.2. Depletion of macrophages in vivo

For in vivo depletion of macrophages, clodronate liposomes were used. The clodronate (dichloromethylene bisphosphonate) is a non toxic drug as well as liposomes (Rooijen and Sanders 1994). The liposomes are used as a trojan horse for the intracellular introduction and

accumulation of clodronate, which acts as an effector molecule that induce apoptosis of macrophages and hence their depletion from organs and tissues (Rooijen and Sanders 1994). The mice were intravenously injected with 100µl/mouse of clodronate liposomes or PBS-liposomes as control and on the next day they were repeatedly injected with 75µl/mouse of the same solution but intranasally. On the following day, the mice were treated intranasally with 3U/kg BLM and 5 days later, the mice were received again clodronate or PBS-liposomes intranasally, 75µl/mouse.

For analysis, mice were euthanized and the bronchoalveolar lavage fluid (BALF), blood samples, lung cells, lung tissue lysate and intact lung tissue were isolated and analysed by different methods.

2.2.1.3. Preparation of bronchoalveolar lavage fluid and lung cells

Euthanized mice were carefully lavaged by injecting 1ml of PBS supplemented with 2 mM of EDTA into a trachea using a syringe with 20 G cannula. The procedure was repeated twice, so that ~ 2ml of bronchoalveolar lavage fluid (BALF) were recovered from each mouse. The BALF was then centrifuged at 300xg for 10 minutes at 4°C, and the supernatant was aliquoted and frozen at -80°C until analysis.

To obtain a single lung cell suspension, the lung tissue was cut into tiny pieces and placed in 15ml falcon with 3-4 ml RPMI 1640 medium containing 0.7mg/ml colagenase A and 100 Kunitz-Units/ml DNase I and incubated at 37°C in a water bath for 30 min, after which the digested tissue was pipetted several times through a 20 G syringe needle. The digested tissue was then passed through a "filter-cartide" (falcon) in order to separate larger tissue pieces. The filtrate was centrifuged at 400xg at 4°C for 7-10 minutes. The pellet was then resuspended with erythrocyte lysis buffer and centrifuged again and resuspended in FACS-PBS (5% FCS in PBS) for analysis. Total cell counts of cell pellets were performed by Neubaur hemocytometer.

2.2.1.4. Preparation of lung tissue lysates

After isolation of mouse lungs, the lung tissue was cut into tiny pieces and distributed into two lysing matrix D tubes, one of which contained 500µl RIPA buffer without SDS for protein lysates, while the other tube contain 1000 µl Trizol reagent for RT-PCR lysates. The obtained samples were stored in -80 °C until use.

2.2.1.5. Isolation of peritoneal murine macrophages

For in vitro experiments, abdominal viscera macrophages were obtained from mice that have been injected intraperitoneally (i.p.) 3 days before with 1 ml of 4% starch solution in PBS (for accumulation of the macrophages in abdominal cavity). The macrophages were washed out from abdominal cavity of euthanizes mice with 5 ml of sterile PBS and centrifuged at 1200 rpm at 4°C for 5 min. The cells were washed two times with PBS by centrifugation, resuspended in DMEM with 2% fetal calf serum (FCS) and 50 µg/ml gentamicin and adjusted to a concentration of $1*10^6$ macrophages/ml and 2 ml of the cell suspension were plated into 6-well dishes and incubated for 3-4 h at 37°C in a humidified incubator under 5% CO2. Non-adherent cells were then removed by washing the dishes twice with PBS and the remained macrophages were stimulated with different stimulator reagents.

2.2.2. Tissue culture and cells methods

2.2.2.1. Tissue cell culture

2.2.2.1.1. General culturing of eukaryotic cells

The mammalian cell lines were placed into media shown below and grown in disposable culture flasks or petri-dishes at 37 °C and 5% CO2. All cells were regularly split before or upon reaching confluency. For this purpose, the medium was aspirated and the cells were washed once with PBS and incubated with trypsin-EDTA solution (1 ml per 75 cm^2 dish) at 37 °C for about two to five minutes. When the cells had become detached, they were resuspended infresh serum-containing medium, counted and depending on the experimental design cultivated further in appropriate media.

For determination of cell amounts, the cell suspension was diluted 1:1 with trypan blue solution and the number of cells was counted under light microscopy using Neubauer hemocytometer.

cell line	**cultur medium**	**additives**
HEK209	D-MEM high glucose	10% FCS, Pen/Strep
HeLa	D-MEM high glucose	10% FCS, Pen/Strep
Machrophages	D-MEM high glucose	2% FCS, Pen/Strep
Murine fibroblasts	D-MEM high glucose	10% FCS, Pen/Strep

2.2.2.1.2. Freezing and thawing of eukaryotic cells

To store cells for longer time, aliquots were frozen in liquid nitrogen (-181 °C). To prepare the cells for storage, they were grown in T175 flask or 10 cm dishes to 100% confluence and the cells were detached with trypsin-EDTA and centrifuged at 1200 rpm for five minutes. They were then resuspended in freezing medium (4 ml for a 10 cm dish) and 1ml of the suspension was distributed into cryotubes. These were kept overnight in polystyrene boxes at -70 °C to cool down the cells slowly and then transferred into liquid nitrogen tank, where they were stored.

The so-frozen cells were thawed, if needed, in a 37 °C water bath and then pipetted into a ten-fold excess of culture medium. To remove the DMSO, the suspension was centrifuged (1200

rpm, five minutes) and placed into the respective cell culture medium and cultured in an incubator. Fresh medium was added on the next day.

2.2.2.1.3. Transfection and stimulation of eukaryotic cells

Transfection of peritoneal machrophages with plasmid DNA

Transfection of expression plasmids into peritoneal mouse macrophages was performed with Amaxa apparatus and the Amaxa mouse Machrophage Nucleofector kit (Lonza, Cologne) according to the manufacturer's instructions. For each transfection set $1*10^6$cells were used. After transfection, the cells were incubated for 2-3 hours at 37 °C and 5% CO2. Then the medium was changed and the cells optionally stimulated with lipopolysaccharide (1µg/ml) or BLM (15U/ml) and mouse lung tissue lysate (contains carbohydrate) for additional 24 h.

Stimulation of peritoneal murine macrophages

After isolation of peritoneal mouse macrophages, as described in section (2.2.1.5), these cells were stimulated with lipopolysaccharide (1µg/ml) or BLM (15U/ml) and mouse lung tissue lysate (contains carbohydrate) for 24 h.

To obtained the lung lysate that was used for macrophage stimulation, lungs from two WT mice were minced, placed into 5 ml of PBS, 4 times repeatedly frozen in liquid nitrogen and thawed at 37°C water bath, sonified on ice for 30 second three times and centrifuged. The supernatant was filtered sterile and used for stimulation of macrophages in a dilution of 1:100. The optimal dilution was estimated in preliminary experiments. The lung lysate was used as a source of released endogenous damage-associated molecular pattern molecules.

Transfection of eukaryotic cells with PEI

For transfection of RNA or plasmid DNA into eukaryotic cells, different transfection strategies were applied. For efficient transfection of eukaryotic cells (e.g. HEK209, HeLa and fibroblasts) the transfection reagent polyethylenimine (PEI) was used. The cells were seeded at a 50% confluence the day before the experiment. On the day of trasfection, growth medium

was replaced by transfection medium (without penicillin/streptomycin). For a 35mm dish (6-well) a mixture of 10µl PEI and 200µl OPTI-MEM was incubated for 5 minutes at room temperature before adding DNA. The PEI-mixture and DNA were incubated for 15 minutes at room temperature and then added to the cells. The cells were incubated with the transfection mix for different times depending on the experimental schedule.

FHL2 knockdown by siRNA

For suppression of the cellular FHL2 expression, fibroblasts were treated with "small interfering RNA (siRNA). Transfection of fibroblasts with FHL2-specific siRNA (Eurofins MWG Operon, Germany) was performed using the HiPerFect transfection kit (Qiagen, Cologne) according to manufacturer's instructions (end concentration: 2-5 nM siRNA). After 24 hours, the cells were lysed and used for analysis. As a control, so-called "scrambled" siRNA (2-5 nM siRNA) was used.

2.2.2.2. Flow cytometry assay (FACS analysis)

The prepared BAL fluid cells or tissue cells described in section (2.2.1.3) were stained with different fluorochrome-labeled antibodies for FACS analysis (Table 7).

The cells were count and at least $2*10^6$ cells for each sample were distributed into 1.5 ml FACS tubes for staining. Usually controls including unstained cells were included. The cells were centrifuged at 400xg for 5-10 min at 4C° and after pouring off the liquid the tubes were inverted on a paper towel. The cell pellets were resuspended in 50 µl staining solution (contains fluorochrome-conjugated secondary antibodies) and incubated for 17 min on ice. For the remaining 3 min of incubation, the 7AAD dye (for dead cells) was added with 50 µl per batch. After 20 min (total incubation), the cells were again pelleted and then taken up in 50-500 µl FACS-PBS. The cells were than ready for FACS analysis.

Marker-dye	**FACS channel**	**Marker-dye**	**FACS channel**
FITC	FL1	PI	FL3
PE	FL2	APC	FL4

2.2.3. DNA/RNA methods

2.2.3.1. Transformation and isolation of plasmid-DNA from bacteria

Chemically competent E.coli was transformed with a plasmid using the heat-shock method. For the transformation, the corresponding plasmid DNA (1µg) was mixed with 100µl of a suspension of heat shock competent bacteria and incubated for 20 minutes on ice. Then a heat shock at 42 °C for 45 seconds was performed and the bacteria were cooled on ice and cultivated at 37 °C in 500µl LB medium without ampicillin but with shaking for one hour and then plated on agar plates with appropriate antibiotics. On next day, individual bacterial colonies were picked and cultured in 4 mL of LB medium with antibiotic for 12 hours. From these pre-cultures, cells were then transferred to 150ml of LB medium with ampicillin (100 µg /ml) and cultivated overnight.

The obtained cell suspension was centrifuged and the plasmid DNA was isolated using the QIA filter plasmid maxi kit (Qiagen, Hilden, Germany) according to manufacturer's instructions. This kit is based on the method originally published by Birnboim and Doly (Birnboim and Doly 1979).

2.2.3.2. Isolation of RNA from cells and tissue

By using the Qiagen RNeasy® Mini kit:

In order to determine the transcript amounts of certain genes by real-time quantitative reverse transcription PCR, RNA had to be isolated from cells or tissues. The Qiagen RNeasy® Mini kit was used according to manufacturer's recommendations for isolaton of total RNA from animal cells or animal tissue. For experiments with eukaryotic cells, the cells were cultured in 6cm dishes or 35mm dishes (6-well dishes). Cells were washed with PBS and lysed with 600µl/6cm dish or 350µl/35mm dish RLT buffer containing β-mecaptoethanol. The samples were homogenized and mixed with 1:1 (v/v) 70% ethanol and applied on spin columms, washed and eluted with RNase-free water. Then the RNA was stored at -80°C.

By using TRIZOL Reagent:

Total RNA was isolated from lung tissue by using the Trizol reagent according to the manufacturer's protocol. Briefly, the lung tissue, described in section (2.2.1.4) was homogenized using the Ultra-Turrax Homogeniser Type T8 (IKA-Werke, Staufen, Germany) and mixed with Trizol lysis solution and incubated for 5 min at room temperature. RNA was then recovered from the lysate by adding 200 µl chloroform (Sigma) followed by centrifugation at 9000 rpm for 20 min at 4 °C. The aqueous layer was then transferred into a clean microcentrifuge tube. RNA was precipitated by adding isopropanol and pelleted by centrifugation at 9000 rpm for 20 min at 4 °C. The pellet was dissolved in 300 µl Na acetate (0.3 M & pH 5.2) and 300 µl phenols (pH 4.1-5.6) was added and centrifuged for 5 min at 4 °C and at 13000 rpm. Equal volume (1:1) of chloroform was added into the aqueous phase and again centerfuged. 1.5 ml of cold 96% ethanol was added to the aqueous phase of the probe, mixed, placed for 30 sec into liquid N2 and centrifuged again for 20 min. The pellet was washed with 80% ethanol, air dried, and resuspended in 30-50 µl RNase-free water and stored at -70°C until using.

2.2.3.3. cDNA synthesis

After determination of the RNA concentration by the NanoDrop spectrophotometer; equal amounts of total RNA were reverse-transcribed using a High-Capacity cDNA Reverse Transcription Kit (ABI 4368814) according to the manufacturer's recommendations. For example, 25µl of total RNA with defined concentration were mixed with 25µl Master Mix cDNA kit (10x RT Random Primers, 10x RT Buffer, 25x dNTPs MIX (Stock 100mM), RNase Inhibitor, Reverse Transcriptase and d. H2O) in PCR-microtubes and after short vortexing and short centrifuging, the mixed samples were run in Thermocycler (N99nBiometra T Gradient) according to the program listed below and obtained cDNA samples were stored at -20°C.

Programm of the Thermocycler:

Heating	**Step1**	**Step2**	**Step3**	**Step4**
25C°	25C° - 10 min	37C°-120 min	85C° - 5 sec (1 min)	4C°

2.2.3.4. Real-Time quantitative Polymerase Chain Reaction (qRT-PCR)

The polymerase chain reaction (PCR) is a method for exponential amplification of DNA by a thermo stable DNA-dependent DNA polymerase. This technique was further refined by the discovery of reverse transcriptases and the possible detection of PCR product amounts while the reaction is still in progress. Today, during the reaction ("real-time") the amount of cDNA of certain transcripts (mRNA) can be quantified after reverse transcription either by using a specific fluorescence labeled reporter probe (Taqman technique) or by the incorporation of a fluorescence dye (e.g. SYBR Green) into the amplified DNA double strand.

Taqman-PCR:

The cDNA samples were diluted 1:10 for TaqMan-PCR. For this technique aTaqMan®-Meister Mix [4.4µl H2O, 0.2µl primer L (20µM), 0.2µl primer R (20µM), 0.2µl Taqman probe (20µM) and 10µl Master Mix (MM)] was used. 15 µl Master Mix and 5 µl template (cDNA sample) were pipetted in duplicate into a 96 well- RT-PCR plate. The RT-PCR plate was covered and centrifuged for 2 min at 1000 rpm at room temperature and subjected to the Taqman RT-PCR Cycler machine. The relative transcription levels of target and reference genes (Cytochrom C and GAPDH) were determined and an absolute quantification and a relative quantification were calculated by RT-PCR Cycler software. The particular steps of the qRT-PCR procedure are shown in Table 11.

SYBR Green® PCR:

For this technique the Brilliant II SYBR Green QPCR Master Mix was used for detection of amplified DNA. The Brilliant II SYBR Green QPCR Master Mix contained all qPCR relevant reagents: SYBR Green, Taq polymerase and dNTPS in the appropriate buffer. 4 µl of Brilliant III SYBR Green QPCR Master Mix and 0.2 µl Reference Dye (33,3nM) and 0.6 µl of 10 µg target gene specific primer (forward and reverse primer mix) were applied per well (96-well plat). 0.5µl of each cDNA sample was diluted in 6.7 µl sterile H2O per well and added. Each sample was measured as doublet. The qRT-PCR was performed on the Roche light cycler 480III under following conditions, as summarized in Table 11.

The increasing fluorescence was measured after each elongation step. The melting curve of PCR products at the end of the reaction was performed to determine the specificity of each target gene primer pair. The determination of the ct-values was carried out automatically by the PCR Cycler software. In addition to the transcription level of the genes of interest, the transcription levels of a housekeeping gene (GAPDH) were determined to eliminate differences in overall transcription levels caused by possible toxic effects of sample`s treatment. Therefore the $2^{-\Delta\Delta ct}$ method was used (Livak & Schmittgen, 2001), and changes in amounts of transcripts were calculated as n-fold of the untreated control.

Table 11: Thermal profile of RT-PCR:

step	**temperature**	**time**
activation of polymerase	95°C	10 min
denaturation	95°C	30 s *
annealing	60°C	1 min *
extension	72°C	1 min *
denaturation	95°C	30 s
melting curve	55°C - 95°C	10 min

* 40 cycles

2.2.3.3. Gene reporter assay (Luciferase assay)

To study the activity of a promoter, it is possible to set the expression of a so called “reporter gene” (usually an enzyme) under the control of the promoter of interest. The activity of the promoter can then be measured directly by measuring the activity of the enzyme. A common reporter gene is the luciferase of photinus pyralis. The substrate of this enzyme is luciferin, which will be converted into oxyl-luciferin thereby emitting light. This emission can be detected by a luminometer (LB96V) and the activity is determined as relative light unit (RLU*s). For reporter gene assay, cells were grown in 12-well dish to 60% confluence and on next day transfected with appropriate plasmids. The transfection of a plasmid that carried the luciferin gene under the control of the promoter of interest was carried out as described earlier

using PEI (section 2.2.2.1.3). After 24 hours of transfection, the cells were lysed for at least 30 minutes at 4C° with 150 µl luciferase harvest buffer. In a 96-well microtiter plate 50 µl of sample lysates were added to 50 µl luciferase assay buffer. The samples were then measured two seconds after addition of luciferin solution for the duration of 10 seconds. Relative light units (RLUs) were calculated in relation to protein amounts and data were plotted in GraphPad Prism diagrams.

2.2.4. Protein methods

2.2.4.1. Preparation of protein samples from cells and tissue

Preparation of protein lysates from cells

Cell lysates were prepared by using different lysis buffers (TLB, RIPA or Harvesting buffer). The medium was aspirated and cells were washed with PBS. For a 6-well dish 200µl of lysis buffer were added and cells were incubated for 10-15 minutes at 4°C or in ice. Protein lysates were collected and centrifuged at 10000 rpm for 10 minutes at 4°C; supernatants were collected in a 1.5 ml tube and stored at -20°C.

Preparation of protein lysates from tissue samples

Tissue samples described in section (2.2.1.4) were mechanically minced on ice in RIPA-Buffer using Ultra-Turrax Homogeniser Type T8 (IKA-Werke, Staufen, Germany). The lysates were frozen and thawed once before pelleting the debris by centrifugation at 13000 rpm (4°C). Supernatants were collected and stored at -20 °C for downstream applications.

2.2.4.2. Determination of protein amounts

By using the Bradford reagent:

The protein amounts were determened using Bradford reagent (BioRad protein assay solution, BioRad, Muenchen). 400µl of the 1:5 diluted stock solutions (with d. water) were incubated with 2 µl of lysate samples for 5 minutes at room temperature. In the presence of ethanol and phosphate acid, the absorption of Coomassie brilliant blue G250 is shifted from 465nm to 595nm upon binding of proteins, which is used for determination of protein concentration, as the rising extinction is proportional to rising protein amount (Bradford 1976). To determine absolute protein concentrations different BSA solutions with defined protein concentrations were measured and these counts were used as calibration values.

By using the BCA Protein Assay Kit:

Protein concentrations were determined with the BCA Protein Assay Kit (Pierce, Bonn, Germany) according to the manufactures instructions. Routinely, 20 µl of protein lysates were mixed with 400 µl of the working reagent of the kit that was diluted 1:50 as described in the product manual. After incubation of the mix at 37°C for 30 min the extinction levels of the samples were determined using the Bio Photometer (Eppendorf) with BSA-standard probes used for calculation of the calibration values.

2.2.4.2. Sodium-Dodecyl-Sulfate gel electrophoresis (SDS-PAGE)

Sodium-dodecyl-sulfate gel electrophoresis (SDS-PAGE) is an efficient method to separate heterogeneous protein samples by the means of electrophoresis according to their size (Laemmli 1970). The gel was poured between two glass plates (Bio-Rad apparatus) and this gel is formed by the monomers acrylamide and bis-acrylamide, which copolymerize in the presence of APS and TEMED. The percentage of acrylamide/bis-acrylamide in a gel solution determines the size of the pores.

In a discontinuous SDS-PAGE the sample first enters the large pores of the stacking gel before entering the narrow pores of the resolving gel. The samples were mixed with 1:3 with sample buffer containing β-mercapto-ethanol and the anionic detergent SDS. The samples were heated at 95 °C for 5 minutes to denature the proteins. The β-mercapto-ethanol disrupts disulfide bonds between cysteine residues and SDS coats the protein molecules with a negative charge, thereby destroying the secondary, tertiary and quaternary structures of the proteins. The proteins have now all the same electrical charge and can be separated by their specific size. For every experiment, gels were prepared freshly. Separation of samples was done at 100-150V in 1x SDS running buffer. One line was loaded for a pre-stained protein marker.

Separating gel	**7 %**	**9 %**	**10 %**	**12.5 %**
Bis-acrylamide	2.2 ml	3 ml	3.3 ml	4.2 ml
H2O	3.9 ml	3.1 ml	2.8 ml	1.9 ml

Add 3.7 µl Tris/HCL (PH 8.9), 50 µl SDS-solution (20%), 100 µl APS (10%) and 2 µl TEMED.

Stacking gel: 7.15 ml Bis-acrylamide, 8.9 ml 1M Tris/HCL (PH 6.8), 33.2 ml distilled water and 250 µl SDS-solution (20%) → mix and keep at 4°C.

Add fresh: 50 µl APS (10%) and 5 µl TEMED for 5 ml mix of the stacking solution.

2.2.5. Immunological methods

2.2.5.1. Western blot (Immunoblot)

Protein samples previously separated in a SDS-PAGE can be transferred to a solid membrane for further immunological analysis. In order to do that an electric field was applied to force the proteins to transfer through the gel and to be bound to the nitrocellulose membrane at the same geometrical arrangement. The protein migrates from the negative charged cathode to the positive charged anode. In all experiments the transfer was done under wet condition using a BioRad "tank blot chamber". The blot was set up as follows: on both sides one sponge pad and two Whatman GB002 paper (Schleicher & Schuell, Dassel), in between the SDS-gel and nitrocellulose membrane (Schleicher & Schuell, Dassel). The nitrocellulose membrane was soaked in buffer before use. This "sandwich" was fitted in the chamber so that the membrane is directed to anode (+) and the SDS gel to cathode (-). The transfer was done at 400mA for 1 hour in blotting buffer at room temperature. Once the transfer was finished the membrane was rinsed in TBS-T. Unspecific binding sites were saturated by blocking with 5% BSA or 5% low-fat milk in TBS-T buffer for a minimum of 30 minutes at room temperature or overnight at 4°C. BSA or low-fat milk was used as instructed by the manufactures of the antibodies. Incubation with primary antibodies was done on a shaker either overnight at 4°C or 1-2 hours at room temperatures. Before incubation with the secondary antibody, the membranes were washed with TBS-T three times for ten minutes. Incubation with the secondary antibody was carried out for 30 mints- 1 hour at room temperature, followed by washing three times for ten minutes.

All antibodies were obtained from animal sources; the secondary antibodies were raised against the constant region of the target specific primary antibodies.

Detection of specific bands was done by incubation of the membrane with chemiluminescence substrate (ECL detection reagent) for one minute. Specific bands were visualized by using the digital detection system Stella with AIDA Image Analyzer software (Raytest Isotopenmeßgerate GmbH, Straubenhardt, Germany).

If the blot was analyzed with multiple antibodies, the antibodies of the first staining were removed after ECL detection. The membrane was swirled a half hour at 60 °C in stripping buffer and washed for one hour in water or TBST and finally blocked for one hour in 3% law-fat milk powder in TBST.

2.2.5.1. Sircol-assay

The Sircol Assay is a dye-binding method designed for the analysis of total (acid and pepsin-soluble) collagens. This assay can assess the rate of newly synthesized collagen produced during periods of rapid growth and development. New collagen is also generated during inflammation, wound healing and development of fibrosis. To detect the production rate of collagens, the Sircol Soluble COLLAGEN Assay kit was used according to the manufacturer's instructions. Briefly, 50 µl from the prepared BALF described in section (2.2.1.3) were used and Sirius red reagent was added to each sample and mixed for 30 min. The collagen–dye complex was precipitated and separated by centrifugation at 12,000g for 10 min, and dissolved in alkali reagent. Finally, the samples were loaded into a microtiterplate reader and the absorbance was determined at 555 nm.

2.2.5.3. Immunohistochemistry (IHC)

Immunohistochemistry (IHC) combines anatomical, immunological and biochemical techniques to identify discrete tissue components by the interaction of target antigens with specific antibodies tagged with a visible label. IHC consists of the following steps: 1) primary antibody binds to specific antigen; 2) antibody-antigen complex is bound by a secondary, enzyme-conjugated, antibody; 3) in the presence of a substrate and a chromogen, the enzyme forms a colored deposit at the sites of antibody-antigen binding.

For tissue staining by IHC, the tissue lung sections were deparaffinized and rehydrated by using histol and alcohol series. Antigens were retrieved by 5 min proteinase K digestion of samples at room temperature or by cooking the samples for 30 minutes in 10mM citrate buffer, pH 6.0 and cooling at room temperature or ice. The sections were treated with 3%

H_2O_2 for 10 min and then incubated with blocking buffer (0.1% Triton and 10% FCS in PBS) for 30 min, followed by incubation with specific target antibody (primary antibody) for 1h at room temperature or overnight at 4°C. After three washes by wash-block buffer, a biotinylated secondary antibody was applied for 30 minutes after which the samples were washed again with wash-block buffer. For the color reaction, the Vectastain ABC kit (Vector Laboratories / Linaris GmbH) was used according to manufacturer's instructions. The A and B solution (Vector Laboratories / Linaris GmbH) were added for 30 minutes with following washing with wash-block buffer. Finally, the sections were incubated in Red Alkaline Phosphatase Substrate solution (Vector Laboratories / Linaris GmbH) for 30 minutes at room temorature.

After that, the stained sections were counterstained with haematoxylin and slides were dehydrated with graded series of alcohol (80%, 96%, 100% isopropanol), cleared in histol and mounted in Roti-Histol or Tissue-Tek Glas mounting medium and analyzed with digital camera microscopy.

2.2.6. Histological methods

2.2.6.1. Fixation and paraffin embedding of lung tissue samples

For histological analysis, mice lung tissues were fixed and embedded into paraffin. For this purpose, the tissue pieces were fixed in 4% paraformaldehyde (in PBS) in 15 ml falcon for 4-6 h at room temperature. To remove the air from lung tissue, the tubes were placed into an exicator and vacuum was generated for about 20-30 min by using an air pump. This procedure was repeated until tissue pieces slided to the bottom of falcon tubes. Fixed tissues were washed two times with PBS before ascending the alcohol dehydrationseries (70%, 90%, 96% and 100% isopropanol). Then the tissue pieces were incubated in histol for 4 h at room temperature. Subsequently, the specimens were transferred to 60°C pure paraffin (the paraffin was changed several times, 1, 2 and 3 types of paraffin were used) and incubated for 6 h or for overnight (each type of paraffin). Finally, the samples were cast into paraffin blocks by using a tissue embedding machine (EG1150H, Leica, Germany) and then stored at 4 °C.
For staining the lung tissue specimens were cut into 4mm thick sections using a microtome.

2.2.6.2. Haematoxylin and Eosin (HE) & Trichrome staining

Formalin fixed and paraffin-embedded murine lung tissue sections were routinely stained with haematoxylin and eosin (HE) stains and with AZAN- Trichrome stainaccording to Heidenhein. After deparaffinization of lung tissue sections by using histol, the sections were rehydrated for three minutes in an ascending alcohol series (100%, 96%, 90%, 80% and 70% isopropanol) and incubated with haemotoxylin for 4 minutes and differentiated in tap water for 10 minutes and then incubated with eosin for 5 minutes. Finally the sections were dehydrated with the alcohol series (80%, 96% and 100% isopropanol) and in histol-cleared. The section slides were then covered by cover slipsand Roti-Histol or Tissue-Tek Glas mounting medium and analyzed with digital camera microscopy.

2.2.6.3. Continuous numerical scale system

A continuous numerical scale system was used for determining the degree of fibrosis in lung specimens (Ashcroft et al. 1988). The grading was scored on a scale from 0 to 8, using the average of microscope field scores, as in table 2. The system allows measuring the degree of fibrosis in small samples of tissue (1 cm) and can provide a detailed description of changes in the lung (Ashcroft et al. 1988).

To score the degree of fibrosis, three-four fields of several sections of lung tissue were photographed, numbered and scored by 3-4 observers in a blinded fashion. The mean scoresof each observer for each lung were calculated and mean score value of all observers defined the degree of fibrosis for that particular lung.

Table 12: Criteria for grading lung fibrosis (Ashcroft et al. 1988).

Grade of fibrosis	**Histologicalfeatures**
0-1	Normal lung
1-2	Minimal fibrous thickening of alveolar or bronchiolar walls
3-4	Moderate thickening of walls without obvious damage to lung architecture
5-6	Increased fibrosis with definite damage to lung structure and formation of fibrous bands or small fibrous masses
6-7	Severe distortion of structure and large fibrous areas; "honeycomb lung" is placed in this category
8	Total fibrous obliteration of the field

2.2.7. Data analysis

Data are expressed as the mean ± SEM or ± SD. Statistical analyses were performed with Graphpad Prism 4.02 software. Means between two groups were compared with 2- tailed unpaired Student's T-test, Wilcoxon test or 2-way ANOVA. $P < 0.05$ was considered as statistically significant.

3. Results and Discussion

3.1. Sensitivity of WT and FHL2KO mice to BLM treatment

To analyse the potential role of FHL2 in development of lung fibrosis, WT and FHL2-deficient mice were first treated with different doses of BLM to compare their sensitivity to the drug. Unexpectedly, the FHL2 knockout mice showed a higher mortality rate to BLM than WT mice. At 5 U/kg BLM almost 50% of FHL2-negative animals died during the first 10 days of drug application, while the vast majority (89%) of WT mice survived the treatment (Figure 9A). A dose of 2 U/kg was toxic for 15% of FHL2KO mice but for none of WT mice and 100% of both WT and FHL2-KO mice survived the application of 1U/kg (Figure 9A). The higher sensitivity of FHL2-/- mice to the antibiotic was also reflected by the stronger loose and slower recovery of their body weight after a single application of lower BLM doses (Figure 9B). As result, FHL2 knockout mice are more severe affected upon BLM treatment compared with WT mice.

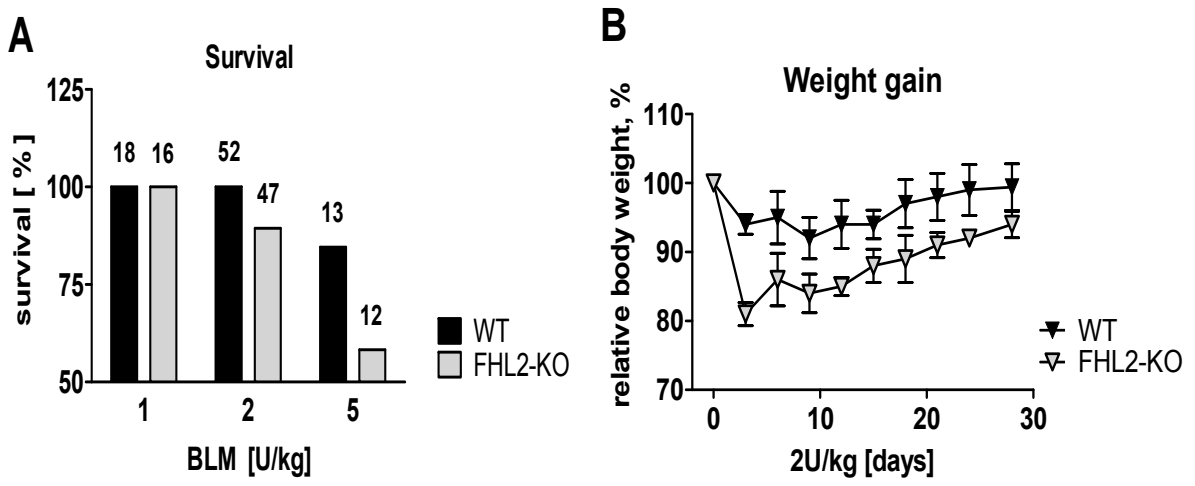

Figure 9: Sensitivity of FHL2WT and KO mice to BLM treatment. **(A)** The mice have received intranasally a single dose of BLM and were scored for mortality rate 10 days later. Cipher over columns show the number of analyzed animals. **(B)** Body weight alteration of FHL2WT and KO mice after a single intranasal application (2 U/kg) of BLM. n= 5-6 for each time point.

3.2. Development of BLM-induced lung fibrosis

BLM causes lung tissue damage at early steps after application and fibrosing of lung tissue at later steps. Fibrosis usually occurs when secretion and deposition of ECM proteins, primarily collagens, exceeds their degradation (Wynn 2011; Krieg et al. 2007). This might be a result of disturbed wound healing or chronic inflammation (Wynn 2011). To reveal whether the observed differences between WT and FHL2-KO mice also went along with dissimilar pulmonary aberrations and to clarify whether the pathology is of fibrotic nature or not, we performed a comparative histological analysis of WT and FHL2-deficient lungs at various time after BLM application. The H&E staining of lung sections showed a clear increase in swelling of alveoli and interstitial tissues as well as an accumulation of infiltrating cells in both WT and knockout lungs (Figure 10A). These alterations were transient and reached the maximum rate in both types of mice two weeks after BLM application, which is in agreement with published data showing that BLM-induced lung fibrosis in mice is severe but transient, which distinguishes the mouse BLM-mediated pulmonary fibrosis from that of humans (Hay et al. 1991; Walters & Kleeberger 2008). To reveal whether the expression and deposition of connective tissue is changed changed in mice after BLM injection, serial lung sections were stained with AZAN trichrome according to Heidenhein. The stains showed that the observed alterations were indeed accompanied in both WT and FHL2-null lungs with increased expression of extracellular matrix proteins, indicating that lung changes are mainly of fibrotic nature (Figure 10B). A further detailed mouse comparison showed that these changes arose in FHL2 knockout mice faster and decreased after reaching the peak at two weeks more slowly compared with WT mice. Quantification of lung fibrosis according to Ashcroft criteria (Asheroft et al. 1988) confirmed the difference in development of fibrosis between WT and knockout animals and further showed that the fibrotic changes are highly significant at early time of BLM application, but reach similar levels after two weeks and decline significantly faster in WT mice (Figure 10C). As fibrosis always goes along with alterations in collagen deposition, we compared their amount in WT and FHL2-KO lungs. Measuring collagen amounts in bronchoalveolar lavage fluids (BALF) by the Sircol Collagen Assay showed an

increase after BLM treatment in WT and in FHL2-/- mice as well, but the revealed differences were minimal (Figure 10D). A further unexpected observation made from these analyses was that lungs of non-treated control FHL2-/-mice already showed some fibrotic properties. Despite of a large variability between animals, FHL2 knockout lungs generally displayed a denser lung structure with a stronger expression of connective tissue in interstitial spaces (Figure 10B). Ashcroft values and amounts of Sircol measured collagens confirmed this observation and showed that the differences are significant (Figure 10E & F).

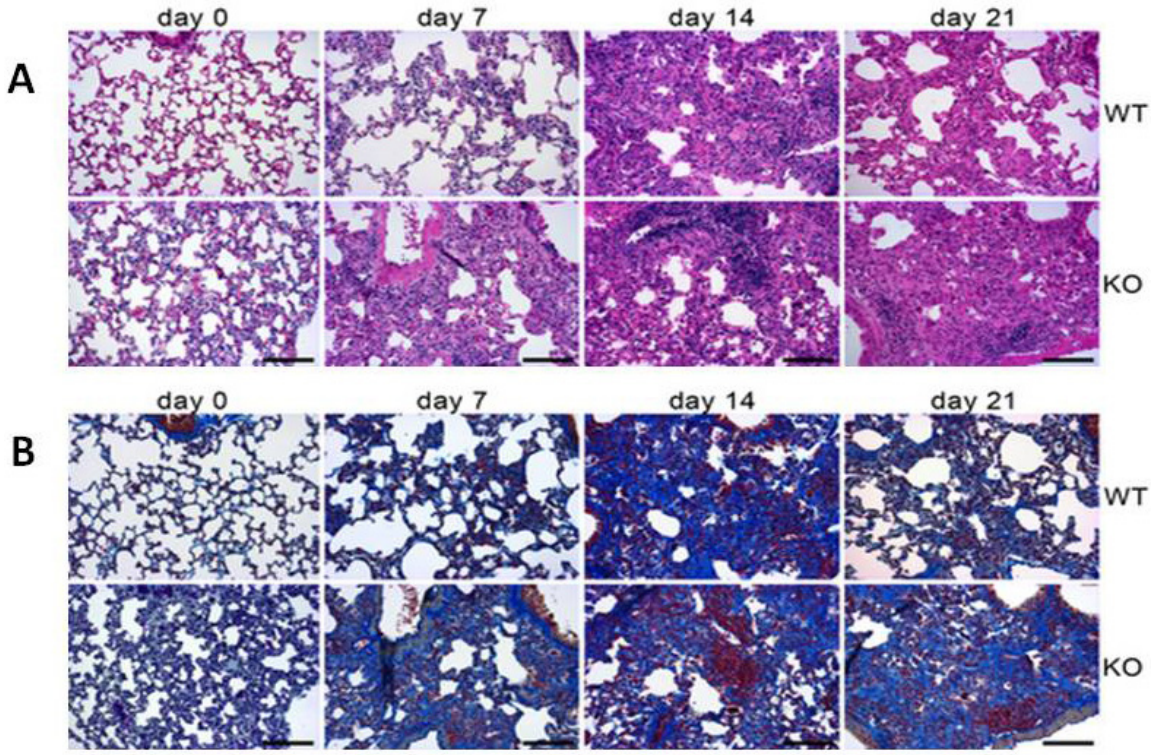

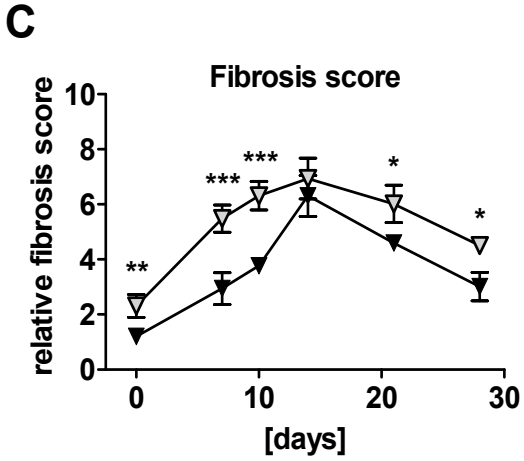

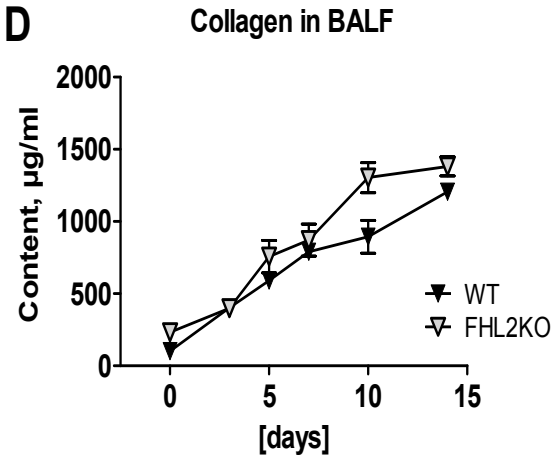

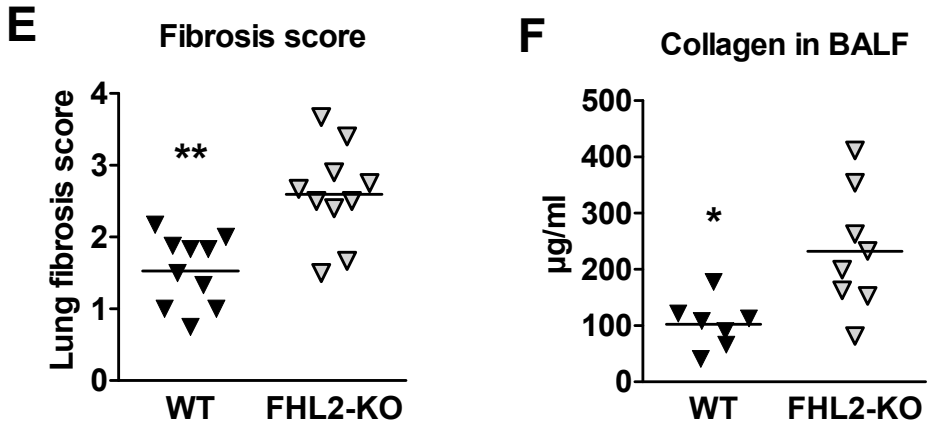

Figure 10: Development of BLM-induced lung fibrosis in FHL2 wild type and knockout mice. **A&B,** WT and FHL2-KO mice obtained a single intranasal application of BLM (2 U/kg) and the right lungs were fixed in PBS with 4% paraformaldehyde, embedded into paraffin and 4µ-thick sections were stained with Hematoxylin and eosin **(A)** or AZAN trichrome according to Heidenhain **(B)**. Bar=200 µm. **(C)** Lung sections shown in A&B were scored for fibrotic alterations according to Ashcroft criteria (Ashcroft et al. 1988) by three observer in a blinded fashion. Lungs from four mice with at least four different sections per lung were analyzed for each time point. (**D)** The collagen amount in bronchoalveolar spaces of BLM treated mice (2 U/kg) was measured by Sircol Collagen Assay. The number of analyzed animals per time point varied from three to eight. Mean values ± SE are shown. **(E&F)** Lung fibrosis score and collagen content in BALF, respectively, of non-induced control mice are shown.

3.3. Expression of ECM proteins during BLM-induced lung fibrosis

Fibrotic alterations are usually paired with excess expression of different extracellular matrix proteins. Therefore we compared alterations in ECM protein amounts in lungs of WT and FHL2 KO mice after BLM treatment by Western blot technique. As shown in Figure11A no significant differences in up-regulation of collagen type I, laminins (studied by expression of the laminin gamma-1 chain), fibronectin or α-smooth muscle actin were detected. Also collagen type III, the major profibrotic protein, showed only minor differences between FHL2 WT and KO lungs. However, tenascin C (TNC) showed a stronger and long-lasting induction in FHL2 knockout lungs, which could also be confirmed by immunohistochemistry (Figure11B). All together, these data are in good consistency with the histological and Sircol analysis (Figure 10). They confirmed that connective tissue proteins are induced in lungs of both FHL2 WT and KO mice and that there are only minor differences between them, with a slight trend to a stronger induction in FHL2 knockout lungs. The acute lung inflammation plays an important role in the development of BLM-induced lung fibrosis (Shaw & Martin 2009; Wynn 2011). During the acute inflammation phase many changes occur, in first line expression and secretion of inflammatory molecules takes place. TNC is a matrix protein that is always up-regulated in response to inflammation and tissue remodelling (Tucker et al. 2009). Its expression kinetic in FHL2 knockout lungs assume a stronger ongoing inflammation at early stages of BLM treatment and a slower ceasing of inflammatory and tissue damaging processes in later stages.

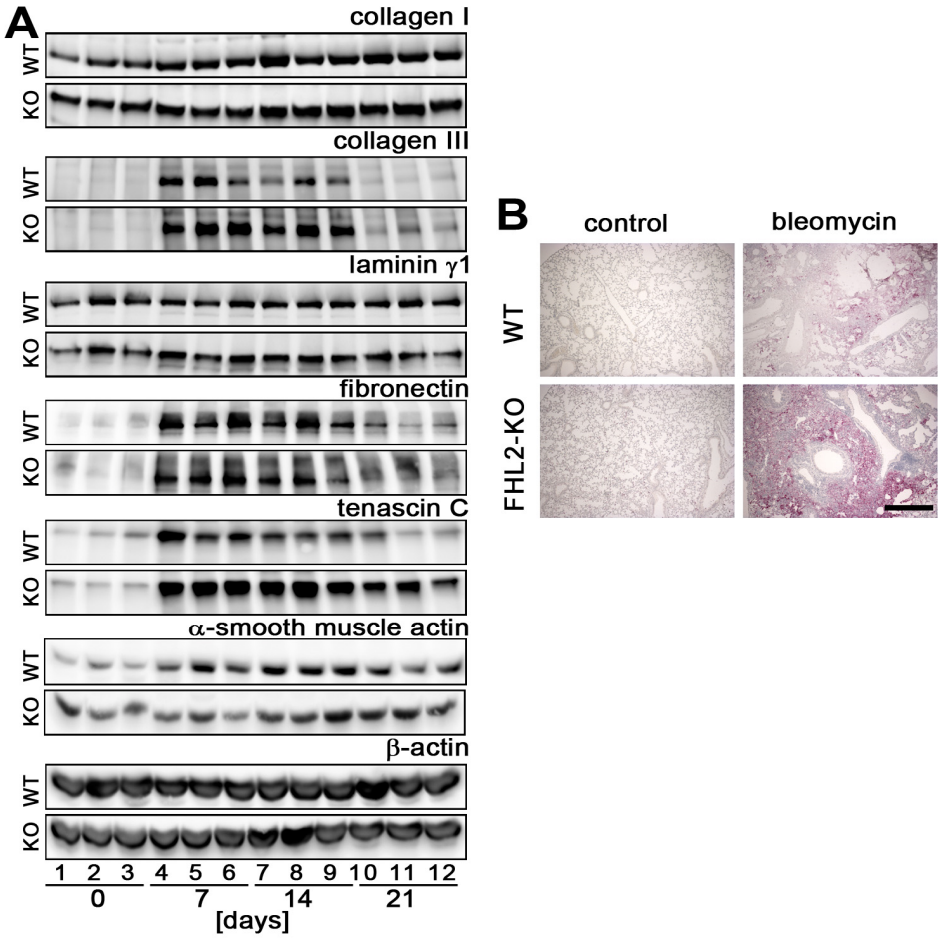

Figure 11: ECM protein expression. (**A)** FHL2WT and knockout mice have been instilled intranasal with BLM (2 U/kg) for indicated times. The left lung was then lysed with RIPA buffer and 20 µg of total lysates were analyzed by Western blotting for expression of different proteins. Lung lysates from three animals per each time point were studied. Equal protein loads were verified by β-actin immunoblotting. (**B)** Paraffin lung sections of control and BLM-induced (for 10 days) were stained for tenascin C (red). Nuclei (blue) were counterstained with hematoxylin. Bar=500 µm.

3.4. FHL2 inhibits expression of tenascin C

To define whether FHL2 regulates the expression of the proinflammatoryTNC protein, we knocked down the FHL2 in mouse fibroblasts that spontaneously express high levels of TNC and could show that this leads to increase in TNC transcripts (Figure 12A). Further, FHL2 strongly inhibited the TNC promoter activity in different cell lines when it was co-expressed

with a reporter gene construct containing the tenascin C promoter sequence in front of a luciferase gene and, the complete FHL2 protein was needed for an efficient inhibition, as our N-terminal and C-terminal truncation analysis of the human FHL2 protein showed (Figure 12B-D). As result, FHL2 reduces the expression of TNC via inhibition of its transcriptional level.

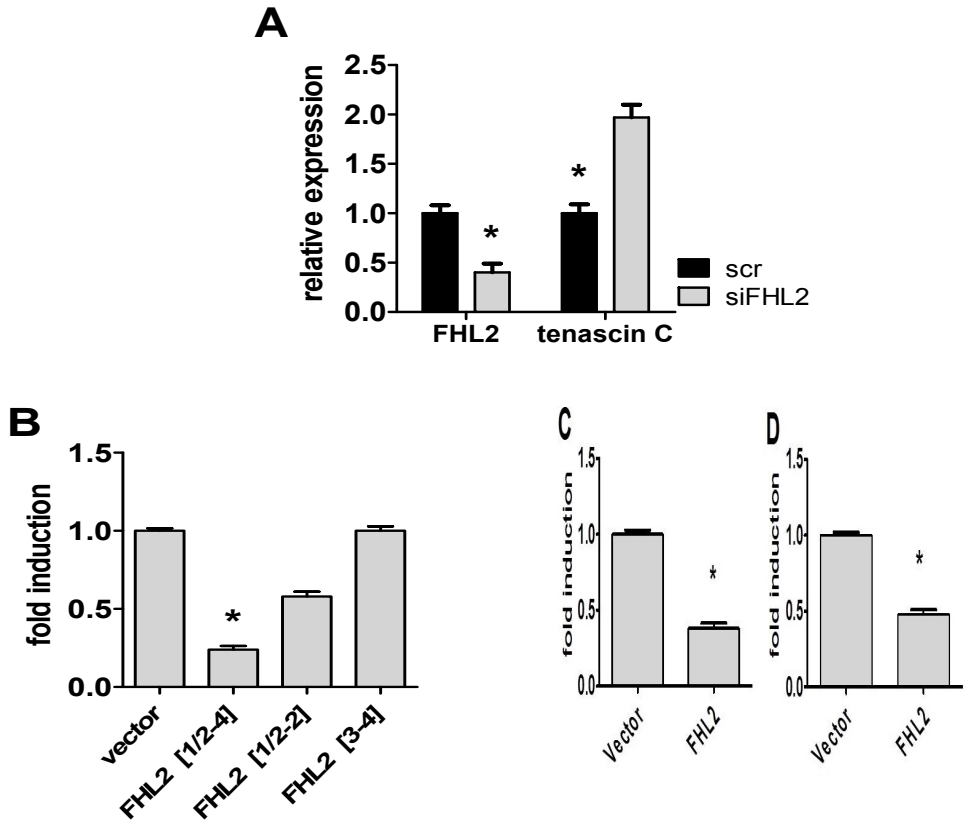

Figure 12: Effect of FHL2 on expression of tenascin C. **(A)** Immortalized embryonal fibroblasts from C57Bl/6 mice was transfected with scrambled or FHL2 specific siRNA for 24 h and the expression of FHL2 and tenascin C was analyzed by TaqManqRT-PCR. **(B)** HEK 293 cells were transfected for 30 h with a luciferase reporter gene construct containing a 2000 bp long tenascin C promoter sequence and plasmids containing either the empty vector, the full-length [1/2-4], the C- [1/2-2] or N- [3-4] terminal truncation mutants of human FHL2 and the luciferase activity was measured. **(C and D)** The dependency of the TNC promoter activity on expression of FHL2 was also studied in HeLa cell and embryonal fibroblast from WT mice. As in (B) a luciferase reporter gene construct containing the tenascin C promoter sequence and plasmids containing either the empty vector or the full-length of FHL2 were cotransfected in these cells. Relative scores are presented. Mean values ± SD are shown.

3.5. FHL2-deficient mice have a higher inflammation status in lungs

The alarmins S100A8 and S100A9 are calcium-binding proteins that belong to the damage-associated molecular pattern proteins and are released by neutrophils and macrophages very early during inflammation. They are increasingly used as biomarkers for ongoing inflammatory processes (Chan et al. 2012). Our results indicate a higher inflammation state in lungs of FHL2-KO than inWT animals on BLM induction. Therefore, we measured the extent of the S100A8/A9 heterodimer protein in bronchoalveolar fluid. Its amount was indeed permanently higher in FHL2-/- mice (Figure 13A) and interestingly, non-stimulated control FHL2-/-mice already contained significantly higher levels of the S100A8/A9 proteins in the BALF and in serum as well (Figure 13B). Neutrophils are not only the major source of the S100A8/A9 alarmin, but also are the cells that infiltrate as first the inflamed or injured tissue, where they release the S100A8/A9 protein complex that acts then as a proinflammatory cytokine (Burns et al. 2003; Vogl et al. 2008). Staining of lung sections for S100A9 showed in WT lungs the number of S100A9-positive neutrophils grew rapidly after BLM instillation, reaching a peak at day 14 and declining afterwards, thus resembling the fibrotic kinetic shown in Figure 13D. However, control FHL2-deficient mice already contained a significantly higher number of S100A9-expressing cells than WT lungs did, and their number did not increase but rather decreased after BLM application shown in Figure 10. Thus, the knockout mice seem to have a disturbed inflammation process. During inflammation many pro-inflammatory and pro-fibrotic cytokines are secreated by damage dresident and infiltrated and immune cells (Wynn 2011). Especially TGFβ and TNFα seem to play an importent role during both inflammation and fibrosis, with TGF-β being the major profibrotic cytokine and activator of myofibroblasts (Krieg et al. 2007). Therefore we measured the levels of these cytokines in BLM-injured lungs by qRT-PCR. These experiments showed that control FHL2-KO lungs already contained higher levels of TGFβ mRNA than the lungs of WT control mice but on BLM induction the amounts of TGFβ were equalized (Figure14A). To the contrary, TNFα amounts did not show differences in control mice but on BLM application WT lungs expressed higher levels of this cytokine than FHL2-KO lungs. It is intriguing to speculate that

the higher expression of TGFβ in control FHL2-KO compared with control WT lungs is probably responsible for the more dense, almost fibrotic, lung structure of knockout mice as well as for the increased expression of S100A8/A9 in these mice. It is known that during an immune response, TGFβ promotes the recruitment and activation of neutrophils, the source of S100A8/A9 (Yang et al. 2010). Further, TGFβ regulates the production of S100A8 and S100A9, at least in the distant premetastatic lungs of tumor-bearing mice (Hiratsuka et al. 2006).

Given that absence of FHL2 facilitates a higher inflammation state and that the BLM-mediated development of lung fibrosis is driven by acute pulmonary inflammation due to high destruction of lung tissue, it is conceivable that the amount of FHL2 in WT lungs will decrease during lung fibrosis. Indeed, both qRT-PCR and Western blot analysis of FHL2 expression showed that it was down-regulated during the early destructive stage of BLM-treatment but increased again at later stages (Figure 15A-B). The pro-fibrotic cytokine TGFβ induces FHL2 expression, while the pro-inflammatory cytokine TNFα down-regulates it (Muller et al. 2002; Joos et al. 2008). And, the kinetic of FHL2 down-regulation upon BLM treatment reflects very well the up-regulation of TNFα, indicating a possible causality between these two events (Figure 14B and 15). Taken together, our data indicate that the more severe lung phenotype observed in FHL2-deficient mice is probably based on the stronger induction of inflammation at early stages of BLM application. Remarkable is that in WT mice the FHL2 is down-regulated at this time and its expression increase again when the acute inflammation/destruction phase passed on to tissue regenerative phase.

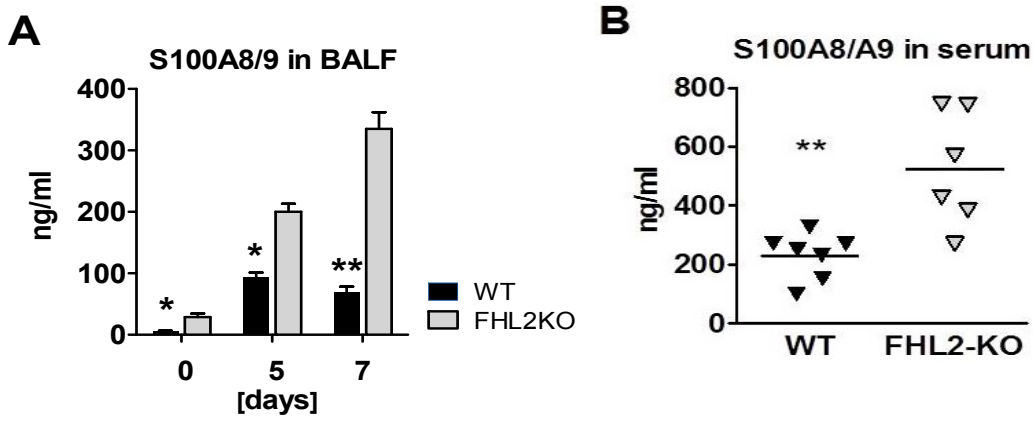

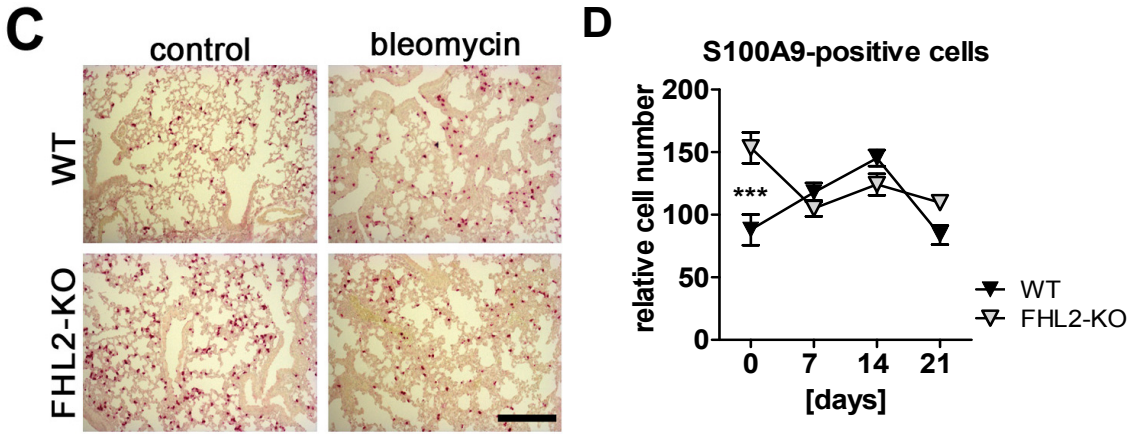

Figure 13: S100A8/A9 expression in FHL2 WT and KO mice. **(A)** The content of S100A8/A9 protein complex was measured in BALF by ELISA. The number of analyzed animals per time point varied from 3 to 8. **(B)** Concentration of S100A8/A9 proteins in serum of control mice measured by ELISA. **(C)** Paraffin lung sections of control and BLM-induced (7 days) mice were stained for S100A9 (red). Bar=250 µm. **(D)** Quantification of S100A9-positive cells shown in C. The S100A9-positive cells were counted in five microscopic fields of a size of 0.75 mm^2 for each lung sample. Lungs of four mice with at least four different sections per lung were analyzed for each time point.

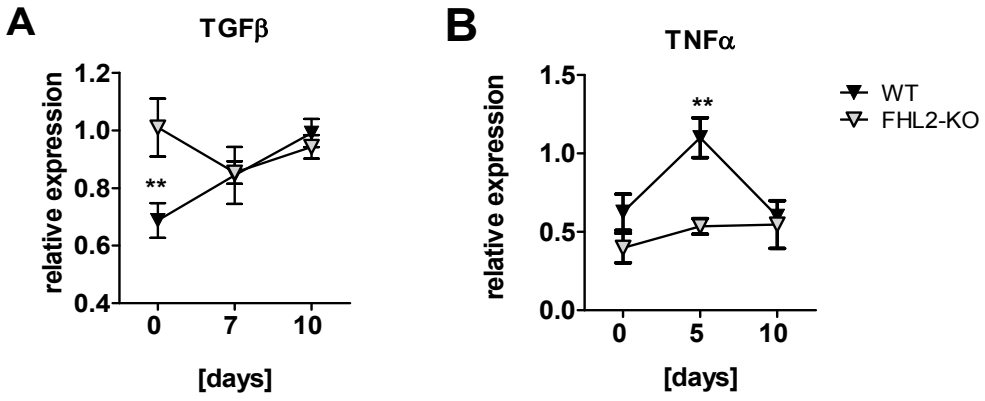

Figure 14: The expression of pro-fibrotic **(A)** and pro-inflammatory **(B)** cytokines in FHL2 WT and KO miceafter BLM treatment. The lung lysates of WT mice and FHL2KO mice treated with 2U/kg BLM were analyzed by RT-PCR. Lungs of 5-6 mice were used per each time point. Mean values ± SE are shown.

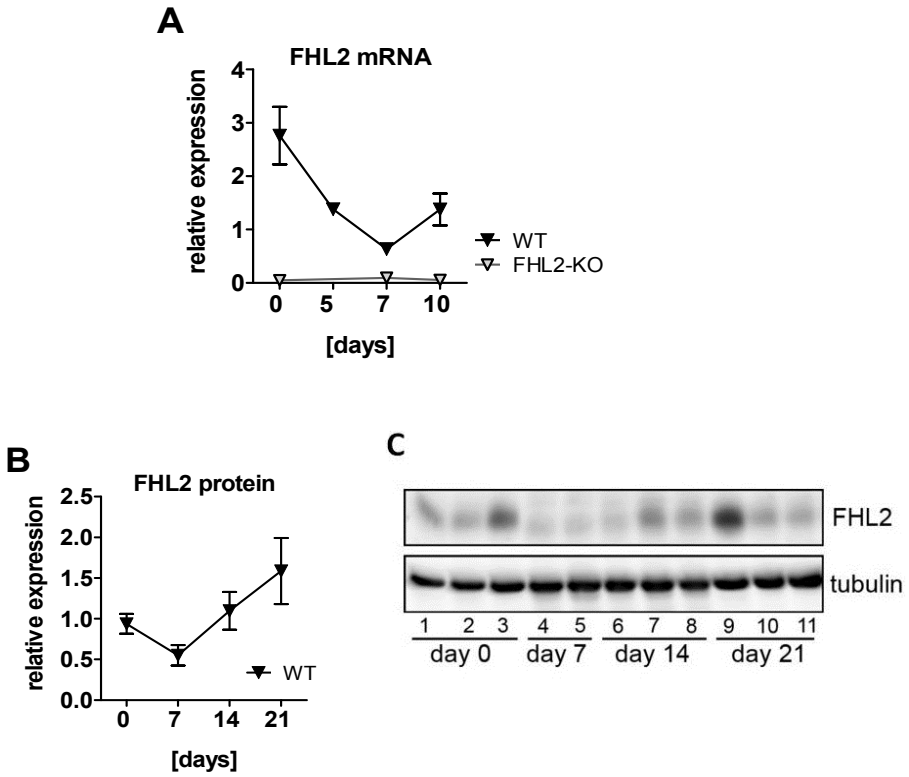

Figure 15: FHL2 expression after BLM treatment. **(A)** FHL2 transcripts in lungs of BLM-treated mice were estimated by TaqManqRT-PCR. **(B)** Western Blot analysis of FHL2 expression in lungs of WT mice after BLM-treatment (2U/kg). **(C)** Quantification of images shown in B. The FHL2 amount was estimated densitometrically as the relative intensity of the FHL2 bands to the loading controls. Values at time point 0 were taken as unity. The number of animals analyzed per time point varied from 6 to 12. Mean values ± SD are shown.

3.6. Immune status of bleomycin-treated lungs

To study changes in the immune response to BLM-mediated lung tissue injury, single cell suspension of WT and FHL2-KO lungs were analysed by flow cytometry. In control mice, no significant differences in number of immune cells present in lungs of the two mouse types were seen (Figure 16A). On BLM administration the number of immune cells that extravagated into lungs increased as already published (Walters & Kleeberger 2008) but again, no differences between WT and FHL2-KO mice could be measured for all analysed types of immune cells except for macrophages. A slight but significant lower number of F4/80-positive cells were measured in FHL2-KO compared with WT lungs (Figure 16B), suggesting that absence of the FHL2 protein either impairs macrophage migration into injured lung or their activation in response to BLM-induced tissue damage. Immunohistochemical analysis of lung sections confirmed the increase of immune cell infiltration into BLM-injured lungs and showed in accordance with flow cytometry data that no difference in T-lymphocyte content between WT and KO lungs could be detected (Figure 16C). However the macrophages abundance was much more pregnant in WT compared with FHL2-KO lungs (Figure 16D), which confirms again the results of the flow cytometry analysis. Interestingly, the amount of B-lymphocytes was in contrary increased in FHL2 knockout treated lungs in comparison to WT lungs (Figure 16E). Lymphocytes migrate into inflamed or injured later into the site of injury. The high infiltration of B-lymphocytes into FHL2 knockout lungs probably supports the inflammatory process. Indeed, the role of B-lymphocytes in development of pulmonary fibrosis is already well documented. Injection of anti-B-lymphocyte antibodies results in decreased fibrosis and mice with defective B-lymphocytes develop only mild forms of lung fibrosis (Yoshizaki et al. 2008). The depletion of B cells in the tight-skin mouse model for systemic sclerosis results in reducing of skin fibrosis and autoimmune response (Hasegawa et al. 2006). Our data showing that FHL2 deficiency results in a strong B-lymphocyte infiltration into BLM-injured and fibrotic lung raises of course the question, how FHL2 regulates B-lymphocyte infiltration into or proliferation in the inflamed lung. This, however, is atopic for future studies.

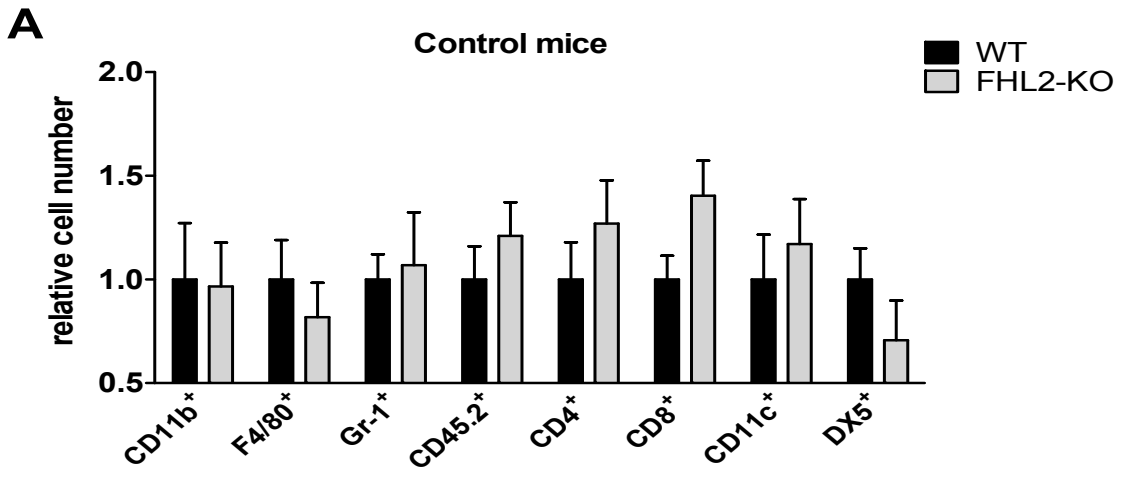
A
Control mice
WT
FHL2-KO
relative cell number
2.0
1.5
1.0
0.5
CD11b+
F4/80+
Gr-1+
CD45.2+
CD4+
CD8+
CD11c+
DX5+

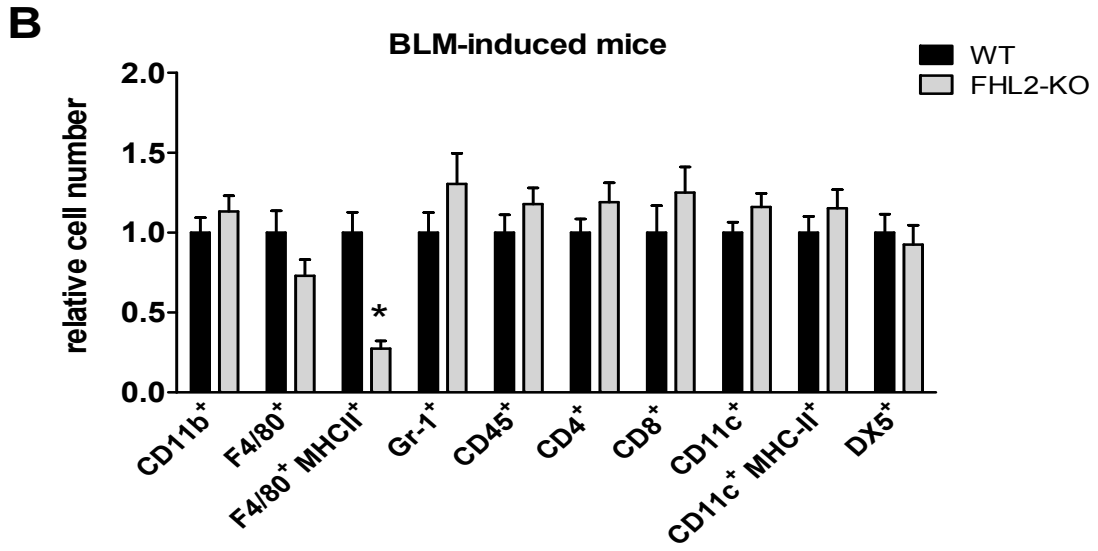
B
BLM-induced mice
WT
FHL2-KO
relative cell number
2.0
1.5
1.0
0.5
0.0
*
CD11b+
F4/80+
F4/80+ MHCII+
Gr-1+
CD45+
CD4+
CD8+
CD11c+
CD11c+ MHC-II+
DX5+

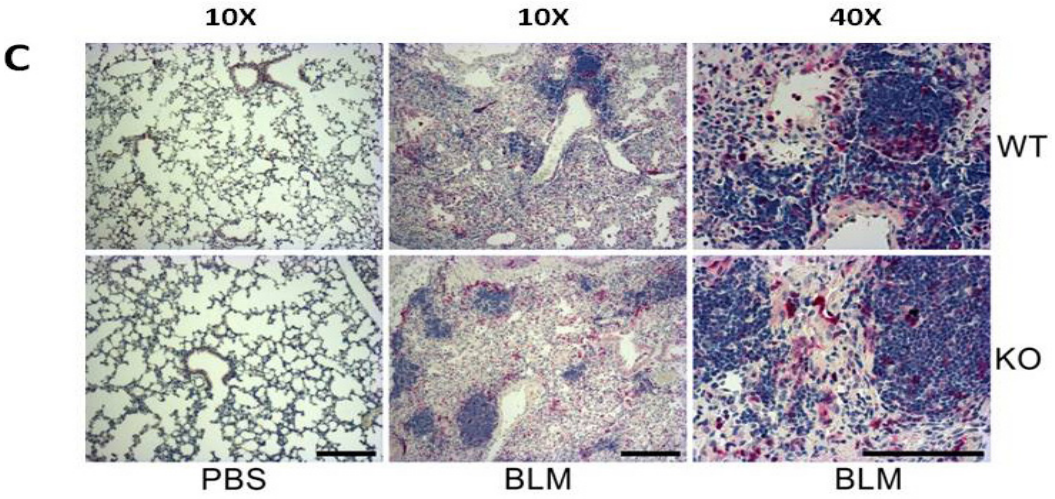
C
10X
10X
40X
WT
KO
PBS
BLM
BLM

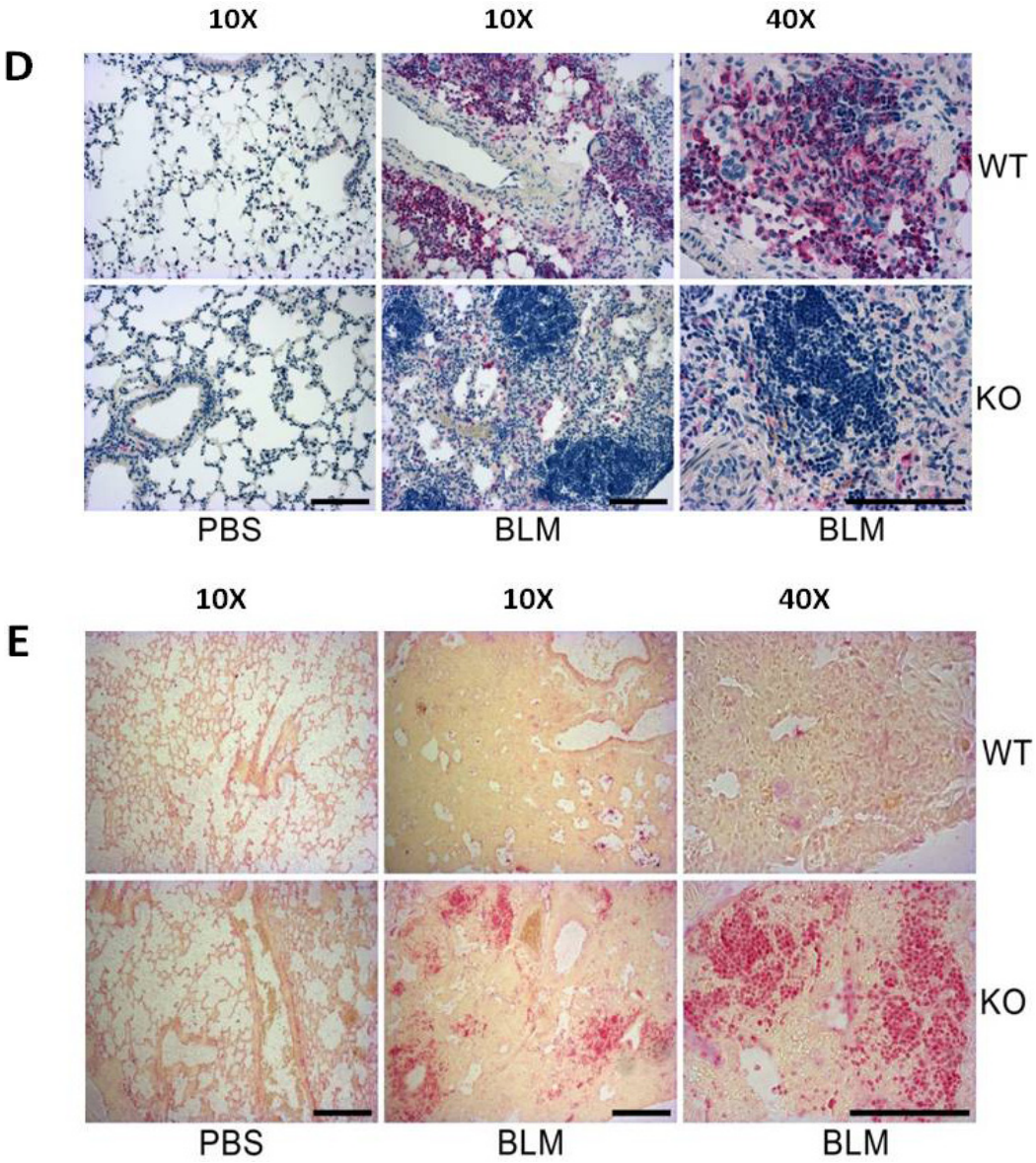

Figure 16: Immune cell infiltration into BLM-treated lungs of WT and FHL2KO mice. Single cell suspensions of lung tissue from control **(A)** or 8 days long BLM-stimulated **(B)** mice were studied for indicated surface receptors by flow cytometry. A total of 10^5 lung cells were analyzed and percentages of positively-stained cells are shown. n= 4-6 mice for each time point. **(C-E)** Paraffin sections from control and BLM-induced (for 10 days) mice were stained with specific antibodies to T-lymphocytes (**C**; CD3), to macrophages (**D**; F4/80) or B-lymphocytes (**E;** CD3). Immune cells are shown in red, while all nuclei (blue) were counterstained with hematoxline. 4-5 lungs were used in each case.

3.7. Macrophages activation during BLM-induce lung fibrosis

The macrophages migrate into damaged tissue and play different roles in inhibition and resolution of the lung inflammation and fibrosis. They induce myofibroblast apoptosis, clearance of alveolar oedema fluid and they remove dead cells. Further, activated macrophages secrete different cytokines, such as TNFα or IL-6 that that have an important role in regulation of inflammation (Herold et al. 2011; Wynn 2011). Also, MHCII molecule is expressed on the surface of macrophages and a lack of this protein expression lead to severe immune-deficiency (Mach et al. 1996). Phenotype analysis of the immigrated macrophages showed that FHL2-deficient cells failed to be activated, as they expressed only low amounts of MHCII receptors as well as TNFα and IL-6 cytokines (Figure 17). This clears that, low infiltration of FHL2KO macrophages into lung tissue damage lead to low activation of these cells.

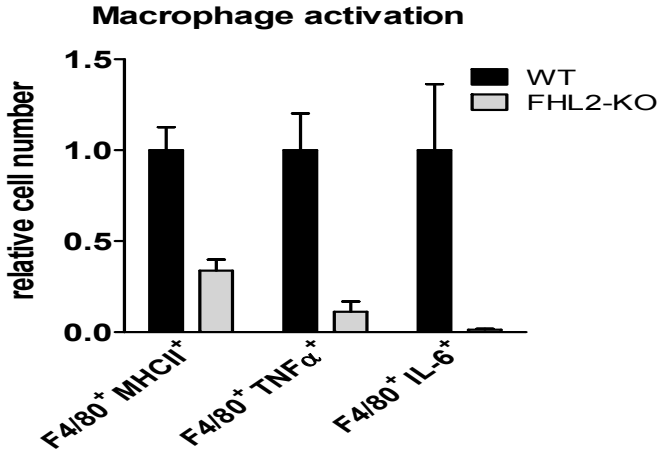

Figure 17: Activation of macrophages in bleomycin-treated lungs of FHL2 WT and KO mice. Single cell suspensions of lung tissue from control or 10 days BLM-stimulated mice were studied by flow cytometry. A total of 10^5 lung cells were analyzed and percentages of positively-stained cells are shown. The F4/80-positive macrophages were analyzed for expression of activation markers, the MHC-II receptor and the intracellular TNFα and IL-6 proteins.

3.8. FHL2 deficiency abrogates DC-SIGN-mediated activation of macrophages

To study whether absence of FHL2 inhibits the activation of macrophages in general or the observed effect was specific for BLM-induced lung damage only, we isolated peritoneal macrophages from WT and FHL2-KO mice, stimulated them in vitro with lipopolysaccharide (LPS) or with BLM plus lung lysate and analysed them for activation markers. The latter stimuli should imitate the situation in the lung after BLM application (the high lung tissue damage). As data of Figure 18A and B show, activation of FHL2 knockout macrophages was not disabled when they were stimulated with LPS, but was prevented on stimulation with lung lysate and BLM. LPS is known to stimulate macrophages via binding the TLR4 receptor (Vogl et al. 2008). On lung tissue damage, however, large amounts of carbohydrates are released, which may activate macrophages via the CD209a (DC-SIGN) receptor (Van den Berg et al. 2012). qRT-PCR analysis of CD209a transcripts showed only a marginal expression in non-activated WT and KO macrophages and its amount was not changed on LPS stimulation. However, when cells were incubated with lung lysate and BLM, the transcription of CD209a increased dramatically, but only in WT macrophages (Figure 17C). Lung analysis also confirmed the negligible expression of CD209a in FHL2-/- mice, which did not change after BLM treatment (Figure 18D), suggesting that FHL2 is probably involved in the transcriptional regulation of CD209a. To test this, peritoneal macrophages from FHL2 knockout mice were transfected with a plasmid containing cDNA for human FHL2 and stimulated with LPS or lung lysate plus BLM.Analysis of their phenotype showed that expression of recombinant FHL2, but not the empty vector rescued the transcriptional activation of CD209a on stimulation with carbohydrate-reach lung lysate. As expected, rescue of FHL2 had no influence on LPS mediated activation of FHL2-KO macrophages but significantly improved the macrophage activation on lung lysate and BLM stimulation (Figure 19A-D).

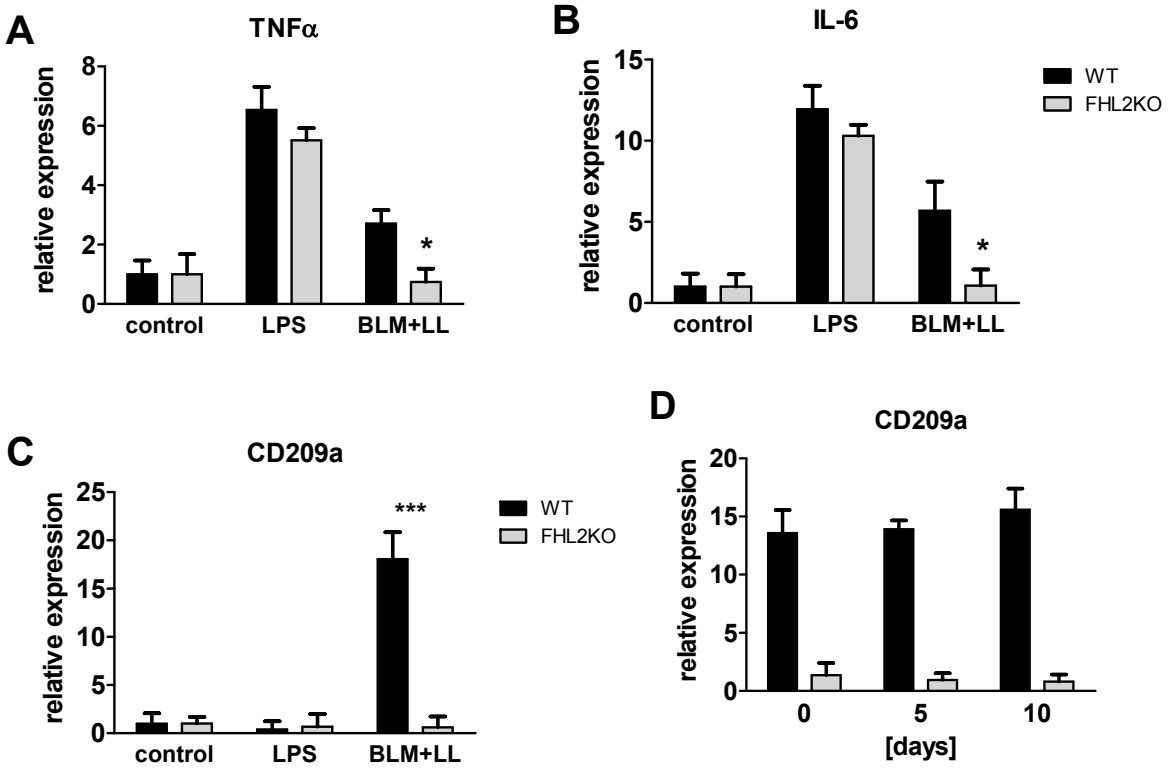

Figure 18: FHL2 deficiency abrogates DC-SIGN-mediated activation of macrophages. **(A-C)** FHL2 WT or knockout mice were injected i.p. with 0.8 ml of 4% starch in PBS and three days later peritoneal macrophages were isolated, plated into 6-well plate dishes and stimulated with LPS (1µg/ml) or BLM (15U/ml) plus mouse lung tissue lysate for 24 h. After isolation of total RNA, the transcripts of indicated genes were determined by TaqManqRT-PCR. Mean values of three repeated experiments ± SD are shown. **(D)** The mRNA levels for DC209a in lungs of WT and FHL2-KO mice were determined by qRT-PCR (n=4-5 per case).

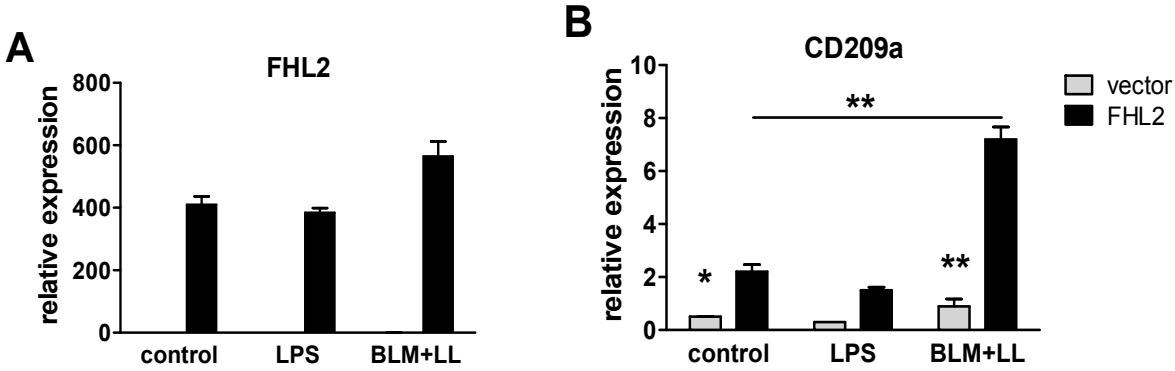

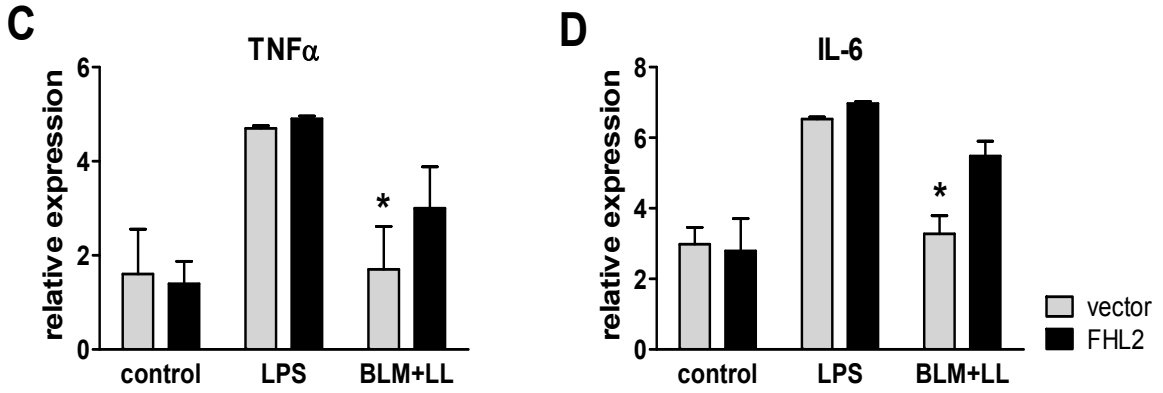

Figure 19: Rescue of FHL2 in FHL2-deficient macrophages restores their ability to up-regulate the CD209a receptor and to respond to BLM and lung lysate. Peritoneal macrophages from FHL2-KO mice were transfected with empty vector or human FHL2 cDNA, stimulated with LPS or BLM plus mouse lung lysate (LL) and analyzed for expression of human FHL2 (**A**) and for endogenous mouse CD209a **(B)**, TNFα **(C)** and IL-6 **(D)** by TaqManqRT-PCR. Mean values ± SD are shown.

3.9. FHL2 enhances macrophages MMP-12 expression

Macrophages abundantly infiltrate the damaged tissue at early stages of wound healing and replace the neutrophils that migrate into injured tissue first. The macrophages not only remove the injured tissue debris but also play an important role in ceasing the inflammation and the initiation of regenerative processes by releasing cytokine- and chemokine-blunting proteases and other MMPs, such as MMP-12 (Dean et al. 2008; Yoshizaki et al. 2008). The macrophage-specific MMP-12 protease is extracellular enzyme know as an important mediator of inflammation. MMP-12 not only degrades extracellular matrix proteins, but also regulates the recruitment of inflammatory cells and cleaves many pro-inflammatory cytokines and chemokines, which results in reducing of inflammation and consequently of fibrosis as well (Dean et al. 2008; Masashi & Kenji 2008). Our data show that expression of MMP-12 is increased after BLM treatment in both types of mice, but the degree of induction is lower in lungs of FHL2-KO mice (Figure 20A) compared with WT lungs. Also, immunohistochemical staining of lung sections with anti-MMP-12 specific antibodies and quantification of these

stains by means of morphometry revealed an increase of the staining intensity with time of BLM treatment but to a lower degree in FHL2-KO samples (Figure 20B &C). Of note, the reduced expression of MMP-12 in FHL2 deficient mice correlated with the lower amount of activated macrophages in the lung (Figure 17). An additional question of future study is how FHL2 regulates the expression of the macrophage-specific MMP-12 enzyme.

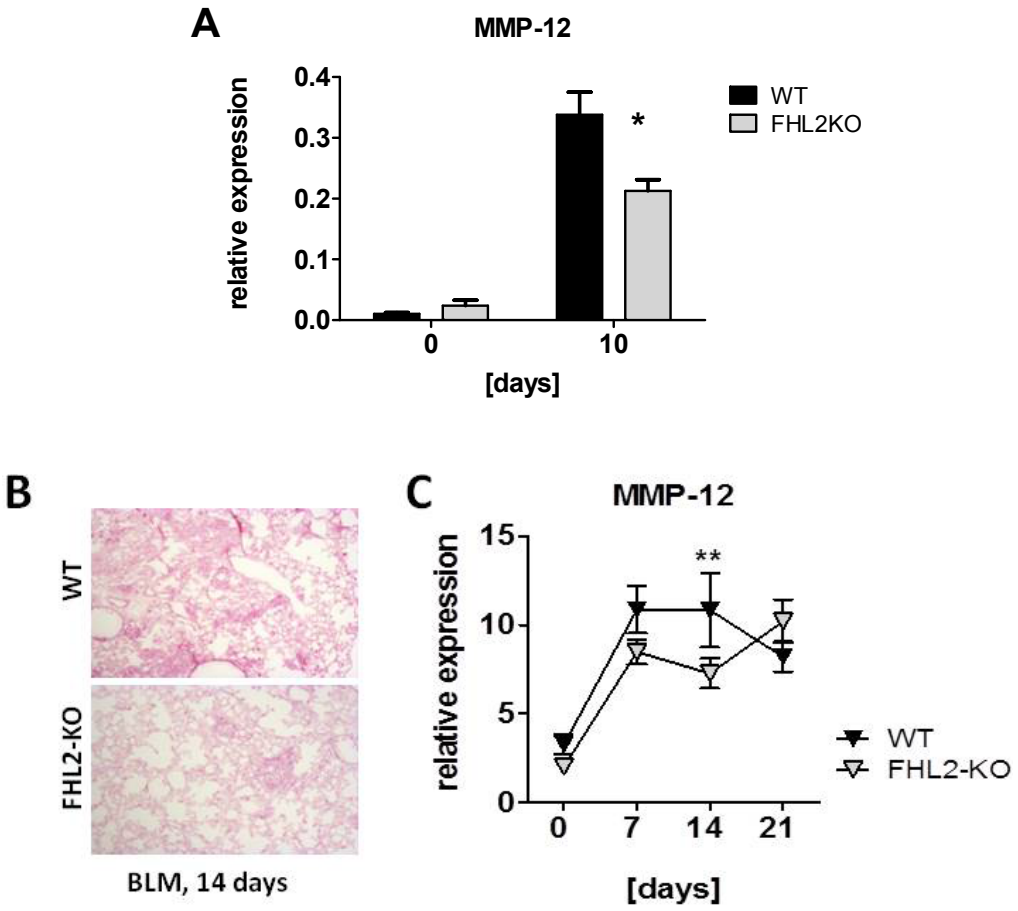

Figure 20: The expression of macrophage MMP-12 after BLM treatment. **(A)** Lung lysates of FHL2WT and KO mice after 10 days of 5U/kg BLM treatment were analyzed by RT-PCR to show the expression of MMP-12 (n= 4 mice for time point). **(B)** Paraffin lung sections of control and 2U/kg BLM-induced (7, 14 & 21 days) mice were stained for MMP-12 (red). Bar=250 µm. **(C)** quantification of MMP-12 expression shown in B. The MMP-12 expression was analyzed in five microscopic fields of a size of 0.75 mm2 for each lung sample. Lungs of four mice with at least four different sections per lung were analyzed for each time point.

3.10. Macrophage depletion aggravates lung fibrosis

Finally, we wished to test to what extent the inadequate amount of activated macrophages in lungs of FHL2-deficient mice accounted for the observed rapid fibrotic changes. Therefore the macrophage pools of WT and FHL2-knockout mice were depleted by injection of clodronate-liposomes and lung fibrosis was scored after BLM application (Figure 21). Ashcroft criteria revealed a significant increase in lung fibrosis after macrophage depletion in lungs of both WT and FHL2-knockout mice but to a similar degree, showing thus that successful activation and recruitment of macrophages into injured lung is needed to circumvent fibrotic changes. Interestingly, the enhanced fibrotic alterations in clodronate-terated mice went along with increased accumulation of collagens in BALF and increased amounts of T-lymphocytes that infiltrate the lungs, but no difference between WT and FHL2-KO mice were registrered, which is in good agreement with observed aggravation but disappearance of differences between mice lines in the severity of fibrosis. Remarkable also is that the levels of MMP-12 mRNA did not differ any more between WT and FHL2-KO mice and the total amount was decreased and reached the level of untreated FHL2 knockout lungs, additionally underlying the importance of MMP-12 up-regulation for the resolution of tissue damage.

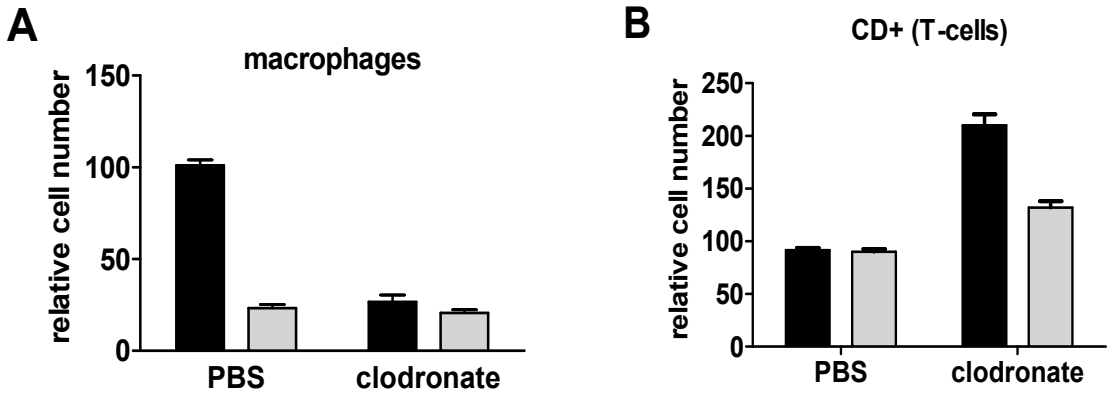

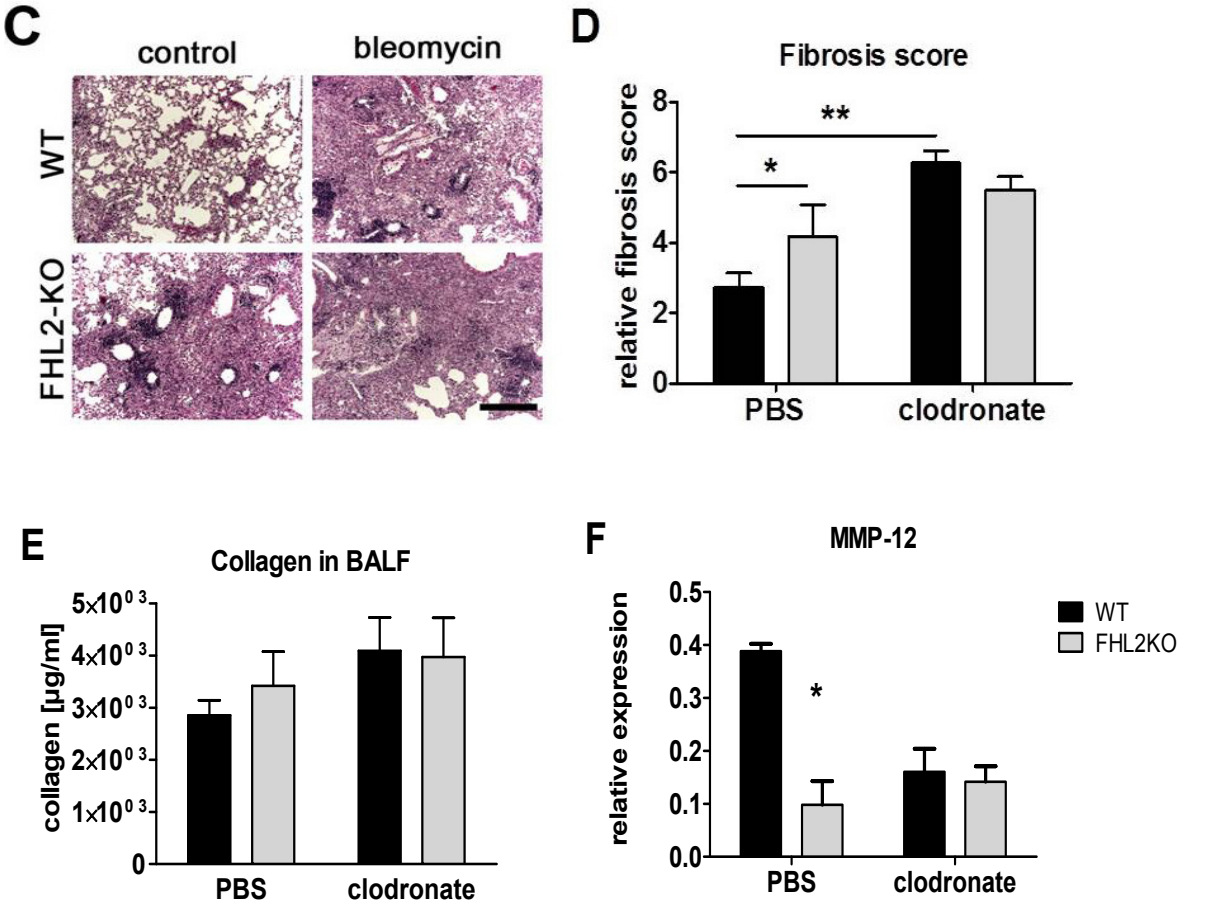

Figure 21: Depletion of macrophages aggravates lung fibrosis. FHL2 WT and KO mice were injected i.v. with 100µl/mouse of PBS- or clodronate-liposomes. On the next day they repeatedly received 75 µl/mouse of the same solution but intranasal. On the following day, the mice obtained 3U/kg of BLM intranasal and 5 days later, they had received again a dose of PBS- or clodronate-liposomes mixture intranasal. On day 10 after BLM application the lungs were fixed, embedded into paraffin and analysed for the presence of macrophages and T-lymphocytes by immunohistochemistry using the anti-F4/80 and Cd3 antibodies, respectively, **(A and B)** and for fibrotic alterations **(C and D)**, whereby the image of the panel **C** represents a H&E staining and the panel **D** the quantification of fibrotic alterations according to Ashcroft criteria. The F4/80- and CD3-positive cells were counted in five microscopic fields of a size of 0.75 mm^2 for each lung sample. **(E)** The collagen amount in BALF of these mice was measured by the Sircoll Collagen Assay. **(F)** Lung lysates of these mice were analyzed by RT-PCR for MMP-12 expression. Four animals for each experiment were analyzed. Mean values ± SD are shown.

In this study, we have shown that absence of the adaptor protein FHL2 aggravates BLM-mediated lung fibrosis. Not the final extent of fibrotic alteration was increased but its development at early steps was augmented and the resolution of the disease at later stages was retarded. Further, we have shown here for the first time that FHL2 inhibits at transcriptional level the expression of the pro-inflammatory ECM protein tenascin C and the DS-SIGN C-type lectin receptor of macrophages. Consequently, a higher inflammation developed in FHL2-deficient lungs that were further aggravated by the inability of macrophages to be activated in the injured tissue due to the absence of the CD209a receptor. As a result, a delayed restoration of lung injury took place. This was unexpected, as FHL2 has been reported to positively regulate the expression of collagens type I and III, and αSMA and to promote the assembly of ECM proteins (Park et al. 2008; Kirfel et al. 2008; Hamidouche et al. 2008). Unexpected also was the observation that the inflammation state in the lung of control FHL2 knockout mice per se was elevated, with measurable increased amounts of the inflammation marker protein S100A8/A9 in lungs and sera as well.

While the exact mechanism of BLM-induced lung fibrosis is not deciphered so far, many data indicate that an acute lung inflammation plays an important role (Shaw & Martin 2009; Wynn 2011). Upon BLM application large tissue damage takes place and results in release of damage-associated molecular pattern molecules that initiate a non-infectious immune response. Neutrophils are the most abundant immune cells that infiltrate into damaged tissue very quickly after injury and are replaced soon by macrophages. Together with neutrophils macrophages remove the injured tissue debris but also play an important role in ceasing the inflammation and in initiating the regenerative processes by releasing cytokine- and chemokine-blunting proteases and other MMPs (Dean et al. 2008; Yoshizaki et al. 2008). The insufficient number of activated macrophages in the wounded lung tissue of FHL2-knockout mice probably accounts for the delayed recovery from fibrotic alterations. Depletion of macrophages during the recovery phase of renal fibrosis has been shown to lead to failure of matrix degradation and persistent scarring (Nishida & Hamaoka 2008). Also myocardial wound healing was impaired when macrophages have been depleted (Van Amerongen et al. 2007). These data are in good agreement with our results showing an increase in lung fibrosis

upon clodronate-liposome depletion of macrophages. The absence of differences in fibrotic changes between WT and FHL2-knockout mice after this procedure further supports our hypothesis that the inability of FHL2-KO macrophages to be activated by BLM-injured tissue was mainly responsible for the severe progression of lung pathology in FHL2-deficient mice.

In summary, FHL2-knockout mice are not protected against BLM-induced lung fibrosis as was initially expected, but develop a severe and long-lasting lung inflammation that leads to greater lung pathology than in WT mice. The reasons for that are probably i) the inhibitory function of FHL2 on transcription of the pro-inflammatory protein TNC and ii) the promoting function of FHL2 on transcription of the macrophage-activation receptor CD209a. As a result, the injured FHL2-KO lungs display high amounts of TNC and contain a reduced number activated and inflammation ceasing macrophages.

4. References

Annie P. & Moisés S. (2002): Molecular mechanisms of pulmonary fibrosis. *Frontiers in Bioscience 7, d1743-1761.*

Ashcroft T., et al. (1988): Simple method of estimating severity of pulmonary fibrosis on a numerical scale. *J Clin Pathol; 41:467-470.*

Atamas, S. P., White, B. (2003): Cytokine regulation of pulmonary fibrosis in scleroderma. *Cytokine Growth Factor Rev. 14, 537–550.*

Bach I. (2000): The LIM Domain: regulation by association. *Mech Dev; 91: 5–17.*

Bai S., et al. (2005): FHL2 inhibits the activated osteoclast in a TRAF6-dependent manner. *J Clin Invest 115(10):2742-2751.*

Bargagli, Elena, et al. (2011): Calgranulin B (S100A9/MRP14) - A Key Molecule in Idiopathic Pulmonary Fibrosis? *Inflammation, Vol. 34, No. 2.*

Beg AA, Baltimore D. (1996): An essential role for NF-kappaB in preventing TNF alpha induced cell death. *Science; 274:782–4.*

Belvisi MG, et al. (2003): The role of matrix metalloproteinases (MMPs) in the pathophysiology of chronic obstructive pulmonary disease (COPD): a therapeutic role for inhibitors of MMPs? *Inflamm Res 52: 95- 100.*

Bennett J M, Reich SD (1979): Drugs five years later - Bleomycin. *Ann Int Med 90: 945-948.*

Bernabei P., et al. (1999): Functional analysis of T lymphocytes infiltrating the dermis and epidermis of post-burn hypertrophic scar tissues. *Burns; 25(1):43–48.*

Bethany B. Moore and Cory M. Hogaboam (2008): Murine models of pulmonary fibrosis. *Am J Physiol Lung Cell Mol Physiol 294: L152–L160.*

Birnboim H C and Doly J. (1979): A rapid alkaline extraction procedure for screening recombinant plasmid DNA. *Nucl. Acid. Res. 7:1513-23.*

Bode W., et al. (1999): Structural properties of matrix metalloproteinases. *Cell Mol Life Sci; 55(4):639- 52.*

Borish LC and Steinke JW (2003): Cytokines and chemokines. *J Allergy Clin Immunol 111:S460-475.*

Boyce DE, et al. (2000): The role of lymphocytes in human dermal wound healing. *Br J Dermatol; 143(1):59–65.*

Bradford, M. (1976): A dye binding assay for protein. *Anal. Biochem. 72:248-254.*

Breuer R., et al. (1995): Abatement of bleomycin-induced pulmonary injury by cell-impermeable inhibitor of phospholipase A2. *Life Sci 57: 237-240.*

Brew K, et al. (2000): Tissue inhibitors of metalloproteinases: evolution, structure and function. *Biochim Biophys Acta; 1477(1-2):267-83.*

Burns AR, et al. (2003): Unique structural features that influence neutrophil emigration into the lung. *Physiol Rev: 83(2): 309-336.*

Calderwood et al. (1997): the integrin a1 A-domain is a ligand binding site for collagens and lamminin. *JOURNAL OF BIOLOGICAL CHEMISTRY Vol. 272, No. 19, pp. 12311–12317, 199.*

Cambi, Alessandra and Figdor, Carl G (2003): Dual function of C-type lectin-like receptors in the immune system. *Current Opinion in Cell Biology, 15:539–546.*

Chan JK, et al. (2012): Alarmins: awaiting a clinical response. *J Clin Invest: 122(8): 2711-2719.*

Chan K., et al. (1998): Molecular cloning and characterization of FHL2, a novel LIM domain protein preferentially expressed in human heart. *Gene 210: 345–350.*

Chang Y., et al. (1995): Binding of Tenascin-C to Soluble Fibronectin and Matrix Fibrils. *Vol. 270, No. 48, pp. 29012–29017.*

Charles A Janeway, et al. (2001): Immuno biology-5. *Garland pulishing 181.I454.*

Chen, D., et al. (2003): SKI activates Wnt/beta-catenin signaling in human melanoma. *Cancer Res. 63 (20):6626-34.*

Chi-Hang Wonga, et al. (2012): The LIM-only protein FHL2 regulates interleukin-6 expression through p38 MAPK mediated NF-jB pathway in muscle cells. *Cytokine 59 286–293.*

Chung KF. (2001): Cytokines in chronic obstructive pulmonary disease. *Eur Respir J Suppl 34:50s-59s.*

Cinzia Bizzarri, et al. (2006): ELR+ CXC chemokines and their receptors (CXC chemokine receptor 1 and CXC chemokine receptor 2) as new therapeutic targets. *Pharmacology & Therapeutics 112- 139–149.*

Coghill, I. D., et al. (2003): FHL3 is an actin-binding protein that regulates alpha-actinin-mediated actin bundling: FHL3 localizes to actin stress fibers and enhances cell spreading and stress fiber disassembly. *J Biol Chem 278, 24139-52.*

Commins SP, et al. (2010): Immunologic messenger molecules: cytokines, interferons, and chemokines. *J Allergy Clin Immunol 125:S53-72.*

Curtis BM, et al. (1992): Sequence and expression of a membrane-associated C-type lectin that exhibits CD4-independent binding of human immunodeficiency virus envelope glycoprotein gp120. *Proc. Natl. Acad. Sci. U.S.A. 89 (17): 8356–60.*

Daniil, Z. D., et al. (1999): A histologic pattern of nonspecific interstitial pneumonia is associated with a better prognosis than usual interstitial pneumonia in patients with cryptogenic fibrosing alveolitis. Am. J. Respir. *Crit. Care Med. 160, 899–905.*

David Danon, et al. (1989): Promotion of wound repair in old mice by local injection of macrophages. *Vol. 86, pp. 2018 2020.*

Dawid IB, et al. (1998): LIM domains: multiple roles as adapters and functional modifiers in protein interactions. *Trends Genet; 14: 156–162.*

Dean, R.A., et al. (2008): Macrophage-specific metalloelastase (MMP-12) truncates and inactivates ELR+ CXC chemokines and generates CCL2, -7, -8, and -13 antagonists: potential role of the macrophage in terminating polymorphonuclear leukocyte influx. *Blood, 112(8): p. 3455-64.*

Debra H., et al. (1996): TNF-a Inactivation of Collagen Receptors. *The Journal of Immunology, 156: 4354-436.*

Degryse, A.L. and Lawson, W.E. (2011): Progress toward improving animal models for idiopathic pulmonary fibrosis. *The American journal of the medical sciences. 341(6): p. 444-9.*

Driss El Kebir and Janos G. Filep (2010): Role of Neutrophil Apoptosis in the Resolution of Inflammation. *ISSN 1537-744X; DOI 10.1100/tsw.169.*

Du X, et al. (2002): The LIM-only coactivator FHL2 modulates WT1 transcriptional activity during gonadal differentiation. *Biochim Biophys Acta; 1577: 93-101.*

Eckes, et al. (2000): Interactions of fibroblasts with the extracellular matrix: implications for the understanding of fibrosis. *Springer S. Imm. 21:415-429.*

El Mourabit, H., et al. (2004): Analysis of the adaptor function of the LIM domain-containing protein FHL2 using an affinity chromatography approach. *J Cell Biochem 92, 612-25.*

Emmet E., et al. (2011): TNF- related apoptosis-inducing ligand (TRAIL) regulates inflammatory neutrophil apoptosis and enhances resolution of inflammation. *J. Leukoc. Biol. 90:855-865.*

End P, et al. (1992): Tenascin- a modulator of cell growth. *Eur J Biochem; 209:1041–51.*

Fanying Meng and Clifford A. Lowell (1997): Lipopolysaccharide (LPS)-induced Macrophage Activation and Signal Transduction in the Absence of Src-Family Kinases Hck, Fgr, and Lyn. *J Exp Med.;185(9):1661-70.*

Feldmann M & Maini RN (2003): Lasker Clinical Medical Research Award. TNF defined as a therapeutic target for rheumatoid arthritis and other autoimmune diseases. Nat Med.;9(10):1245–1250.

Fimia, G. M., et al. (2000): A family of LIM-only transcriptional coactivators- tissue-specific expression and selective activation of CREB and CREM. *Mol Cell Biol 20, 8613-22.*

Foell, D., and Roth, J. (2004): Proinflammatory S100 proteins in arthritis and autoimmune diseases. *Arthritis and Rheumatism 50: 3762–3771.*

Fridlender, et al. (2007): Telomerase activity in bleomycin-induced epithelial cell apoptosis and lung fibrosis. *Eur Respir J, 30: 205-213.*

Fui G. Goh, et al. (2010): Transcriptional Regulation of the Endogenous Danger Signal Tenascin-C: A Novel Autocrine Loop in Inflammation. *The Journal of Immunology, 184: 2655–2662.*

Fumitake, et al. (2008): role of interleukin-6 in bleomycin-induced lung inflammatory changes in mice. *Respir Cell Mol Biol Vol 38, pp 566-571.*

Gabriel, B., et al. (2004): Focal adhesion kinase interacts with the transcriptional coactivator FHL2 and both are overexpressed in epithelial ovarian cancer. *Anticancer Res 24, 921-7.*

Gabriel, et al. (2009): Expression of the Transcriptional Coregulator FHL2 in Human Breast Cancer - A Clinicopathologic Study. *J Soc Gznecol Investig. 13(1):69-75.*

Gay StefSan & Miller E.J. (1979): Collagen in the Physiology and Pathology of Connective Tissue, *Am J Hum Genet. 31(3):396-398.*

Gebhardt, C., et al. (2006): S100A8 and S100A9 in inflammation and cancer. *Biochemical Pharmacology 72: 1622–1631.*

Genini M, et al. (1997): Substractive cloning and characterization of DRAL, a novel LIM-domain protein down-regulated in rhabdomyosarcoma. *DNA Cell Biol; 16: 433–442.*

Grant, S. G. N., et al. (1990): Differential plasmid rescue from transgenic mouse DNAs into Escherichia coli methylation-restriction mutants. *Proc Natl Acad Sci U S A 87, 4645–4649.*

Hamidouche Z, et al. (2008): FHL2 mediates dexamethasone-induced mesenchymal cell differentiation into osteoblasts by activating Wnt/beta-catenin signaling-dependent Runx2 expression. *Faseb J: 22(11): 3813-3822.*

Hasegawa, et al. (2006): B-Lymphocyte Depletion Reduces Skin Fibrosis and Autoimmunity in the Tight-Skin Mouse Model for Systemic Sclerosis. *The American Journal of Pathology, Vol. 169, No. 3.*

Hay, John, et al. (1991): Mechanisms of bleomycin-induced lung damage. *Arch Toxicol 65:81-94.*

Henke, M. M. (2007): Die Role von FHL2 als Transkriptionskofaktor in der karzinogenese Oraler Plattenepithelkarzinome. *PhD thesis; DER HOHEN MEDIZINISCHEN FAKULTÄT, UNIVERSITÄT BONN, Germany.*

Herbert Y. Reynolds (2005): Lung Inflammation and Fibrosis: An Alveolar Macrophage–centered Perspective from the 1970s to 1980s. *Respir Crit Care Med Vol 171. pp 98–102.*

Herold et al. (2011): Acute lung injury: how macrophages orchestrate resolution of inflammation and tissue repair. *doi: 10.3389/fimmu.00065.*

Hinz, Boris (2007): Formation and function of the myofibroblast during tissue repair. *J Invest Dermatol 127, 526-537.*

Hinz, Boris, et al. (2007): Biological Perspectives - The Myofibroblast: One Function, Multiple Origins. *The American Journal of Pathology, Vol. 170, (6) 070112.*

Hiratsuka, S. et al. (2006): Tumour-mediated upregulation of chemoattractants and recruitment of myeloid cells predetermines lung metastasis. *Nat. Cell Biol. 8 (12), 1369–1375*

Hogan, Vanessa, et al. (2010): Role of B Cells in Rheumatic Autoimmune Disease. *The Open Arthritis Journal, 3, 32-36.*

Ilic, D., et al. (2004): FAK promotes organization of fibronectin matrix and fibrillar adhesions. *J Cell Sci 117, 177-87.*

Iredale JP, et al. (1998): Mechanism of spontaneous resolution of rat liver fibrosis - hepatic stellate cell apoptosis and reduced hepatic expression of metalloproteinase inhibitors. *J Clin Invest; 102: 538–549.*

Irina G., et al. (2008): Roles of T lymphocytes in pulmonary fibrosis. *Jleukoc. Biol. 83:237-244.*

Jack Gauldie, et al. (1993): Cytokines and pulmonary fibrosis. *T7horax; 48:931-935.*

Jantz M.A. & Antony V.B. (2006): Pleural fibrosis. *Clin. Chest Med. 27, 181–191.*

Ji Y. Kim, et al. (2009): Early and Late Changes of MMP-2 and MMP-9 in Bleomycin- Induced Pulmonary Fibrosis. *Yonsei Med J 50(1):68 – 77.*

Johannessen, M., et al. (2006): The multifunctional roles of the four-and-a-half-LIM only protein FHL2. *Cell Mol Life Sci 63, 268-84.*

Jones FS and Jones PL (2000): The tenascin family of ECM glycoproteins: structure, function, and regulation during embryonic development and tissue remodeling. *Dev Dyn 218:235-259.*

Joos, H., et al. (2008): IL-1beta regulates FHL2 and other cytoskeleton-related genes in human chondrocytes. *Mol Med.14 (3 4):150-9.*

Kaarteenaho-Wiik R, et al. (2001): Distribution and mRNA expression of tenascin-C in developing human lung. *Am J Respir Cell Mol Biol 25:341-346.*

Kadrmas JL & Beckerle MC (2004): The LIM domain: from the cytoskeleton to the nucleus. *Nat Re Mol Cell Biol; 5: 920-931.*

Kanayama, M., et al. (2009): α9 Integrin and its ligands constitute critical joint microenvironments for development of autoimmune arthritis. *J. Immunol. 182: 8015–8025.*

Kerrigan Ann M. & Brown, Gordon D. (2009): C-type lectins and phagocytosis. *Immunobiology 214 562–575.*

Kettritz, Ralph, et al. (2000): TNFα- mediated neutrophil apoptosis involves Ly-GDI, a Rho GTPase regulator. *J. Leukoc. Biol. 68:277-283.*

Khazen, W., et al. (2005): Expression of macrophage-selective markers in human and rodent adipocytes. *FEBS Lett. 579 (25): 5631–4.*

Kirfel, J., et al. (2008): Impaired intestinal wound healing in Fhl2-deficient mice is due to disturbed collagen metabolism. *Experimental cell research,. 314(20): p. 3684-91.*

Kisseleva, Tatiana and Brenner, David A. (2008): Mechanisms of Fibrogenesis. *Experimental Biology and Medicine, 233:109-122.*

Kolb, M., et al. (2001): Transient expression of IL-1beta induces acute lung injury and chronic repair leading to pulmonary fibrosis. *J. Clin. Invest. 107:1529–1536.*

Konig, Katharina, et al. (2010): Four and a Half LIM Domain Protein 2 Is a Novel Regulator of Sphingosine 1-Phosphate Receptor 1 in C-C Motif Chemokine Ligand 19-Induced Dendritic Cell Migration. *Published, doi:10.4049/jimmunol.0903449.*

Korpos, E., et al. (2010): Role of the extracellular matrix in lymphocyte migration. *Cell Tissue Res. 339, 47-57.*

Krieg, T., et al. (2007): Fibrosis in connective tissue disease: the role of the myofibroblast and fibroblast-epithelial cell interactions. *Arthritis Res Ther 9 Suppl 2, S4.*

Labalette, C., et al. (2004): Interaction and functional cooperation between the LIM proteins FHL2, CBP/p300, and beta-catenin. *Mol Cell Biol 24, 10689-702.*

Laemmli U. K. (1970): Cleavage of structural proteins during the assembly of the head of bacteriophage T4. *Nature Vol. 227.*

LI HY, et al. (2001): Translocation of a human focal adhesion LIM-only protein, FHL2, during myofibrillogenesis and identification of LIM2 as the principal determinants of FHL2 focal dehesion localization. *Cell Motil Cytoskeleton; 48: 11-23.*

Lisha Patel, et al. (2011): Tenascin-C induces inflammatory mediators and matrix degradation in osteoarthritic cartilage. *BMC Musculoskeletal Disorders, 12:164.*

Livak, Kenneth J. and Schmittgen, Thomas D. (2001): Analysis of Relative Gene Expression Data Using Real- Time Quantitative PCR and the 2-ddCT Method. *METHODS 25, 402–408.*

Lorenz, E., et al. (2008): Different expression ratio of S100A8/A9 and S100A12 in acute and chronic lung diseases. *Respiratory Medicine 102: 567–573.*

Mach, B., et al. (1996): Regulation of MHC class II genes: lessons from a disease. *Annu. Rev. Immunol. 14:301.*

Martin G. Schwacha, (2009): γδ T-Cells: Potential Regulators of the Post-Burn Inflammatory Response. *Burns; 35(3): 318–326.*

Martin, B., et al. (2002): The LIM-only protein FHL2 interacts with beta-catenin and promotes differentiation of mouse myoblasts. *J Cell Biol 159, 113-22.*

Martin, B.T., et al. (2007): FHL2 regulates cell cycle-dependent and doxorubicin-induced p21Cip1/Waf1 expression in breast cancer cells. *Cell Cycle.6 (14):1779-88.*

Masashi Nishida & Kenji Hamaoka (2008): Macrophage Phenotype and Renal Fibrosis in Obstructive Nephropathy. *Nephron Exp Nephrol; 110:e31–e36.*

Maseruka H, et al. (1997): TulloTenascin-C expression in normal, inflamed, and scarred human corneas. *British Journal of Ophthalmology; 81:677–682.*

Mauri C, et al. (2003): Prevention of arthritis by interleukin 10 producing B cells. *J Exp Med; 197:489-501.*

McGrath, M. J., et al. (2006): Four and a half LIM protein 1 binds myosin-binding protein C and regulates myosin filament formation and sarcomere assembly. *J Biol Chem 281, 7666-83.*

McGreal E, et al. (2005): Ligand recognition by antigen-presenting cell C-type lectin receptors. *Curr Opin Immunol 17 (1): 18–24.*

McGreal, Eamon P., et al. (2006): The carbohydrate-recognition domain of Dectin-2 is a C-type lectin with specificity for high mannose. *Glycobiology vol. 16 no. 5 pp. 422–430.*

Meyer, (2008): Die Rolle des Four-and-a-half-LIM-only-Protein 2 (FHL2) in der Gelenkzerstörung bei Rheumatoider Arthritis. *PhD Thesis; Biologie, uni. Münster- Germany.*

Midwood, K. and Orend, G. (2009): The role of tenascin-C in tissue injury and tumorigenesis. *J. Cell Commun. Signal. 3: 287–310.*

Midwood, K., et al. (2009): Tenascin-C is an endogenous activator of Toll-like receptor 4 that is essential for maintaining inflammation in arthritic joint disease. *Nat. Med. 15: 774–780.*

Mitra, S. K., et al. (2005): Focal adhesion kinase: in command and control of cell motility. *Nat Rev Mol Cell Biol 6, 56-68.*

Moises Selman and Annie Pardo (2006): Role of Epithelial Cells in Idiopathic Pulmonary Fibrosis. *Proc Am Thorac Soc Vol 3. pp 364–372.*

Moore BB & Hogaboam CM. (2008): Murine models of pulmonary fibrosis. *American journal of physiology Lung cellular and molecular physiology; 294(2):L152- L160.*

Morgan MJ & Madgwick AJ (1996): Slim defines a novel family of LIM-proteins expressed in skeletal muscle. *Biochem Biophys Res Commun; 225: 632–638.*

Morgan MJ & Madgwick AJ (1999a): The LIM proteins FHL1 and FHL3 are expressed differently in skeletal muscle. *Biochem Biophys Res Commun; 255: 245–250.*

Morgan MJ & Madgwick AJ (1999b): The fourth member of the FHL family of LIM proteins is expressed exclusively in the testis. *Biochem Biophys Res Commun; 255: 251–255.*

Morgan MJ & Whawell SA (2000): The structure of the human LIM protein ACT gene and its expression in tumor cell lines. *Biochem Biophys Res Commun; 273: 776-783.*

Morlon, A. and Sassone-Corsi, P. (2003): The LIM-only protein FHL2 is a serum-inducible transcriptional coactivator of AP-1. *Proc Natl Acad Sci U S A 100, 3977-82.*

Mouratis MA. and Aidinis V. (2011): Modeling pulmonary fibrosis with bleomycin. *Curr Opin Pulm Med. 17(5):355-61.*

Muller, J. M., et al. (2000): FHL2, a novel tissue-specific coactivator of the androgen receptor. *Embo J 19, 359-69.*

Muller, J.M, et al. (2002): The transcriptional coactivator FHL2 transmits Rho signals from the cell membrane into the nucleus. *Embo J 21(4):736-48.*

Mungunsukh O., et al. (2010): Bleomycin induces the extrinsic apoptotic pathway in pulmonary endothelial cells. *Am J Physiol Lung Cell Mol Physiol 298: L696-L703.*

Murray, M. (2010): Metalloproteinase Expression in Bone Marrow-derived Macrophages: Roles in Cell Migration. *PhD thesis; University of East Anglia, School of Biological Sciences, Norwich, NR4 7TJ.*

Mutsaers SE, et al. (1997): Mechanisms of tissue repair: from wound healing to fibrosis. *Int J Biochem Cell Biol; 29: 5–17.*

Nagase H, Woessner JF (1999): Matrix metalloproteinases. *J Biol Chem; 274(31):21491-4.*

Naohito Suzuki, et al. (1996): T lymphocytes and silica-induced pulmonary inflammation and fibrosis in mice. *Thorax; 51:1036-1042.*

Nkyimbeng Takwi, E.H. (2008): Regulation and pathomechanistic role of matrix metalloproteinases in Idiopathic Pulmonary Fibrosis. *PhD thesis; department of Internal Medicine II, Universitätklinikum Giessen und Marburg GmbH, Germany.*

Nordhoff, et al. (2012): The adaptor protein FHL2 enhances the cellular innate immune response to influenza A virus infection. *Cellular Microbiology, 14(7), 1135–1147.*

Norihiro Nishimoto, et al. (2000): IL-6 inhibits the proliferation of fibroblastic synovial cells from rheumatoid arthritis patients in the presence of soluble IL-6 receptor. *International Immunology, Vol. 12, No.2, p.187-193.*

Nuno R. Grande, et al. (1998): Lung fibrosis induced by bleomycin – structural changes and overview of recent advances. *Scanning Microscopy Vol. 12, No. 3, Pages 487-494.*

Olson MW, et al. (1997): Kinetic analysis of the binding of human matrix metalloproteinase-2 and -9 to tissue inhibitor of metalloproteinase (TIMP)-1 and TIMP-2. *J Biol Chem; 272(47):29975-83.*

Overall CM & Lopez-Otin C (2002): Strategies for MMP inhibition in cancer: Innovations for the post-trial era. *Nat Rev Cancer Nat Rev Cancer; 2(9):657-72.*

Pankov, R. and Yamada, K.M. (2002): Fibronectin at a glance. *J. Cell Sci. 115, 3861-3863.*

Papanicolaou DA, et al. (1998): The pathophysiologic roles of interleukin-6 in human disease. *Ann Intern Med; 128:127–37.*

Park J, et al. (2008): Deficiency in the LIM-only protein FHL2 impairs assembly of extracellular matrix proteins. *FASEB J. (7):2508-20.*

Parks WC, et al. (2004): Matrix metalloproteinases as modulators of inflammation and innate immunity. *Nat Rev Immunol; 4(8):617-29.*

Peter Lloyd Jonesa & Frederick Scheetz Jones (2000): Tenascin-C in development and disease: gene regulation and cell function. *Matrix Biology 19 -581-596.*

Philippar, U., et al. (2004): The SRF target gene Fhl2 antagonizes RhoA/MAL-dependent activation of SRF. *Mol Cell 16, 867-80.*

Philippe Van Lint and Claude Libert (2007): Chemokine and cytokine processing by matrix metalloproteinases and its effect on leukocyte migration and inflammation. *J Leukoc Biol.;82(6):1375-81.*

Pinart M., et al. (2008): Inflammatory related changes in lung tissue mechanics after bleomycin-induced lung injury. *Respiratory Physiology & Neurobiology 160, 196–203.*

Pottier, Nicolas, et al. (2007): Relationships between Early Inflammatory Response to Bleomycin and Sensitivity to Lung Fibrosis. *Am J Respir Crit Care Med Vol 176. pp 1098–1107.*

Purcell, N. H., et al. (2004): Extracellular signal-regulated kinase 2 interacts with and is negatively regulated by the LIM-only protein FHL2 in cardiomyocytes. *Mol Cell Biol 24, 1081-95.*

Purva Singh, et al. (2010): Schwarzbauer Assembly of Fibronectin Extracellular Matrix. *Annu. Rev. Cell Dev. Biol. 26:397–419.*

Raghu, G., et al. (2006): Incidence and prevalence of idiopathic pulmonary fibrosis. *Am. J. Respir. Crit. Care Med. 174, 810–816.*

Rajendra Raghow (1994): The role of extracellular matrix in postinflammatory wound healing and fibrosis. *FASEB J. 8: 823-831.*

Ramirez, Francesco, et al. (2006): Transcriptional regulation of the human α2 (I) collagen gene (COL1A2), an informative model system to study fibrotic diseases. *Matrix Biology 25- 365–372.*

Razzaque, Mohammed S. and Taguchi, Takashi (2003): Pulmonary fibrosis: Cellular and molecular events. *Pathology International; 53: 133–145.*

Robert J. Homer, et al. (2011): Modern Concepts on the Role of Inflammation in Pulmonary Fibrosis. *Arch Pathol Lab Med.; 135:780–788.*

Robert J. Mason, et al. (2010): Murray and Nadel`s Texbook of Respiratory Medicine. *Saunders; 5 edition; ISBN-13:978-1416047100.*

Roderick J. Tan, et al. (2006): Matrix Metalloproteinases Promote Inflammation and Fibrosis in Asbestos-Induced Lung Injury in Mice. *Am J Respir Cell Mol Biol Vol 35. pp 289–297.*

Rooijen, N.and Sanders, A. (1994): Liposome mediated depletion of macrophages: mechanism of action, preparation of liposomes and applications. *J. of Immunological methods 174, 83-93.*

Ruiz, Victor, et al. (2003): Unbalanced collagenases/TIMP-1 expression and epithelial apoptosis in experimental lung fibrosis. *Am J Physiol Lung Cell Mol Physiol 285: L1026–L1036.*

Russell Ross (1994): The role of T lymphocytes in inflammation. *Proc Natl Acad Sci USA. 91(8):2879.*

Ryckman, C., et al. (2003): Proinflammatory activities of S100 - Proteins S100A8, S100A9 and S100A8/A9 induce neutrophil chemotaxis and adhesion. *Journal of Immunology 170: 3233-3242.*

Samson, T., et al. (2004): The LIM-only proteins FHL2 and FHL3 interact with alpha- and beta-subunits of the muscle alpha7 beta1 integrin receptor. *J Biol Chem 279, 28641-52.*

Scholl FA, et al. (2000): DRAL is a p53-responsive gene whose four and a half LIM domain protein product induces apotosis. *J Cell Biol; 151: 495-506.*

Schuppan D, et al. (2001): Matrix as a modulator of hepatic fibrogenesis. *Semin Liver Dis; 21(3):351–372.*

Shaw TJ, et al. (2009): Wound repair at a glance. *J Cell Sci: 122(Pt 18): 3209-3213.*

Shiokawa, et al. (1999): Functional Role of Arg-Gly-Asp (RGD)-Binding Sites on b1 Integrin in Embryo Implantation Using Mouse Blastocysts and Human Decidua. *BIOLOGY OF REPRODUCTION 60, 1468–1474.*

Sieg, D. J., et al. (2000): FAK integrates growth-factor and integrin signals to promote cell migration. *Nat Cell Biol 2, 249-56.*

Smith RE, et al. (1994): Production and function of murine macrophage inflammatory protein-1α in bleomycin-induced lung injury. *J Immunol; 153(10):4704–4712.*

Smith RE, et al. (1995): A role for C–C chemokines in fibrotic lung disease. *J Leukoc Biol; 57(5):782–787.*

Soazig Nénan, et al. (2005): Macrophage elastase (MMP-12): a pro-inflammatory mediator? *Mem Inst Oswaldo Cruz, Rio de Janeiro, Vol. 100 (Suppl. I): 167-172.*

Soilleux, Elizabeth J., et al. (2002): Constitutive and induced expression of DC-SIGN on dendritic cell and macrophage subpopulations in situ and in vitro. *J. Leukoc. Biol. 71: 445–457.*

Steven E. Mutsaers, et al. (1997): Mechanisms of Tissue Repair: from Wound Healing to Fibrosis. J. Biochem. *Cell Bid. Vol. 29, No. 1, pp. 5-17.*

Strieter RM, et al. (2007): The role of CXC chemokines in pulmonary fibrosis. *J Clin Invest 117:549–556.*

Timothy A. Butterfield; et al. (2006): The Dual Roles of Neutrophils and Macrophages in Inflammation: A Critical Balance Between Tissue Damage and Repair. *Journal of Athletic Training; 41(4):457–465.*

Tomoaki Yoshinoa, et al. (2005): Multiple proteins are involved in the protein–DNA complex in the proximal promoter of the human a1 (III) collagen gene (COL3A1). *Biochimica et Biophysica Acta 1729, 94 – 104.*

Tucker RP, et al. (2009): The regulation of tenascin expression by tissue microenvironments. *Biochim Biophys Acta: 1793(5): 888-892.*

Umezawa H, et al. (1966): New antibiotics, bleomycin A and B. *Cancer 19:201-209.*

Van Amerongen, Machteld J., et al. (2007): Macrophage Depletion Impairs Wound Healing and Increases Left Ventricular Remodeling after Myocardial Injury in Mice. *Am J Pathol, 170:818–829.*

van den Berg LM, et al. (2012): An evolutionary perspective on C-type lectins in infection and immunity. *Ann N Y Acad Sci: 1253: 149-158.*

Van der Rest, Michel and Garrone, Robert, (1991): Collagen family of proteins. *FASEB J. 5- 2814– 2823.*

Vincent Lagente, et al. (2009): Macrophage metalloelastase (MMP-12) as a target for inflammatory respiratory diseases. *Informa UK Ltd ISSN 1472-8222.*

Visse R & Nagase H. (2003): Matrix metalloproteinases and tissue inhibitors of metalloproteinases structure, function, and biochemistry. *Circ Res Circ Res;92(8):827-39.*

Vogl TJ, et al. (2008): Palliative hepatic intraarterial chemotherapy (HIC) using a novel combination of gemcitabine and mitomycin C: results in hepatic metastases. *Eur Radiol: 18(3): 468-476.*

Walters DM, et al. (2008): Mouse models of bleomycin-induced pulmonary fibrosis. Curr Protoc Pharmacol: Chapter 5: Unit 5 46.

Wei, Y., et al. (2003): Identification of the LIM protein FHL2 as a coactivator of beta-catenin. *J Biol Chem 278, 5188-94.*

Wenjing Zhang, et al. (2010): Four and a half LIM protein 2 (FHL2) promotes invasive potential and epithelialmesenchymal transition in colon cancer. *Carcinogenesis. 31(7):1220-9.*

Wick, Georg, et al. (2009): The immunology of fibrosis: innate and adaptive responses. *Trends in Immunology Vol.31 No.3.*

Wierzbicka-Patynowski, I. and Schwarzbauer, J.E. (2003): The ins and outs of fibronectin matrix assembly. *J. Cell Sci. 116, 3269-3276.*

William A.H. (2007): Inflammation-associated remodeling and fibrosis in the lung: a process and an end point. *Int. J. Exp. Path, 88, 103–110.*

Wixler V., et al. (2000): The LIM-only Protein DRAL/FHL2 Binds to the Cytoplasmic Domain of Several a and b Integrin Chains and Is Recruited to Adhesion Complexes. *J. Biol. Chem., Vol. 275, Issue 43, 33669-33678.*

Wixler, V., et al. (1999): Identification of novel interaction partners for the conserved membrane proximal region of alpha-integrin cytoplasmic domains. *FEBS Lett 445, 351-5.*

Wixler, V., et al. (2007): Deficiency in the LIM-only protein Fhl2 impairs skin wound healing. *J Cell Biol 177(1):163-72.*

Woessner JF, Jr (1994): The family of matrix metalloproteinases. *Ann N Y Acad Sci; 732:11-21.*

Wynn T.A. (2011): Integrating mechanisms of pulmonary fibrosis. *The Journal of experimental medicine, 208(7): p. 1339-50.*

Wynn TA. (2007): Common and unique mechanisms regulate fibrosis in various fibroproliferative diseases. *J Clin Invest; 117(3):524–529.*

Wynn TA. (2008): Cellular and molecular mechanisms of fibrosis. *J Pathol; 214: 199–210.*

Wynn, T.A. and Barron L. (2010): Macrophages: master regulators of inflammation and fibrosis. Semin. *Liver Dis. 30:245–257.*

Yang, Li et al. (2010): TGF-β and immune cells: an important regulatory axis in the tumor microenvironment and progression. *Trends in Immunology 31, 220–227.*

Yoshizaki A, et al. (2008): CD19 regulates skin and lung fibrosis via Toll-like receptor signaling in a model of bleomycin-induced scleroderma. *Am J Pathol: 172(6): 1650-1663.*

Zhou et al. (2006): DC-SIGN and Immunoregulation. *Cellular & Molecular Immunology; 3(4):279-283.*

Zimmer, B. Danna et al. (1995): The S100 Protein Family- History, Function, and Expression. *Brain Research Bulletin. Vol. 37, No. 4, pp. 417-429.*

Zuo FR, et al. (2002): Gene expression analysis reveals matrilysin as a key regulator of pulmonary fibrosis in mice and humans. *P Natl Acad Sci USA; 99(9):6292-7.*

5. Appendix

5.1. List of Figures

5.2. List of Tables

5.3. List of Symbols

ACT	activator of CREM in testis
AP-1	activator protein- 1
APMA	aminophenylmercuric acetate
AR	androgen receptor
ARDS	acute respiratory distress syndrome
aSMA	alpha-smooth muscle actin
ATP	adenosine triphosphate
BLM	bleomycin
CD209	cluster of differentiation 209
COL	collagen
COPD	chronic obstructive pulmonary disease
CREP	collection of rice expression profiles
DC-SIGN	dendritic cell-specific intercellular adhesion molecule -3- grabbin non-integrin
DNA	deoxyribonucleic acid
DRAL	down regulated in rhabdomyosarkoma LIM protein
E. coli	escherichia coli
ECM	extracellular matrix
EMT	epithelial/endothelial-mesenchymal transition
ERK	extracellular-signal-regulated kinase
FAK	focal adhesion kinase
FGF	fibroblast growth factor family
FHL	four-and-half LIM domains
FN	fibronectin
g	gramm
IAV	influenza A virus
IFN-γ	interferon-gamma
IL	interleukin

IPF	idiopathic pulmonary fibrosis
kb	kilobasenpaar
kDa	kilodalton
kg	kilogramm
l	liter
LPS	lipopolysaccharid
m	milli
M, mM, µM	molar, milimolar, micromolar
MAPK	mitogen-activated protein kinase
MIP	macrophage inflammatory protein
ml	milliliter
MMP	matrix metalloproteinase
mRNA	Messenger RNA
µ	mikro
µl	mikroliter
MΦ	macrophages
NAD	nicotinamide adenine dinucleotide
NF-*k*B	nuclear factor -*k* B
NK cell	natural killer cells
OA	osteoarthritic cartilage
PAMPs	pathogen associated molecular patterns
PDGF	platelet-derived growth factor
PMN	polymorphonuclear leucocytes
RA	rheumatoid arthritis
RANK	receptor activator of nuclear factor *k* B
RNA	Ribonucleic acid
ROS	reactive oxygen species
S1P	sphingosine-1-phosphate
SLIM	skeletal muscle LIM-protein

°C	temperatur in Grad Celsius
TGF- β	transforming growth factor beta
TIMP	tissue inhibitors of metalloproteinases
TLR	toll-like receptors
TNC	tenascin-C
TNF-α	tumor necrosis factor - alpha
TRAF	tumor necrosis factor receptor-associted factor

Acknowledgement:

My special thanks to my supervisor Dr. Victor Wixler for his supervision, his direction and his strong efforts to succeed this project. I learned a lot of things from him in my field. Also, I would like to thank Prof. Dr. Shtephan Ludwig; (the head of our institute), Prof. Dr. Martin Bähler (second referee) and Prof. Dr. Volker Gerke (available as an examiner) for their support and help to finish this work. Finally, I would like to thank my colleagues and all other people who contributed to this work.

CURRICULUM VITA